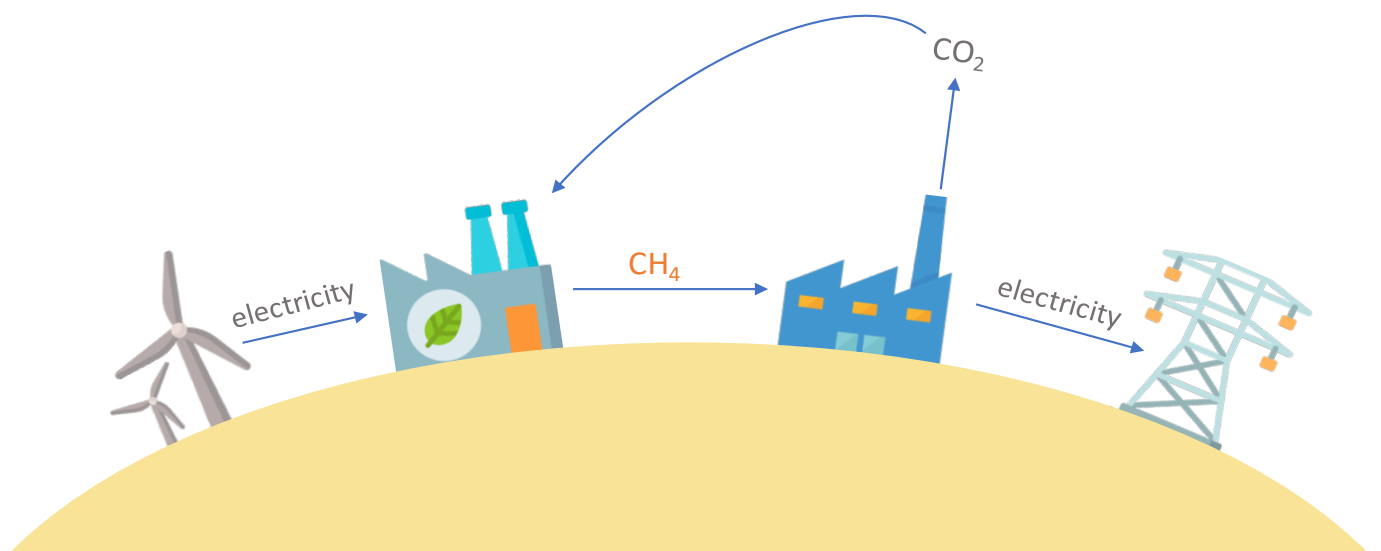


Power to Methane to Power

Performance analysis of a closed loop energy storage system

M.Goorden



Power to methane to power

Performance analysis of a closed loop energy storage system

by

M. Goorden

to obtain the degree of Master of Science
at the Delft University of Technology,
to be defended publicly on Monday September 2, 2019 at 11:30 AM.

Student number: 4076362
Project duration: February 15, 2019 – September 2, 2019
Thesis committee: Dr. R. Kortlever, TU Delft, supervisor
Prof. dr. ir. C. A. Ramirez, TU Delft
Prof. dr. ir. W. de Jong, TU Delft
Ir. C. Nijhof, Vattenfall

This thesis is confidential and cannot be made public until August 26, 2019.

An electronic version of this thesis is available at <http://repository.tudelft.nl/>.



The work in this thesis was supported by Vattenfall. Their cooperation is hereby gratefully acknowledged.



Preface

It is not difficult to substantiate why working on renewable energy solutions is important. To me, it is also a lot of fun. The field of renewable energy, and specifically energy storage, is the field where two of my major interests are combined: sustainability and puzzling. With great enthusiasm I worked on this thesis, puzzling a power-to-methane-to-power system together and hopefully contributing to a sustainable future.

I would like to thank my supervisors Ruud Kortlever and Andrea Ramirez for being critical on my work, as I have the tendency to lose myself to exciting ideas. Also I would like to thank all the kind people at Vattenfall for giving me such a great time and brainstorming on the content of this thesis. I would like to thank my family and friends for the support and sometimes needed distraction. I would like to thank my parents, Anne-Marie and Louis, for always encouraging me to do what makes me happy. I would like to thank my sisters, Pia and Kristie, for always being there. And I would like to thank Sjoerd for helping me putting this project together and for all his patience and love.

*M. Goorden
Delft, August 2019*

Abstract

The Paris Agreement central aim is to prevent climate change by keeping the global temperature rise this century well below 2 °C above pre-industrial levels and to pursue efforts to limit the temperature increase even further to 1.5 °C. Anthropogenic global warming can be stopped by reaching and sustaining net zero global anthropogenic CO₂ emissions. Electricity and heat generation were the largest sources of CO₂ emissions from fuel combustion in 2016, accounting for 42% of the global total. Reducing CO₂ emissions in this sector has a large effect on total global CO₂ emissions. This can be done by generating energy from renewable sources such as wind and sun. However these sources alone cannot provide a reliable electricity system and therefore an energy storage system is needed.

Power-to-gas is a concept in which surplus renewable electricity is used for the production of a gas fuel. The gas can be stored and is used for electricity production when there is a deficit in renewable electricity. When CO₂ exhaust gases form reactants for new production of the gas the system has no net CO₂ emissions. The gas functions as an energy carrier for electrical energy. Methane could be an interesting gas for large scale energy storage as there is much knowledge about methane transport, storage and combustion and the gas is easier to store than hydrogen. Power-to-gas-to-power conversions come with great electricity losses. Therefore it is interesting to investigate what waste heat streams can be extracted from the process to use for external purposes.

The aim of this thesis is to map the input and output energy streams of a power-to-methane-to-power system operating in 2030 to find the efficiency of the system and to see how efficiency could be maximized by using waste heat streams for external purposes. Also, a power-to-methane-to-power system requires a lot of gas storage capacity. Therefore it is useful to estimate the capacity of the gas storage facility to provide such a system. It should be investigated whether it is technically possible to store such amounts of gas and to see what gas storage does with the efficiency of the system. Last, since the aim is to reduce carbon emissions the (small) CO₂ emissions of the system are calculated. The system is scaled up to a scenario in which it provides a fully renewable electricity grid in the year 2050, to explore the feasibility in terms of carbon emissions and required gas storage capacity. The system is also compared to a power-to-hydrogen-to-power system to find the most feasible solution.

The behavior of the power-to-methane-to-power system highly depends on the amount of electricity surplus and deficit. Therefore a grid an estimate of the grid load in the years 2030 and 2050 is made in Excel. The power-to-methane-to-power system is modeled using Aspen, Cycle Tempo, MATLAB and Excel.

The round trip energy efficiency of the system in 2030 is 88.0 %, which is the sum of an electrical efficiency of 30.9 % and a thermal efficiency of 57.1 %. The total energy efficiency can only be achieved when streams modeled as usable heat output streams can actually be used. This depends highly on the location of the system. The carbon emissions of a system with a 44MW output in 2030 are to be 56.3 t y⁻¹ and the required gas storage capacity is 5.09 × 10⁵ m³ of underground salt caverns. When scaling up the system to provide a fully renewable electricity grid, the total gas storage capacity is 9.34 × 10⁷ m³, which is 5.5 % of the total potential salt cavern volume in the Netherlands. The carbon emissions are 2.78 kt y⁻¹, which is 0.0056 % of the current annual carbon emissions caused by the Dutch power generation sector. Compared to a hydrogen system the methane system performs worse in terms of electrical efficiency, gas storage capacity and carbon emissions.

Power-to-methane and methane-to-power technologies are currently widely investigated and there could be a technological breakthrough in the coming years which could significantly increase the electrical efficiency of the methane system. The results from this thesis are an early stage estimate. Also, the technical details of both a methane and a hydrogen system are not explored as well as the investment costs. To find the most convenient and economically feasible system, an economic analysis should be performed.

List of Abbreviations

AEC	=	Alkaline electrolysis cell
ASU	=	Air separation unit
CAPEX	=	Capital costs of investment
CCS	=	Carbon capture and storage
CCU	=	Carbon utilization and utilization
CES	=	Clean energy system
GHSV	=	Gas hourly space velocity
GT	=	Gas turbine
GtP	=	Gas-to-power
HHV	=	Higher heating value
HPT	=	High pressure turbine
HRSG	=	Heat recycle steam generator
IPT	=	Intermediate pressure turbine
LHV	=	Lower heating value
LPT	=	Low pressure turbine
MtP	=	Methane-to-power
NGCC	=	Natural gas combined cycle
OF-CHP	=	Oxy-fuel combined heat and power plant
OPEX	=	Operational costs of investment
PEM	=	Proton exchange membrane
PtHtP	=	Power-to-hydrogen-to-power
PtG	=	Power-to-gas
PtH	=	Power-to-hydrogen
PtGtP	=	Power-to-gas-to-power
PtHtP	=	Power-to-hydrogen-to-power
PtMtP	=	Power-to-methane-to-power
SCOC-CC	=	Semi-closed oxy-combustion combined cycle
SOEC	=	Solid oxide electrolysis cell
ST	=	Steam turbine

List of Figures

1.1	Power-to-methane-to-power system block scheme	3
1.2	Methodology block scheme	4
2.1	Grid balance 2018, only taking into account electrical input from wind and sun	7
2.2	Grid balance 2030, only taking into account electrical input from wind and sun	9
2.3	Grid balance 2050 low scenario, only taking into account electrical input from wind and sun	10
2.4	Grid balance 2050 mid scenario, only taking into account electrical input from wind and sun	10
2.5	Grid balance 2050 high scenario, only taking into account electrical input from wind and sun	11
3.1	Exergy efficiency for methanation comparing different electrolysis technologies	17
4.1	Equilibrium concentration of a $H_2/CO_2 = 4$ mixture at 30 bar, taken from [30]	21
5.1	Schematic flow sheet of the SCOC-CC	24
5.2	Schematic flow sheet of the Allam cycle	25
5.3	Schematic flow sheet of the CES cycle	25
5.4	Schematic flow sheet of the S-Graz cycle	26
7.1	Oxy-fuel powerplant model from Cycle Tempo	34
7.2	Flowsheet of methanation plant	37
7.3	Total amount of CH_4 produced by methanation plant per hour over the year 2030	42
7.4	Total amount of CH_4 consumed by power plant per hour over the year 2030	42
7.5	Total amount of CO_2 produced by methanation plant per hour over the year 2030	43
7.6	Total amount of CO_2 consumed by methanation plant per hour over the year 2030	43
7.7	Total amount of O_2 produced by methanation plant per hour over the year 2030	44
7.8	Total amount of O_2 consumed by methanation plant per hour over the year 2030	44
7.9	Total amount of H_2 produced by SOEC's per hour over the year 2030	45
7.10	Total amount of H_2 consumed by the methanation plant per hour over the year 2030	46
7.11	Flow sheet from Aspen for gas compression with heat extraction	47
8.1	Amount of CH_4 stored per hour	50
8.2	Amount of CO_2 stored per hour	50
8.3	Amount of O_2 stored per hour	51
8.4	Amount of H_2 stored per hour	52
8.5	System input flows and electrical output flows	61
8.6	System input flows and heat output flows	62
8.7	Build up of round trip electrical efficiency of PtMtP system	63
8.8	Hydrogen produced over one year	65
8.9	Hydrogen consumed over one year	65
8.10	Hydrogen stored over one year	66

List of Tables

2.1	Future installed capacity renewable sources	8
2.2	Factors for supply in demand prognosis	9
2.3	Balance and amount of deficit hours	12
3.1	Parameters of different cell types	17
3.2	Parameters of different electrolysis technologies	17
4.1	Comparison of different methanation technologies	20
4.2	Typical process conditions for catalytical methanation in fixed bed reactors	21
5.1	Comparison of different oxy-fuel power cycles	26
5.2	Equipment specifications of oxy-fuel combined heat and power cycle in PtMtP system	27
6.1	Underground gas storage potential in the Netherlands for different gases taken from [24]	30
7.1	Fuel composition of OFCC model	33
7.2	Turbine inlet temperatures for OF-CHP model	35
7.3	Equipment specifications of OFCC	35
7.4	Reactant flow rates methanation plant	36
7.5	Equipment specifications methanation plant	38
7.6	Electrolyzer specifications Sunfire SOEC [25, 30]	38
7.7	Values for PtMtP system capacity based on first assumption as explained in section 7.2-7.3	39
7.8	Final values for PtMtP system capacity based on first assumption as explained in section 7.4.1	40
7.9	Methane production and consumption rates for PtGtP system, depending on the grid load	41
7.10	Carbon dioxide production and consumption rates for PtGtP system, depending on the grid load	43
7.11	Oxygen production and consumption rates for PtGtP system, depending on the grid load	44
7.12	Hydrogen production and consumption rates for PtGtP system, depending on the grid load	45
7.13	Initial conditions gases before compression for storage	46
8.1	Required storage capacity with actual system flows based on calculation described in chapter 7	52
8.2	Required storage capacity with balanced system flows	52
8.3	Required storage capacity for different scenarios	54
8.4	Amount of gas to be stored for different scenarios	54
8.5	Input and chemical output values of methanation plant	56
8.6	Input and thermal output values of methanation plant	57
8.7	Electrical input and heat output of gas compression for storage	58
8.8	Heat input and output values for compressor cooling	58
8.9	Energy input of PtMtP system	60
8.10	Energy output of PtMtP system	63
8.11	Hydrogen production and consumption rates, depending on the grid load, for a PtHtP system	65
8.12	Storage capacity for different scenarios under storage conditions of 80 bar and 31 °C	67
8.13	Amount of gas to be stored for different scenarios	67
9.1	Annual surplus and deficit for different scenarios	69
9.2	Final system parameters	70

- 9.3 Gas storage capacity of different gases for a PtMtP system in 2050, designed to store enough gas to provide an electricity grid with input only from wind and solar energy . . . 70

Contents

List of Figures	xi
List of Tables	xiii
1 Introduction	1
1.1 Motivation	1
1.2 Power-to-methane-to-power system.	2
1.2.1 Description of the system	2
1.2.2 Context of the system	2
1.2.3 Comparison with a hydrogen system	2
1.3 Objective	3
1.4 Scope	3
1.5 Thesis outline	3
1.6 Methodology	4
2 Grid Analysis	7
2.1 Grid balance 2018	7
2.2 Prognosis supply and demand.	8
2.3 Grid balance 2030 and 2050.	9
2.4 Surplus and deficit hours.	11
2.5 Conclusion on grid analysis	11
3 Electrolysis	15
3.1 Important parameters for electrolysis	15
3.2 Alkaline cells	15
3.3 Proton exchange membrane cells	16
3.4 Solid oxide cells	16
3.5 Heat integration.	16
3.6 Conclusion	17
4 Methanation	19
4.1 Important parameters for methanation	19
4.2 Catalytic methanation	19
4.3 Electrochemical methanation	20
4.4 Biochemical methanation	20
4.5 Conclusion	20
4.6 Methanation process conditions for PtGtP system	20
4.7 Methanation flexibility	21
5 Oxy-fuel power generation	23
5.1 Important parameters	23
5.2 Different cycles	24
5.2.1 SCOC-CC.	24
5.2.2 Allam cycle	25
5.2.3 CES cycle.	25
5.2.4 S-Graz cycle	26
5.3 Conclusion	26
5.4 Oxy-fuel power plant process conditions for PtMtP system	26

6	Gas Storage and Transport	29
6.1	Carbon dioxide storage and transport	29
6.2	Methane storage and transport	30
6.3	Oxygen storage and transport	30
6.4	Hydrogen storage and transport	31
6.5	Conclusion on storage and transport	31
7	Modeling	33
7.1	Oxy-fuel power plant	33
7.2	Methanation plant	35
7.3	Electrolysis plant	38
7.4	Final system values	39
7.4.1	Methanation and electrolysis plant final capacity	39
7.4.2	Steam production and consumption	40
7.5	Transport and storage	41
7.5.1	Transport	41
7.5.2	Storage losses and capacity calculation.	41
7.5.3	Methane storage	41
7.5.4	Carbon dioxide storage	42
7.5.5	Oxygen storage.	43
7.5.6	Hydrogen storage	44
7.5.7	Gas compression.	46
8	Results	49
8.1	Gas storage capacity.	49
8.1.1	Methane storage capacity	49
8.1.2	Carbon dioxide storage capacity.	50
8.1.3	Oxygen storage capacity.	50
8.1.4	Hydrogen storage capacity.	51
8.1.5	Total gas storage capacity	52
8.1.6	Storage capacity sensitivity to methanation flexibility.	53
8.2	Efficiencies	55
8.2.1	Oxy-fuel power plant efficiency	55
8.2.2	Methanation plant efficiency	56
8.2.3	Electrolyzer efficiency	57
8.2.4	Storage energy	57
8.2.5	Power-to-methane efficiency.	59
8.2.6	Methane-to-power efficiency	59
8.2.7	Round trip efficiency	59
8.2.8	Relation between energy efficiency and methanation flexibility	60
8.3	Carbon emissions	64
8.4	Hydrogen system.	64
8.4.1	System design and modeling	64
8.4.2	Storage capacity	65
8.4.3	Efficiency	66
8.5	Comparison between methane system and hydrogen system	66
8.5.1	Storage capacity	66
8.5.2	Efficiency and carbon emissions.	67
9	2050 scenario	69
9.1	Oxy-fuel power plant capacity	69
9.2	Methanation plant capacity and electrolysis capacity.	69
9.3	Efficiency	70
9.4	Storage capacity	70
9.5	Carbon emissions	71

10 Discussion and Recommendations	73
10.1 Grid analysis	73
10.2 Electrolysis	73
10.3 Methanation.	73
10.4 Power generation.	73
10.5 Gas storage.	74
10.6 Modeling	74
10.6.1 Power plant modeling	74
10.6.2 Methanation modeling	74
10.6.3 Gas storage modeling	75
10.7 Power-to-gas efficiency	75
10.8 Round trip efficiency	75
10.9 Hydrogen system.	76
10.10 2050 Scenario	76
11 Conclusion	77
Bibliography	79

Introduction

1.1. Motivation

The Paris Agreement central aim is to prevent climate change by keeping the global temperature rise this century well below 2 °C above pre-industrial levels and to pursue efforts to limit the temperature increase even further to 1.5 °C [44]. Anthropogenic global warming can be stopped by reaching and sustaining net zero global anthropogenic CO₂ emissions [40]. Electricity and heat generation were the largest sources of CO₂ emissions from fuel combustion in 2016, accounting for 42% of the global total [32]. Reducing CO₂ emissions in this sector has a large effect on total global CO₂ emissions. Electricity and heat generation emits CO₂ into the atmosphere via the following principle. Hydrocarbons from under the ground (i.e. oil, coal and gas) are combusted with oxygen above the ground and converted into CO₂ molecules that are emitted into the atmosphere. Net zero CO₂ emissions in electricity and heat generation can be realized by keeping carbon from under the ground, under the ground and by using energy from renewable sources like wind energy, and hydro-power energy. Biomass is also considered a renewable energy source, since the amount of CO₂ emitted by burning biomass equals the amount of CO₂ captured from air by the plant for its growth process. Therefore biomass has a net CO₂ emission of zero. However, the potential for producing biomass energy without negative climate or food security impacts lies mainly in the use of abandoned agricultural lands. The total above ground net primary production on these lands represents just 5% of global energy demand. Demands for land use in agriculture and grazing are unlikely to decrease [22]. Energy security is a problem when using purely wind, solar and hydro power energy due to fluctuating input. Therefore it is necessary to have a storage system. Daily fluctuations can be stored in batteries but they are not suited for long time, seasonal storage. Chemical storage in the form of synthetic gas (i.e., hydrogen, syngas, methane) produced via power-to-gas (PtG) is considered promising for seasonal storage in comparison with other technologies (e.g., pumped hydro, compressed air energy, flywheels, batteries), based on considerations including storage capacity, discharge time, location and distribution [19]. PtG is a concept in which surplus renewable electricity is used for the production of a gas fuel. The gas can be stored and is used for electricity production when there is a deficit in renewable electricity. When CO₂ exhaust gases form reactants for new production of the gas the system has net zero CO₂ emissions. The gas functions as an energy carrier for electrical energy. Some wide studied potential gases for PtG systems are hydrogen, ammonia and methane. Hydrogen can be produced via electrolysis of water with renewable electricity, giving only oxygen as a by-product. Burning hydrogen gives water and no CO₂ emissions. However, hydrogen gas is not easy to store. Burning ammonia gives NO_x emissions, which are also a form of greenhouse gases. These gas could be captured and split into N₂ and O₂. However, burning ammonia is a technological challenge. Methane could be an interesting gas for large scale energy storage as there is much knowledge about methane transport, storage and combustion and the gas is easier to store than hydrogen. Power-to-gas-to-power conversions come with great electricity losses. Therefore it is interesting to investigate what waste heat streams can be extracted from the process to use for external purposes. When heat is also used as form of energy output the total energy efficiency of the system increases. Also less electricity is needed for heating purposes, meaning less electricity needs to be stored.

1.2. Power-to-methane-to-power system

1.2.1. Description of the system

A power-to-methane-to-power system is visualized in figure 1.1. The blocks refer to operational units and the orange molecules indicate material streams. Renewable electricity from wind and sun delivers energy input to the system. Although biomass and bio-gas are considered renewable energy sources, their contribution is not taken into account in this research. The large amount of land required makes it unrealistic to provide the world with this source of energy [22]. Due to a limited amount of data available, input from hydro power is neglected as well. However, hydro power currently delivers a small contribution, a couple percent points of the total green energy mix [9]. The system will be designed in a way that all energy input, i.e. energy for electrolysis, compression and heating, is supplied in the form of electricity. When there is surplus green electricity the surplus is used to split water into oxygen and hydrogen via electrolysis. Oxygen is stored. Hydrogen is further processed to methane in a reaction with carbon monoxide in a methanation process, producing water as a by-product. Ideally these processes would run during periods of green electricity surplus and switched off when there is a green electricity deficit. However it is likely that the methanation plant does not allow this type of flexibility, where the electrolysis process follows the load on the grid. Therefore intermediate hydrogen storage is probably required to keep the methanation plant provided with hydrogen during a period of green electricity shortage, i.e. when the electrolyzers are switched off. The formed methane is then stored. When there is a deficit in wind and solar power, green electricity is generated from the stored methane along with the stored oxygen in an oxy-fuel power plant (block 'electricity generation'). This process produces water as a by-product and carbon dioxide which is captured, stored and used as a reactant for the production of new methane. As can be read above, a power-to-methane-to-power system requires a lot of gas storage capacity. Therefore it is useful to estimate the capacity of the gas storage facility to provide such a system to find if this is technically possible to store such amounts of gas and to see what gas storage does with the efficiency of the system.

1.2.2. Context of the system

A commercial scale system is designed to operate in the Netherlands, in the year 2030, since it is likely that there will already be green electricity surplus hours in this year (section 2). Consequently the green electricity balance prognoses of the Dutch grid in 2030 is taken as the first starting point for the design. Also the outcomes are put in perspective in a Dutch future framework when it comes to, for instance, available storage gas capacity or the usage of excess heat. The 2030 design is not meant to store all surplus peaks or back-up all deficits. It only shows an example of a commercial size system and gives indications of the efficiency and required installed capacity of power generation, methanation, electrolysis and storage. Eventually, the system is scaled up to store enough energy to create a fully renewable Dutch electricity grid in 2050. The feasibility in terms of carbon emissions and storage capacity is analyzed. The reason that scaling up to a fully renewable grid system is only done for the year 2050 and not for the year 2030 is because it is likely that in 2030 there will not be enough renewable electricity supply yet for a 100% renewable grid system. The second starting point of the system design is the capacity of the oxy-fuel power plant, which is predefined as 44 MW. This is 10 times smaller than the Vattenfall Magnum gas power plants and it is in the typical scale of first generation oxy-fuel power plants [3]. Other important system characteristics are the production of heat and the small carbon emissions during methanation and power generation. Making smart use of this form of energy increases the overall system efficiency, this is explained more briefly in section 8. Small carbon emissions make that there is a net carbon output, also described in chapter 8.

1.2.3. Comparison with a hydrogen system

Main advantages of this system, compared to a power-to-hydrogen-to-power system, are the decrease in hydrogen storage, which is a complicated and energy intensive process, and the possibility to make use of existing technologies and infrastructure designed for natural gas. However, turning hydrogen into methane requires an extra conversion step which causes energy losses. Carbon capture too is an extra required step decreasing the overall energy efficiency, but using the by-product oxygen from electrolysis for oxy-fuel power generation significantly enhances this the carbon capture process. Nevertheless, large amounts of oxygen need to be stored which is an energy intensive process. It therefore is of importance to compare the round trip efficiencies of the two systems.

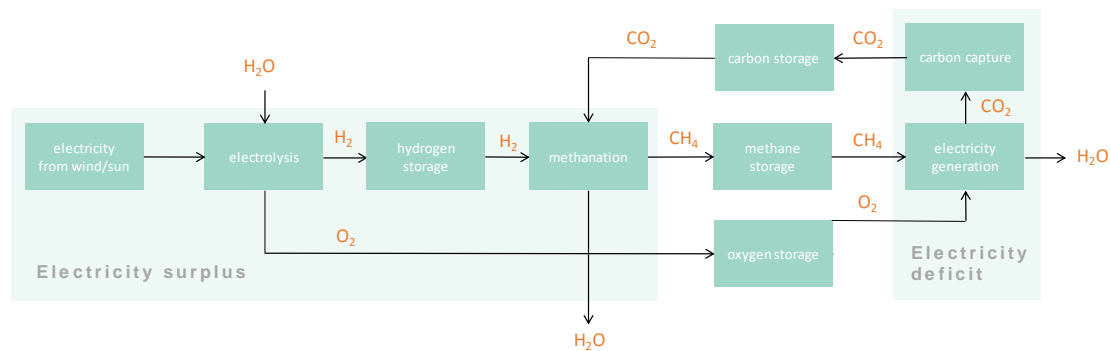


Figure 1.1: Power-to-methane-to-power system block scheme

1.3. Objective

To find investigate how the power-to-methane-to-power system behaves in terms of energy efficiency, storage capacity and carbon emissions and to investigate if it is a better solution that a hydrogen system, the following research question and sub questions are answered in this thesis:

Research question: What are the key factors that influence the energy efficiency of a closed loop system that uses methane as an energy carrier and how does the system preform compared to a system that uses hydrogen as an energy carrier?

Subquestions:

1. What are the energy efficiency, carbon emissions and required gas storage capacity of a closed loop system that uses methane as an energy carrier?
2. How does the allocation between electricity and heat influence the efficiency of the system?
3. How does the system perform in terms of carbon emissions and storage convenience compared to a power-to-hydrogen system and in an all renewable grid scenario?

1.4. Scope

This thesis focuses on modeling of the power-to-methane-to-power system and mapping the energy and mass input and output streams to find system efficiencies, carbon emissions and gas storage capacity. The design choices are based on a literature study but finding the most optimal design is not a key feature of this thesis. Also the more practical features of the PtMtP system such as reactor design, turbine design and design of the storage facility are not investigated. Last, the aim of this thesis is to find the technical behavior of a PtMtP system and the economic performance is not investigated.

1.5. Thesis outline

This subsection describes how this thesis is built up. The methods used to provide an answer to the research question are explained in the next subsection. Chapter 2 describes the grid analysis of the year 2030 and 2050. It concludes with indicating the electricity surplus and the gaps of the year 2030 and 2050, only taking into account electricity supply from wind and sun. The rest of the thesis is divided into 2 parts, focusing on 2 different periods in time.

The first part focusses on the year 2030. In chapter 3 - 8 technologies for a commercial scale power-to-methane-to-power system with intermediate gas storage are explored and modeled and results are evaluated. The 2030 system is not designed as an energy storage system that can provide the whole grid with wind and solar power yet. Chapter 3 is about hydrogen production via electrolysis of water. The most commonly used water electrolysis technologies are explored and compared to eventually choose the most suited one for this system. Chapter 4 dives into methane production. Several technologies are explored and compared and the most suited one is further investigated to develop a plant flow sheet with

operating characteristics. In chapter 5 oxy-power plants are explored. Different cycles are investigated and compared and a flow sheet with operating characteristics is developed. Chapter 6 gives possible solutions for gas storage. No technical details are explored and the gas storage system will not be modeled as this is out of the scope of this research. Chapter 7 describes the modeling of the 2030 system, providing more detailed flow sheets, scaling of the system components and input and output values. In chapter 8 the results from the previous section are evaluated and the efficiency, carbon emissions and gas storage capacity are presented. The allocation of different forms of energy, i.e. electricity and heat, and their utility is discussed in terms of energy efficiency. The system is compared to a power-to-hydrogen-to-power system in terms of storage capacity and carbon emissions.

The second part, chapter 9, focusses on the year 2050 in a scenario in which the power-to-methane-to-power system provides a solution for a full wind and solar electricity grid. The required installed capacity of the 2050 system is calculated so that the system can back up the grid using only input from wind and sun. The carbon emissions and the required gas storage capacity are presented and analyzed.

Last, chapter 10 discussed the outcomes and limitations of the system and gives recommendations for further research. Chapter 11 provides the final conclusion of the research.

1.6. Methodology

The steps that are taken in order to answer the sub questions, and eventually the research question, are visualized in figure 1.2. The green blocks refer to the future grid analysis, which provides input to all sub questions. The blue blocks refer to the power-to-methane-to-power system design that eventually answers sub question 1 at block 'Final system design and efficiency'. The orange block refers to the analysis of the efficiency calculation and answers sub question 2. The yellow blocks refer to a 2050 scenario in which all electricity on the grid comes from wind and sun and where the 2030 system is scaled up to back up the 2050 grid. This scenario eventually answers sub question 3 in block 'Performance comparison'.

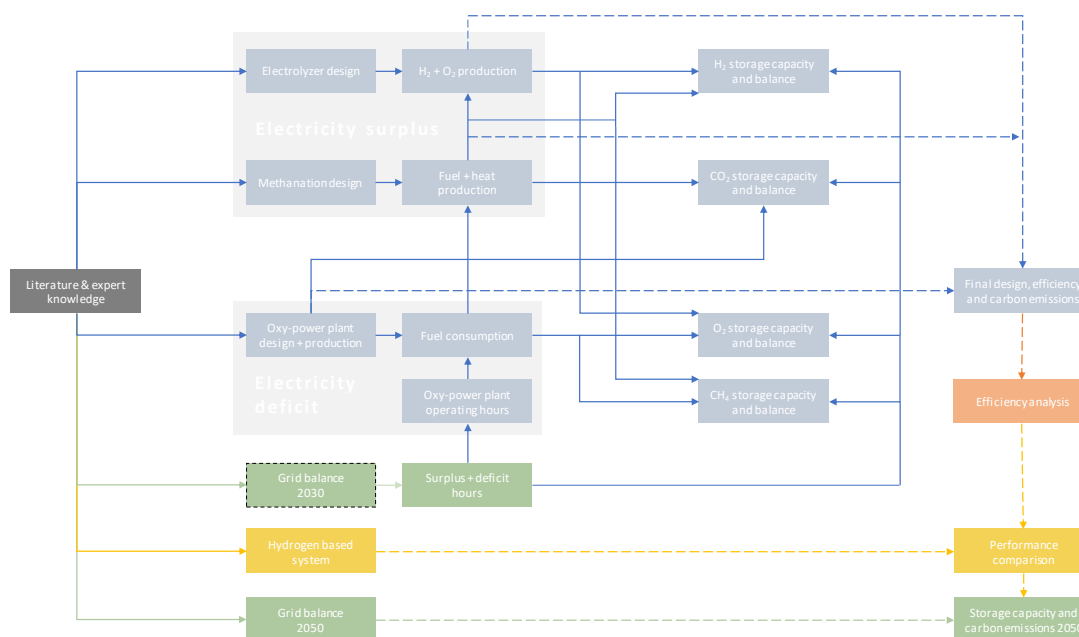


Figure 1.2: Methodology block scheme

The start of this research is making an estimate of the electricity demand and the renewable electricity supply in the year 2030 (green block with the black dashed line: 'Grid balance 2030'). After a literature review on the 2030 electricity supply from wind and sun and the 2030 electricity demand, a 2030 grid balance estimate is made in Excel to estimate the operating hours of the oxy-power plant. The plant will not operate when the renewable electricity supply exceeds the electricity demand and

therefore it runs during deficit hours. Designing the power-to-methane-to-power system is an iterative process, to start with the oxy-power plant. The oxy-power plant design is based on literature and expert knowledge. The plant capacity is pre-defined at 44MW and used as a starting point in calculating the capacity of the system in 2030. It is assumed that the plant always runs at full load during operating hours. With the use of Cycle Tempo the plant is modeled so that the heat production of the plant and the annual fuel consumption are calculated, based on the number of operating hours. Since the annual oxy-power plant fuel consumption equals the annual methanation plant fuel production, the methanation plant can now be scaled and modeled in Aspen One V8.8. The design is based on literature. From the Aspen model the heat production of the methanation plant and the required amount of hydrogen can be extracted. Hydrogen consumption of the methanation plant equals hydrogen production of the electrolyzer stacks, which leads to oxygen production and scaling of the stacks. Stack design is based on literature. The methanation plant fuel output requirements are defined by the oxy-power plant fuel input requirements. The oxy-power plant model first runs on an estimated fuel composition. After designing the methanation plant the oxy-power plant is updated with the final fuel composition. The power output is fixed but the heat output and the fuel consumption can be influenced by a different fuel composition. The new fuel consumption is plugged in as production requirement for the methanation plant, and afterwards the electrolyzer stacks are scaled and the final system design is made. The next steps are estimating the required 2030 gas storage capacity, determining the 2030 carbon emissions and calculating the energy efficiency of the system. Both the grid balance of 2030 and the gas production and consumption of the different system components provide input to the calculation of the of the required gas storage capacity. With the material and energy input and output of all system components the energy efficiency and carbon emissions are calculated. Afterwards, the efficiency calculation is analyzed to determine how the allocation of electricity and heat influence the efficiency of the system. A distinction is made between electrical efficiency, referring to the amount of electrical output to the input, and energy efficiency in which energy in the form of heat is also taken into account. Last, a grid balance estimate for the year 2050 is used to calculate the amount of required gas storage capacity and carbon emissions in a future where all electricity on the grid comes from renewables and the 2030 system is scaled up to balance the 2050 grid. This is also a check to see if the designed system could provide an all renewable electricity grid in terms of efficiency and storage capacity. The results are compared to a power-to-gas-to-power system with hydrogen as energy carrier. Information on the hydrogen based system comes from literature and expert knowledge.

2

Grid Analysis

2.1. Grid balance 2018

The amount of wind and solar energy sources in the Netherlands grows every day and their electricity supply could exceed the electricity demand during peak wind or sun hours in 2030. During these hours power plants are ideally switched off, otherwise they run at minimum load. To estimate the number of operating hours in the year 2030 the amount of surplus green electricity hours is estimated by creating a 2030 grid balance, only taking into account electricity from wind and sun. As a starting point an hourly balance of 2018 is made. The installed capacity wind and solar panels in 2018 and the prognoses for 2030 and 2050 are used to estimate the hourly supply of green electricity in these years respectively. The same method is used for estimating the future demand. The balance is defined as:

$$\text{Balance} = \text{Supply} - \text{Demand} \quad (2.1)$$

Via this method a possible 2030 and 2050 grid balance is calculated, assuming that the weather conditions and distributions of the demand in 2018 are the same in 2030 and 2050.

Data about the hourly Dutch electricity demand in 2018 is extracted from [14]. The hourly electricity generated from solar panels, offshore wind turbines and onshore wind turbines in 2018 is collected separately from [13]. The total supply from wind and sun for one hour is defined as:

$$\text{Supply} = \text{Solar} + \text{Offshore wind} + \text{Onshore wind} \quad (2.2)$$

Performing calculation 2.1 and 2.2 for all hours in the year 2018 and plotting all hours in a graph results in figure 2.1. It shows that in 2018 the electricity supply from wind and sun never exceeded the electricity demand.

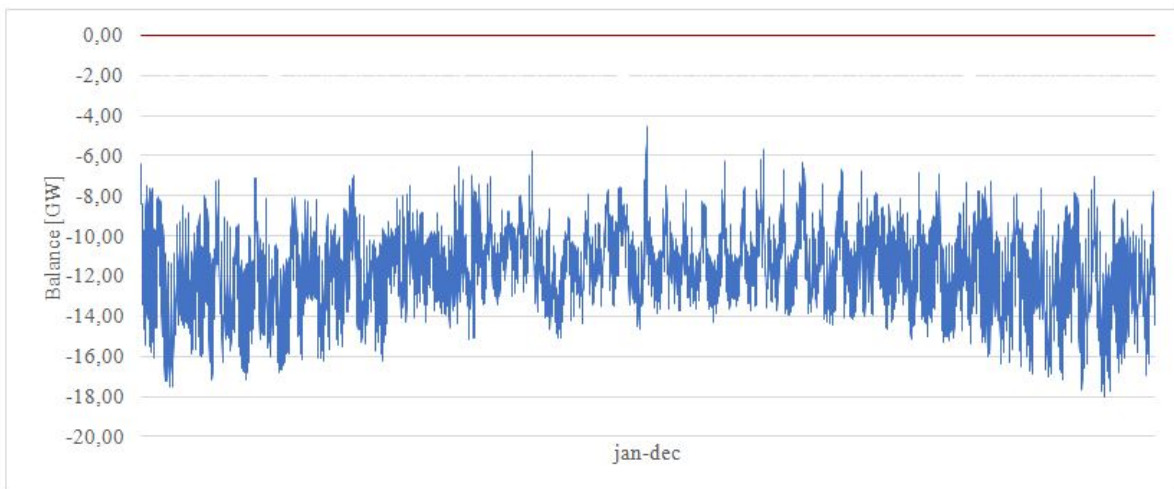


Figure 2.1: Grid balance 2018, only taking into account electrical input from wind and sun

2.2. Prognosis supply and demand

To estimate the future grid balance in the year 2030 and 2050 the installed capacity of wind turbines and solar panels is scaled up to the target years and the same goes for the electricity demand. For the year 2018, the total installed capacity solar panels, offshore wind turbines and onshore wind turbines at the end of 2017 is taken as a reference point. The extra capacity installed during the year 2018 is neglected. The amount of installed capacity is shown in table 2.1.

	Solar [GW _{peak}]	Onshore wind [GW _{peak}]	Offshore wind [GW _{peak}]
2018	2.6 [Folkerts]	0.96 [Wiki]	3.3 [RVO]
2030	22 [PBL]	13	8
2050 low	40	35	7
2050 mid	56	55	9
2050 high	75	75	11

Table 2.1: Future installed capacity renewable sources

According to the Dutch climate agreement the target installed capacity solar panels, offshore wind turbines and onshore wind turbines in 2030 is 21-23 GW_{peak}, 12-14 GW_{peak} and 6-10 GW_{peak} respectively [12]. The average of these values is taken for a 2030 prognoses.

The Dutch Planbureau voor de leefomgeving (PBL) calculated the required installed capacity of renewable sources in 2050 for 95% carbon emission reduction in the Netherlands, optimized in costs. The numbers represent a wide range which is translated in this thesis to a low, mid and high scenario (table 2.1). The low scenario represents the most pessimistic situation with the lowest installed capacity and the highest electricity demand and the high scenario represents the most optimistic situation with the highest installed capacity and lowest electricity demand. An important note to these numbers is that the PBL predicts that a 95% decrease in carbon emission by only building extra wind and solar energy sources, and without the use of carbon capture and storage (CCS, which differs from CCU) and biomass is economically unrealistic, when only technical measures are taken. Also the PBL did not design a solution for a 95% emission reduction of the Dutch electricity grid, but investigated the total emissions of the whole country in all sectors. This means these numbers do not represent an accurate amount of installed capacity of renewable sources for this research. Nevertheless to explore the feasibility of a power-to-methane-to-power system in terms of storage capacity and carbon emissions in 2050 the PBL numbers are used as a reference point.

Based on the numbers in table 2.1 the installed capacity solar panels, offshore wind turbines and onshore wind turbines will increase with a factor 8.5, 14 and 2.5 respectively in the 2030. In the 2050 low scenario the factors are 15 for solar, 37 for offshore wind and 2.2 for onshore wind. In the 2050 mid scenario the factors are 22 for solar, 57 for offshore wind and 2.8 for onshore wind. And In the 2050 high scenario the factors are 29 for solar, 78 for offshore wind and 3.4 for onshore wind.

The electricity demand in 2030 increases from 121 in 2018 to 132 TWh, corresponding to an increase of 10%, according to the Dutch Centraal Bureau voor de Statistiek (CBS) [statline.cbs.nl]. To achieve a 95% carbon emission reduction in 2050 the PBL also calculated the yearly Dutch electricity demand. According to PBL new industrial processes running on electricity are likely to play an important role in the future. Also power-to-fuel, with hydrogen production via electrolysis, plays a role in the PBL future scenario. The electricity demand in 2050 would be 250 TWh – 361 TWh, translated in this thesis to a low, mid and high scenario with an electricity demand of 250 TWh, 306 TWh and 361 TWh respectively. Based on these numbers the electricity demand in the 2050 low, mid and high scenario increases with a factor 3.0, 2.5 and 2.1 respectively. All factors are listed in table REF.

	Solar	Onshore wind	Offshore wind	Demand
2030	8.2	2.5	14	1.1
2050 low	15	2.2	37	3.0
2050 mid	22	2.8	57	2.5
2050 high	29	3.4	78	2.1

Table 2.2: Factors for supply in demand prognosis

2.3. Grid balance 2030 and 2050

With the electricity supply and demand prognoses, described in sub section 2.2, a potential grid balance for the years 2030 and 2050 is calculated. The grid balance from 2018 is used as a starting point. For the year 2030 the hourly supply of solar electricity in 2018 is multiplied by a factor 8.5 (described in subsection 2.2) to find the hourly supply in 2030. The same multiplication is done for onshore wind, offshore wind and demand, using the factors from table 2.2. With the use of equation 2.1 and 2.2 a balance is estimated for the year 2030 (figure 2.2) Via the same method the balances for the 2050 high, mid and low scenarios are estimated (figure 2.3 – 2.5).

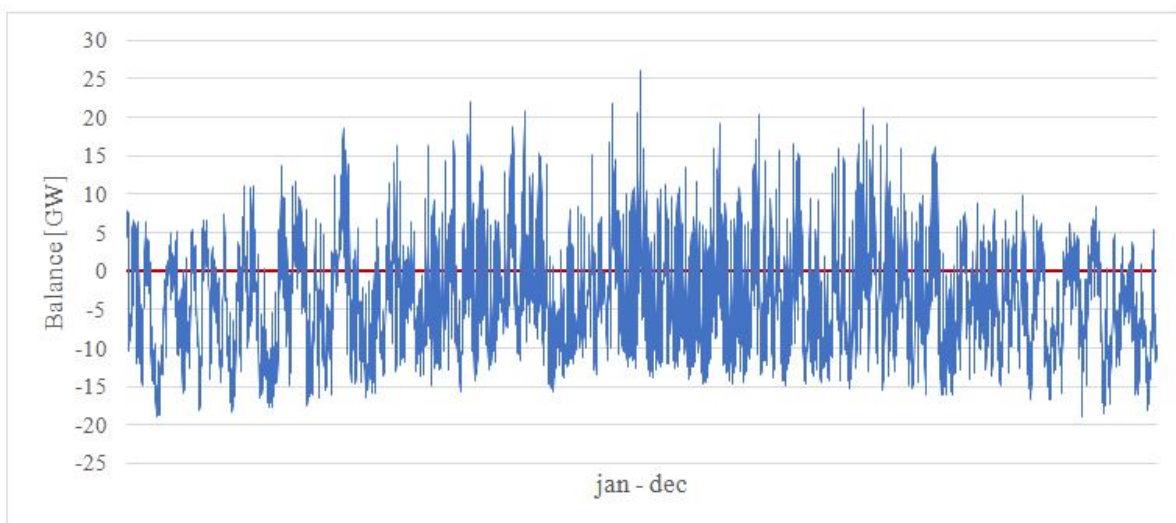


Figure 2.2: Grid balance 2030, only taking into account electrical input from wind and sun

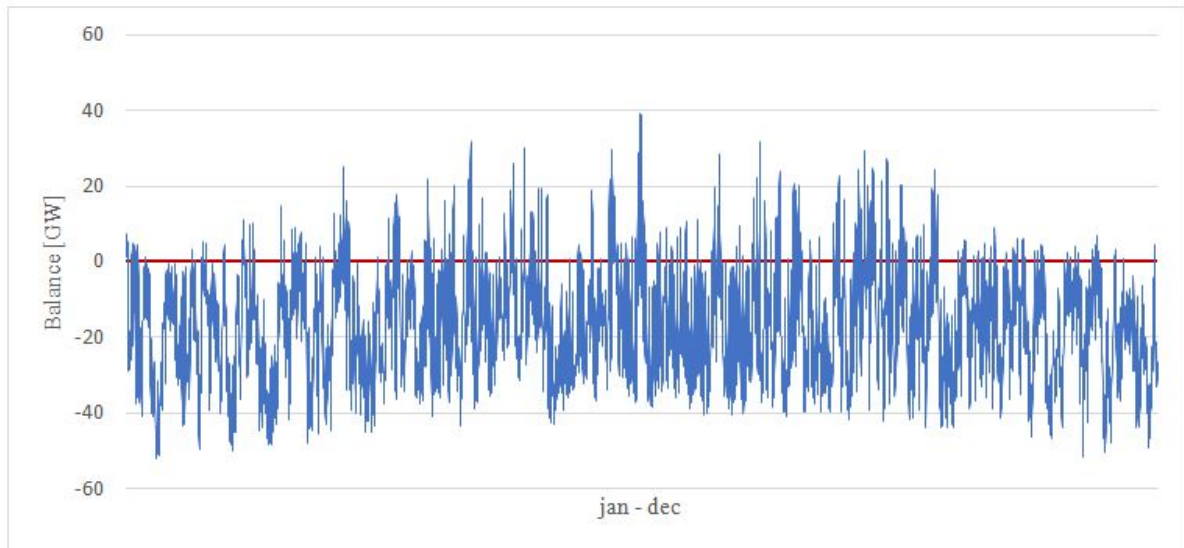


Figure 2.3: Grid balance 2050 low scenario, only taking into account electrical input from wind and sun

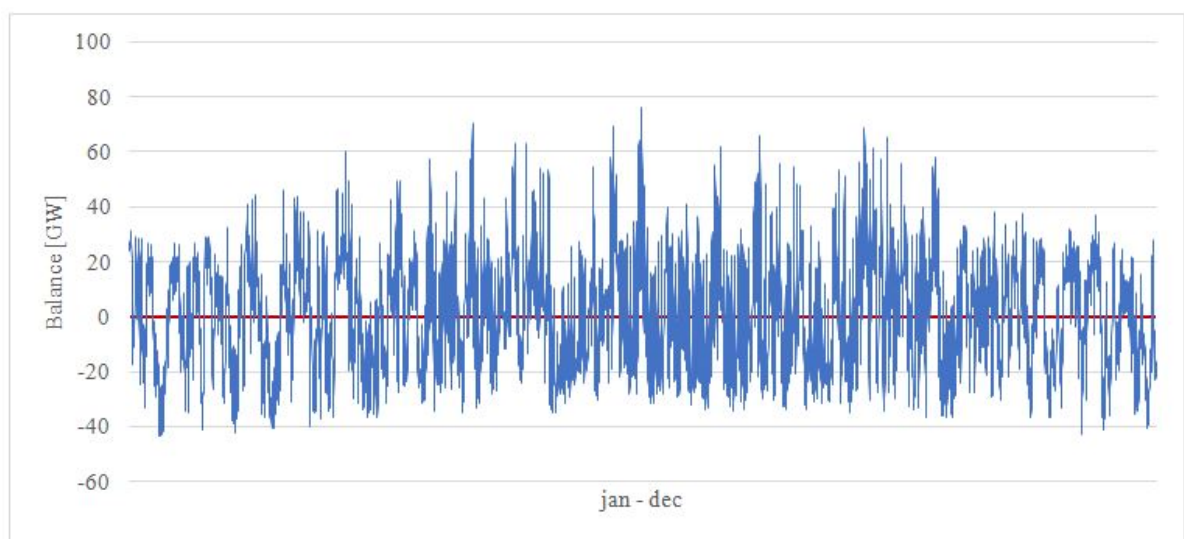


Figure 2.4: Grid balance 2050 mid scenario, only taking into account electrical input from wind and sun

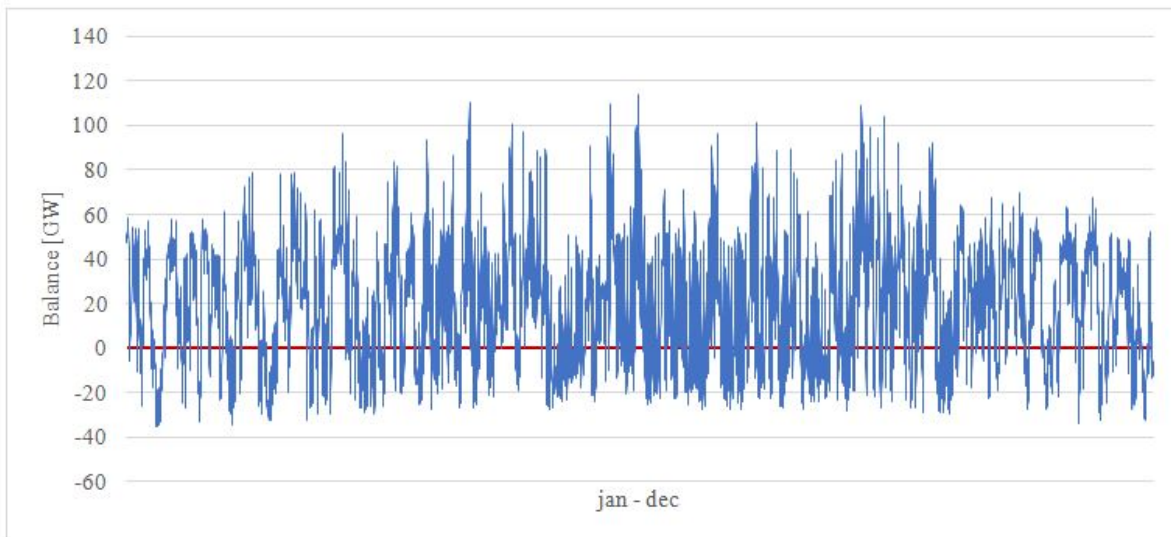


Figure 2.5: Grid balance 2050 high scenario, only taking into account electrical input from wind and sun

2.4. Surplus and deficit hours

The grid balance and the amount of deficit hours per month in 2030 and 2050 are shown in tables 2.3a - 2.3d. The total amount of deficit hours in 2030, i.e. 6131 hours, defines the number of operating hours of the oxy-fuel power plant in 2030. The total amount of deficit hours for the 2050 low, mid and high scenario's is 7634, 4286 and 2675 respectively. After modeling the oxy-fuel power plant the annual fuel production of 2030 can be calculated based on 6131 operating hours. Another interesting conclusion that can be drawn from the results in table 2.3a is that the methanation plant is best shut down during the month December. Operating 8000h per year, which is typical for a chemical plant, requires one month of shut down per year, preferably during the month with the least electricity surplus or the highest electricity deficit.

The 2050 low scenario results in the most negative grid balance and the largest amount electricity deficit hours. The scenario is the most pessimistic scenario for 2050, with the lowest installed capacity wind and solar parks and the largest increase in electricity demand. Therefore the scenario is even more disadvantageous than the 2030 scenario. The data for the 2050 scenarios are used in chapter ?? to check if the systems designed in his thesis could store enough energy to provide a 100% wind and solar electricity grid in 2050. All scenarios have to deal with electricity surplus hours (figure 2.2 - 2.5). However, all energy conversion steps of the PtMtP system come with losses so only a part of the electricity surplus can be provided back to grid after conversion and storage. The storage and conversion losses are calculated in chapters 3 – 8 and finally the round trip efficiency is calculated to find how much electricity can be provided back to the grid after conversion and storage. A side from the number of surplus and deficit hours, an important conclusion that can be drawn from figures 2.2 - 2.5 is that the positive and negative peaks in 2050 are much higher than in 2030. The largest negative peak in 2050 defines the maximum installed capacity of oxy-power plants. In the 2050 low scenario this results in 52 GW installed oxy-power plant, and in the 2050 mid and high scenario's this results in 43 GW and 35 GW respectively. In 2019 a total capacity of 22 GW of power plants was installed in the Netherlands, including coal, natural gas, biomass, blast furnace gas, waste and nuclear power plants. This means that even for the 2050 high scenario the total installed capacity of power plants has to increase by a factor 1.5. This already indicates that a combination of several energy storage systems such as batteries and smart grids could provide an interesting solution, next to power to gas. It also indicates that a decrease in energy consumption is very useful.

2.5. Conclusion on grid analysis

All grid balance scenarios have to deal with green electricity surplus and deficit hours. From the estimate of the grid balance of the years 2030 the number of operating hours of the power plant in 2030 are 6131 hours. The 2050 low, mid and high scenario results in 7634, 4286 and 2675 operating hours

2030	Balance [GWh]	Deficit hours
January	-3242	502
February	-3629	534
March	-2835	506
April	-2303	505
May	-1073	482
June	-2424	511
July	-2286	492
August	-2582	525
September	-1879	478
October	-2624	521
November	-3292	534
December	-3659	541
Total	-31828	6131

(a) 2030

2050 high	Balance [GWh]	Deficit hours
January	14843	187
February	9538	239
March	13654	232
April	13619	213
May	18690	150
June	10448	283
July	11156	276
August	10906	287
September	15344	236
October	15360	184
November	14380	182
December	12462	207
Total	160400	2676

(b) 2050 high

2050 mid	Balance [GWh]	Deficit hours
January	410	352
February	-2350	357
March	153	369
April	1066	339
May	4815	283
June	-977	411
July	-679	398
August	-821	421
September	2563	340
October	1798	324
November	667	339
December	-943	354
Total	5702	4287

(c) 2050 mid

2050 low	Balance [GWh]	Deficit hours
January	-14022	690
February	-14260	624
March	-13349	664
April	-11489	637
May	-9064	610
June	-12405	633
July	-12520	653
August	-12552	632
September	-10221	588
October	-11766	647
November	-13047	672
December	-14349	679
Total	-149044	7729

(d) 2050 low

Table 2.3: Balance and amount of deficit hours

respectively. Based on these numbers and, in the 2050 scenario, the lowest peaks, the annual fuel consumption can be calculated. The lowest peaks for the 2050 low, mid and high scenario are –52 GW, –43 GW and –35 GW respectively. This means much more power plants have to be installed than compared to the current situation. This points towards a combined solution with a PtGtP storage facility as well as other kinds of storage facilities and a reduction in energy consumption. Another finding is that the methanation plant is best shut down during the month December.

3

Electrolysis

3.1. Important parameters for electrolysis

The production of hydrogen, one of the reactants for methane synthesis, from green electricity is done via water electrolysis. This technology splits water into hydrogen and oxygen with an electrical current. The three most widely used cell types are Proton exchange membrane (PEM) cells, Alkaline cells and Solid oxide electrolysis cells (SOEC's). Co-electrolysis, in which CO_2 and H_2O are reduced in one cell to H_2 and CO , could be an interesting technology for the future. It is not evaluated in this thesis since the technology is not mature enough.

To select the most suited cell type three different technologies are compared considering:

Potential of heat integration and efficiency Carbon dioxide methanation is a highly exothermic reaction and the usage of waste increases overall system efficiency. A higher cell stack efficiency increases power-to-gas efficiency and reduces operational costs.

Pressure Pressurized methanation (at 30 bar) is preferred over low pressure methanation, which will be explained in chapter 4. This means hydrogen preferably reacts under pressure. Since compressing water is easier than compressing hydrogen it is advantageous to have electrolysis cells operate under a pressure close to 30 bar.

Process flexibility Due to a fluctuating electricity input a quick system response (in the order of minutes) and broad operating range (10-100%) are beneficial.

Maturity of the technology and scale To back-up the Dutch electricity grid with a power-to-gas system large plants are needed for efficient land use. Also the intent of this research is to design a system that could be built within 10 years. Therefore current maturity of technology and potential scale is important.

Gas purity Since electrolysis products are further processed to methane gas purity is an important parameter. Contaminants in reactant gases could cause unwanted by-products during methanation that reduce power-to-gas efficiency or damage methanation catalysts.

Efficiency A high efficiency of the cells is preferred since it reduces operational costs and installed capacity of electrolysis cells.

3.2. Alkaline cells

The anode and cathode electrodes of an alkaline electrolysis cell (AEC) are immersed in a liquid alkaline electrolyte, most commonly potassium hydroxide. A diaphragm permeable for OH^- between the two electrodes serves to separate the product gases [46]. The electrolyte typically consists of a 20-30% KOH and/or NaOH aqueous solution and nickel materials are used as electrodes. An alkali fog in the generated gas must be removed, for which desorption is typically used [10]. Alkaline cell can operate at pressures up to 30 bar [8]. Alkaline electrolysis is a mature technology, which has been applied on MW-scale since the beginning of the 20th century [8]. The operating temperature is between 60 °C

– 100 °C where water is liquid [8, 46, 47]. The voltage efficiency (HHV) is 62-82% for alkaline cells [8, 46, 47]. These numbers exclude the energy required for heating, compression and rectifying. The AEC system response is in the order of seconds and cold start-up time is <60 minutes [47, 53]. The H₂ gas purity for alkaline electrolysis is 99.5 – 99.8% [8, 10, 47].

3.3. Proton exchange membrane cells

A proton-exchange membrane (PEM) cell consists of two electrodes and a solid polymer electrolyte that is responsible for the conduction of protons, separation of product gases, and electrical insulation of the electrodes. The corrosive acidic regime provided by the proton exchange membrane requires the use of noble metal catalysts like iridium for the anode and platinum for the cathode. The cells feature a more compact module design and higher current density compared to Alkaline cells. This supports high pressure operation up to 50 bar [8]. The technology is introduced in the 1960s and nowadays commercially available. However the technology is not considered mature yet [46, 47]. The operating temperature of PEM cells described is 50 °C – 90 °C [8, 47, 53] which is approximately the same as for AEC's. The voltage efficiency (HHV) of a PEM cell is currently 60-82% [8, 47]. The system response is in the order of milliseconds and re cold start-up time is <20 minutes [47, 53], which makes these cells flexible and suited for fluctuating electricity input. The H₂ gas purity is 99.99% [8, 47, 53].

3.4. Solid oxide cells

A solid oxide electrolysis cell (SOEC) operates at high temperatures. High temperature operation results in higher voltage efficiencies than alkaline or PEM cells but implies a remarkable challenge for material stability. The feed water or steam is pre-heated in a recuperator against the hot product streams leaving the stack. Additionally, extra heating is required to account for the heat of evaporation. After electrolysis the mixture of steam and hydrogen is separated by cooling and condensing of the water. Heat integration with subsequent exothermal synthesis processes represents an interesting application. SOEC electrodes are typically made from nickel and the electrolyte is yttria stabilised zirconia. The development of solid oxide electrolysis was begun in the USA in the 1970s [8] and the German company Sunfire currently offers SOEC's at small scale, up to 150 kW stacks. The technology is not considered mature yet [46, 47]. The operating temperature of an SOEC is in the range of 650 °C-1000 °C [8, 46, 47]. Operating pressure is up to 15 bar [8]. The voltage efficiency (HHV) is <110% [47]. An important note on the voltage efficiency is that it does not take into account the energy required for steam production. The LHV efficiency including steam generation is 67-81% [8] REF SUNFIRE. The stack response is in the order of seconds [23, 39, 47] and Sunfire GmbH claims that flexible operation from 1% to 100% in 15 min is possible when the system is at operating temperature. The cold start-up time however is 1 hour. [8, 47, 51]. However different operation and insulation strategies can be applied in the SOEC-plant in order to keep the plant close to operation temperature [51]. A SOEC module has to be held at the high operating temperature to avoid the risk of thermal stress [8]. Last, the H₂ gas purity of an SOEC is 99.9% [47].

3.5. Heat integration

Luo et al performed an exergy analysis on CO₂ methanation, using green hydrogen, in which a heat integration network linked the electrolysis process and the Sabatier process [38]. The study is based on data from a computer simulation and reveals that the highest exergy efficiency for the whole process (electrolysis and methanation) is reached by using SOEC's (figure 3.1).

The methanation reactor operates at 350 °C and 23 bar. Luo et al. assumed a heat transfer effectiveness of 0.9 and a turbine and compressor efficiency of 0.8. Heat exergy that cannot be utilized is considered as lost. The inlet streams consist out of pure H₂O for the electrolysis cell and pure CO₂ is added to the Sabatier reactor. The AEC operates at 80 °C, the PEM cell at 80 °C, the LSGM-SOEC at 600 °C and the YSZ-SOEC at 800 °C. The H₂/CO₂ ratio in the reactor 2.75. This leads to a maximum exergy efficiency of 41% using AEC's, 58% using PEM cells and 70% using SOEC's. When the H₂/CO₂ ratio is increased to the stoichiometric ratio of 4, the exergy efficiency for SOEC's slightly increases to 70.5%.

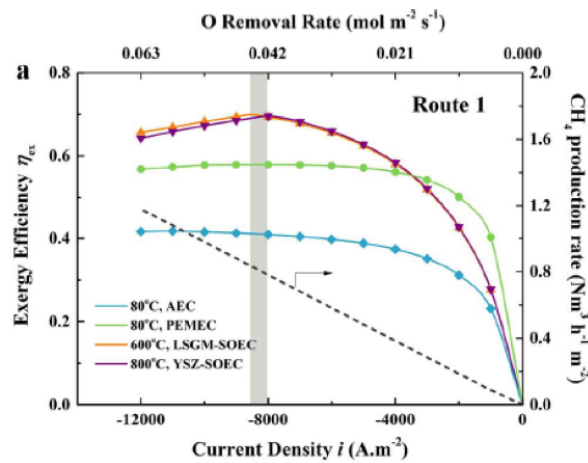


Figure 3.1: Exergy efficiency for methanation comparing different electrolysis technologies

3.6. Conclusion

	Alkaline cell	PEM cell	Solid Oxide cell
Operating temperature [C]	60-80	50-80	650-1000
Voltage efficiency _{LHV} [%]	63-71	60-68	100
System response	seconds	milliseconds	Seconds
Cold start-up time [min]	<60	<20	<60
Gas purity [%]	>99.5	99.99	99.9
Maturity	Mature	Commercial	Commercial

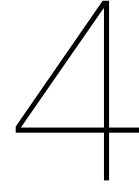
Table 3.1: Parameters of different cell types

In table 3.1 the parameters from sub section 3.1 are listed for alkaline, PEM and solid oxide cells. Luo et al showed that the highest overall efficiency of a power-to-methane system can be reached with SOEC's because of their heat integration potential [39].

	Alkaline	PEM	SOEC
Maturity	+	+	+
Pressure	+	+	+
System response	+	+	+
Start-up time	-	+	-
Heat integration	-	-	+
Efficiency	-	-	+
Gas purity	+	+	+

Table 3.2: Parameters of different electrolysis technologies

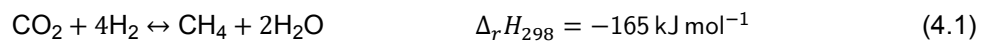
Table 3.2 shows the score of different cell types considering the important electrolysis parameters. After comparing three different cell types SOEC is the preferred one. Although slow start-up time is going to be challenging. PEM cells, due to their high flexibility, could be particularly interesting in power-to-fuel systems that do not have much excess heat.



Methanation

4.1. Important parameters for methanation

Methanation of carbon dioxide and hydrogen occurs via the chemical reaction:



Three possible processes for methanation are 'catalytical methanation', 'electrochemical methanation' and 'biochemical' methanation. To find the most suitable technology for this system a comparison is made concerning:

Gas hourly space velocity (GHSV) in h^{-1} This is the volumetric flow rate of the gas flow per m³ of reactor volume. A high GHSV required less reactor volume and thus lower investment costs.

Potential of heat integration and efficiency Reaction 4.1 is a highly exothermic and waste heat can be used to produce steam for the SOEC's and increase overall system efficiency.

Process flexibility Due to a fluctuating electricity input a quick system response (order of minutes) and broad operating range (10% - 100%) are beneficial.

Maturity of the technology and scale To back-up the Dutch electricity grid with a power-to-gas system large plants are preferred over small plants considering efficiency usage of space. The intent of this research is to design a system that could be built within 10 years. Therefore current maturity of technology is important

4.2. Catalytic methanation

In catalytic methanation CO_2 and H_2 react to CH_4 in a reactor vessel with the presence of a catalyst. Well known catalysts are Ni and Ru based catalysts. Supported Ni catalyst are the most promising catalysts for methanation due to their good catalytic performance and relatively low price [48]. Hydrogen and carbon dioxide react under stoichiometric condition under a pressure of 1-30 bar and within a temperature range of 300 °C – 700 °C, mostly in fixed bed reactors [21, 30, 31, 38, 41, 42]. Catalytic methanation is the most mature technology of all three [28] and has excellent heat integration potential [20, 27–29, 38]. Catalytic methanation in fixed bed reactors with SOEC heat integration has been widely investigated and tested at pilot scale with promising results of 76% PtG efficiency (HHV), [20, 29, 30]. The technology is suited for large scale operation, [27]. A disadvantage of the process is its poor flexibility. The operation range is between 40-100% meaning that during deficit hours the methanation plant still has to run at 40%. Shut down is very costly and the plant has a long start-up time, [27, 28]. Biegger et al. [5] reports about a new honeycomb catalyst used in a multi bed methanation reactor which increases the process flexibility to 12,5% minimum load. The honeycomb catalyst is in its early development stage and are not used on commercial scale for methanation plants. An alternative for fixed bed reactors is three-phase methanation in which solid catalyst powder is suspended in a temperature stable inert liquid. The reaction occurs in a three phase fluidized bed reactor. Three-phase

methanation can run at a minimum of 10-20% load which increases system flexibility. This technology also enables good heat control of the reaction and more effective heat removal. However using a liquid limits mass transfer and reduces reaction rate and CO₂ conversion to 82% compared to 97% in fixed bed methanation [28, 36]. A lower reaction rate requires a more complex plant with gas recycle streams and separation of reactant gases and product gas resulting in higher costs. Without these measures a lower CO₂ conversion results in a larger reactant stream and higher CO₂ emissions, since CO₂ will end up purge streams.

4.3. Electrochemical methanation

As described in section 3.1, producing CH₄ by co-electrolysis of CO₂ and H₂ in an electrochemical cell is called electrochemical methanation. The process is able to run at ambient temperature and pressure which gives electrochemical methanation the potential to be highly flexible and very efficient. However, no electrode catalysts have been developed that can perform the reaction with a low overpotential at reasonable current densities [Peterson]. Therefore currently electrochemical methanation from CO₂ and H₂O is only realized at lab scale with electrical efficiencies of 63% [35]

4.4. Biochemical methanation

In biochemical methanation microorganisms serve as a biocatalysts, converting the hydrogen and carbon dioxide into methane. This is only an option for small scale plants since large reactors are needed due to the low gas hourly space velocity (GHSV). Also the process runs at low temperature which makes the process not suited for SOEC heat integration. An advantage is that the technology is most flexible of all three and load change is a non-issue for biological methanation. Although the process was discovered on 1906, the technical implementation is still an issue [27].

4.5. Conclusion

	Methanation method		
	Catalytic	Electrochemical	Biochemical
GHSV	+	+	-
Process flexibility	-	+	+
Heat integration and efficiency	+	+	-
Maturity	+	-	-

Table 4.1: Comparison of different methanation technologies

Table 4.1 shows the score of different methanation methods considering the important methanation parameters. Although being a highly flexible process the GHSV, heat integration potential and maturity make biochemical methanation not the preferred option. Electrochemical methanation has great potential but the process is only done on lab scale and overpotential is still a problem. This results in a lower electrical efficiency than catalytic methanation with heat integration. Catalytic methanation performs well considering GHSV, heat integration potential and maturity and scale. The flexibility of the process is going to be a challenge in further system design.

4.6. Methanation process conditions for PtGtP system

In catalytic methanation, low reactor temperature enhances a favorable chemical equilibrium (figure 4.1). However, cooling fixed bed methanation reactors is a challenge due to the high exothermic reaction and all components being in gas phase. Methanation in two or more fixed bed reactors in series, with a decreasing temperature from the first reactor to the last, gives an acceptable yield [30, 50]. Intermittent water removal between reactors shifts the equilibrium in towards methane and each following reactor is able to operate at a lower temperature since less heat is dissipated due to a decrease in percentage of reactants (and an increase in percentage of products). A plant with fixed bed reactors in series functions with easy gas separation steps in tanks to achieve a CH₄ gas purity of 97% [30, 50]. Typical process conditions for catalytic methanation in fixed bed reactors are listed in table 4.2. The

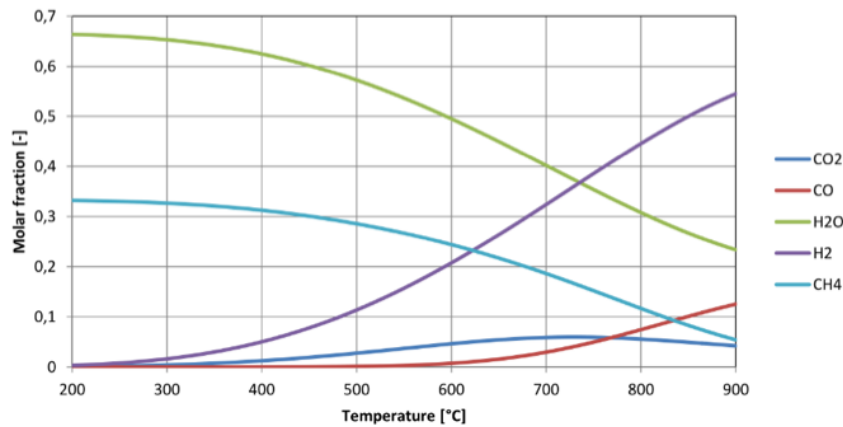


Figure 4.1: Equilibrium concentration of a H₂/CO₂ = 4 mixture at 30 bar, taken from [30]

temperature of the first reactors is typically around 700 °C and the temperature of the following reactors can be cooled down to 200 °C-300 °C when using a four reactor in series system [50]. A higher pressure requires more compressor work but also a more favorable equilibrium (figure 4.1). Since carbon reactants come from pressurized storage facilities high pressure methanation operation is chosen. Currently, SOEC's can operate under 10 bar [25] and operating pressure up to 15 bar is considered achievable, as discussed in section 3.4. This means hydrogen compression from 10 – 30 bar, or 15 – 30 bar is necessary for pressurized methanation in the PtMtP system.

Operating temperature	350 – 700 C
Operating pressure	0 – 30 bar
Catalyst	Nickel or Ruthenium based
H ₂ :CO ₂	4:1
Reactor	Fixed bed reactor, several reactors in series

Table 4.2: Typical process conditions for catalytical methanation in fixed bed reactors

4.7. Methanation flexibility

It is assumed that the methanation plant minimum load is 40% and that the plant cannot be shut down for a couple of hours or days due to long and expensive start-up procedure. Most chemical processes are not optimized for a high flexibility since, in the fossil era, it was economically more feasible to run a chemical plant at full load as much as possible. However, for a load following chemical process, as designed in this thesis, a flexible process is desired. Since the global aim is to limit the use of fossil fuels to a minimum, it is likely that more flexible load following power to gas processes are being built in the future and the need for flexible chemical processes will grow. Also, nowadays electricity prices are more and more fluctuating due to the growing amount of renewable energy sources. It is expected that these fluctuations become more extreme in the future. Therefore it could be economically more feasible to run chemical plants at low load or to shut them down during expensive electricity hours. This enhances the demand for chemical processes with a better flexibility. As described in section 4.2 a process flexibility of 12,5% minimum load in a multi bed methanation reactor is reported [5]. Therefore a methanation plant flexibility of 40% is assumed for now and the effect of highly flexible methanation plant is investigated in chapter 8.

5

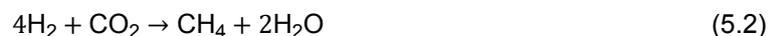
Oxy-fuel power generation

5.1. Important parameters

Oxy-fuel combustion is the combustion of fuel, in this case methane, with pure oxygen. Particulates and SO₂ can be removed by conventional electrostatic precipitator and flue gas desulphurization methods, respectively [37]. But if the streams in the total power-to-methane-to-power system are kept pure and exclusively for this system there should be no contaminants in the gases. Oxygen is a by-product from electrolysis and stoichiometrically exactly enough oxygen is produced to burn the produced amount of CH₄ in the PtMtP system (equation 5.1, 5.2 and 5.3). The chemical reaction in the electrolysis step is



where 4 moles of water produce 4 moles of hydrogen. The latter is further processed in the methanation step according to the reaction



where 4 moles of hydrogen react with 1 mole of CO₂ to 1 mole of methane and water as a side product. Eventually methane reacts with oxygen according to the reaction



where 1 mole of methane produced in the methanation step is combusted with 2 moles of oxygen produced in the electrolysis step. Like electrolysis and methanation, oxy-fuel combustion happens approximately stoichiometrically [49]. In reality the system creates some excess oxygen due to the fact that for every 4 moles of hydrogen produced, two moles of oxygen are always produced but for every 4 moles of hydrogen that react during methanation, a little less than 1 mole CH₄ is produced.

Unlike regular gas power plants the working fluid in oxy-fuel power plants does not mainly consist out of air, but out of a steam and CO₂ mixture, depending on the cycle. Oxy-fuel cycles for gas turbines can be divided into 2 groups, distinguished by the recycled substance to moderate the temperature in the process (the working fluid): CO₂ cycles and H₂O cycles. This has strong effect on the cycle performance and on the components needed in the cycle [49].

CO₂ cycle Exhaust gas from the heat recycle steam generator (HRSG) is cooled and partly recycled to the gas turbine for to cool the equipment. Due to the cooling, most of the water is condensed and thus the recycle stream consists mainly of CO₂. To retain the turbine inlet temperature of air-blown gas turbines recycle ratios of approx. 90% are necessary while the remaining flue gas can be further processed for storage [49].

H₂O cycle Water-based cycles use the condensed water of the exhaust gas instead of the CO₂ for the cooling of the combustion cycle. Temperature is controlled by evaporating liquid water injected to the combustor which generates a working fluid that consists by volume of approx. 90% steam and 10% CO₂ [49].

Some of the leading oxy-GT cycles are: Semi-closed Oxy-combustion Combined Cycle (SCOC-CC), Allam cycle, CES cycle, S-Graz cycle [49]. To find the most suited technology for this system a comparison is made concerning:

Potential scale To provide enough electricity to the Dutch grid, a large installed capacity of power plants is needed. For most efficiency use of space, it is preferred to have several large plants i.e. ~300 MW, instead of a lot of small plants.

Efficiency An efficiency comparable to that of a NGCC power plant ($57\%_{LHV}$) is desired, higher efficiencies are even better. A decrease in power plant efficiency increases electrolysis and methanation plant capacity and gas storage capacity.

Maturity The intent of this research is to design a system that could be built within 10 years. Therefore current maturity of technology is important.

5.2. Different cycles

5.2.1. SCOC-CC

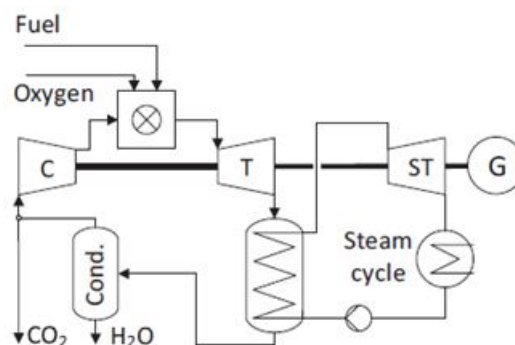


Figure 5.1: Schematic flow sheet of the SCOC-CC

The only differences between an SCOC-CC (figure 5.1) and an NGCC are the pressurized oxygen stream to the combustor and the recycle with condenser going back to the compressor instead of air [49]. The SCOC-CC is a CO_2 based cycle and oxygen is added at near stoichiometric conditions [49]. The cycle has an electrical efficiency of $61.45\%_{LHV}$, without an air separations unit (ASU) and the potential scale of the cycle is ~400 MW [11]. At the moment the technology is developed up to the level of thermodynamic analysis but there are no pilot plants yet [11]. High pressure ratios of the turbines and the different working fluid require the design of new gas turbine components and a redesign of gas turbine burners is necessary to achieve stable combustion for oxyfuel conditions [49]. The high pressure combustor for hydrocarbon fuels in a CO_2/O_2 environment is the most critical part regarding technical maturity. The compressor (C) and turbine (T) for the gas turbine are also challenging whereas the heat recovery steam generator (HRSG), the steam turbine (ST), and the recycle condenser (Cond.) are considered as technically mature [7]. Besides the oxy-fuel gas turbine that needs to be newly designed the other components of the process are considered generally as state-of-the art. The HRSG and other components of the bottoming water steam cycle are standard technology, but some differences in the fluid properties of the exhaust gas need to be considered [49].

5.2.2. Allam cycle

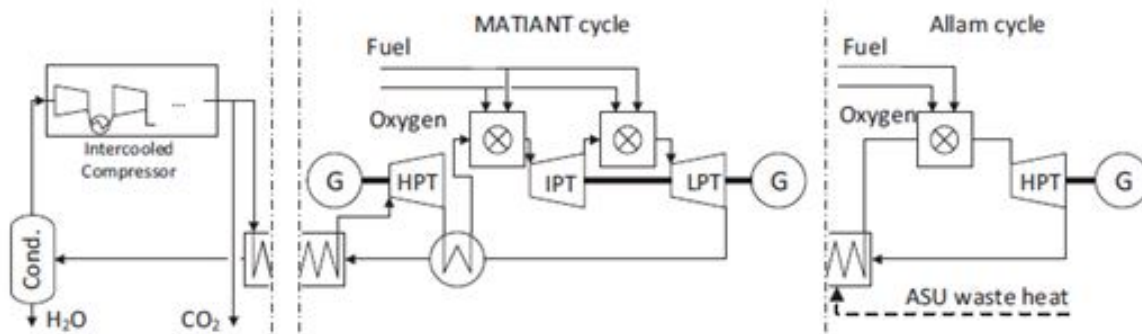


Figure 5.2: Schematic flow sheet of the Allam cycle

The Allam cycle is a semi-closed CO_2 cycles without a bottoming steam cycle (figure 5.2). Instead of using a bottoming cycle an internal recuperator heats the compressed working fluid by cooling the turbine exhaust [49]. The Allam cycle waste heat from the ASU serves as additional heat input to the recuperator. However, in the PtMtP system in this thesis there is no need for an ASU to produce oxygen as this is a by-product from electrolysis. The electrical efficiency of the Allam cycle is $59\%_{\text{LHV}}$, including the energy consumption for air separation [1]. Numbers on efficiency without ASU power consumption were not found but are likely to be slightly higher. The potential scale of the plant is ~ 250 MW [11]. The maturity of the technology is at pilot plant level [11, 45] but detailed and objective research on the process is scarce [49].

5.2.3. CES cycle

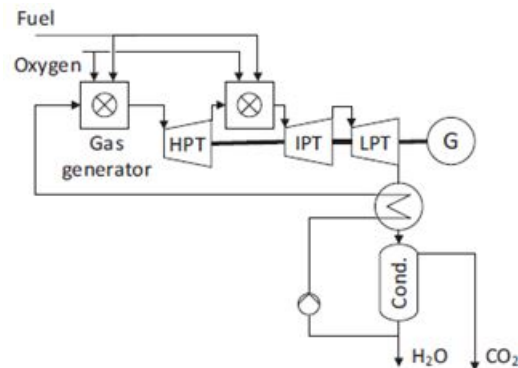


Figure 5.3: Schematic flow sheet of the CES cycle

The CES cycle is based on an internal combustion Rankine cycle [49] and is shown in figure 5.3. The gas generator, i.e. the main combustor, burns natural gas with oxygen and liquid water is injected to moderate the temperature. Due to the evaporation of the water, the working fluid consists approx. 90% of steam and 10% CO_2 . The electrical efficiency of the cycle is around $52\%_{\text{LHV}}$, without energy for air separation [49]. The potential scale of is ~ 400 MW [11] and the technology is developed up to pilot plant scale. From all 4 cycles discussed in this thesis it is the most mature one and no major technological breakthrough is required [17]. HP and LP turbine are considered as a conventional or advanced technology steam turbine. Because of the high outlet temperature of the reheat combustor, the IP turbine is significantly different to a steam turbine but comparable to a gas turbine with advanced materials and cooling technology [4]. Due to higher corrosion rates in CO_2 /steam environments uncoated alloys show a reduction in strain life behavior. In contrast, only minor effects are observed on coated alloys [4].

5.2.4. S-Graz cycle

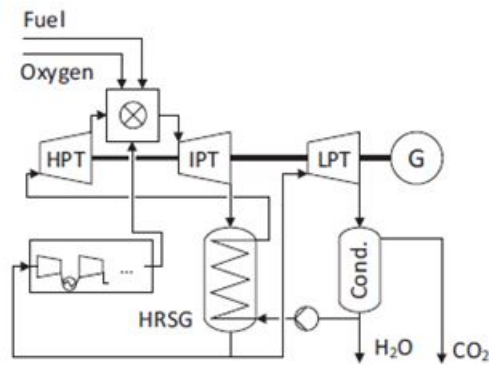


Figure 5.4: Schematic flow sheet of the S-Graz cycle

The S-Graz cycle is shown in figure 5.4. It has two recycle streams to the combustor: one of the recycle streams is pure steam and the other consists out of CO₂ and steam. The steam rich exhaust gas is expanded to approx. atmospheric pressure in the IP turbine (IPT) and cooled in an HRSG. Around 45% of the HRSG outlet stream is further expanded in an LP turbine (LPT) to vacuum conditions where the water is condensed. The water is used as feed water for the HRSG. The steam from the HRSG is expanded in a conventional HP steam turbine (HPT) to the combustor pressure and then used for cooling purposes. The remaining 55% of the working fluid that do not pass the LP turbine are compressed with intercooling and recycled to the combustion chamber [49]. The efficiency of the S-Graz cycle is 64% without an ASU [15] and the potential scale is 82.75 MW Its maturity is at the level of thermodynamic analysis [11]. Two recycle streams cause higher operational challenges than for the other cycles. The combustor technology requires a technological breakthrough whereas the turbines are comparably mature except for the high temperature turbine [17].

5.3. Conclusion

Table 5.1 shows the comparison of the technologies discussed in section 5.2. Both the Allam cycle and the CES cycle score well on all parameters. Since there is only little detailed and objective research available on the Allam cycle, the CES cycle is modeled in this thesis.

Oxy-fuel power cycle				
	SCOC	Allam	CES	S-Graz
Scale	+	+	+	-
Efficiency	+	+	+	+
Maturity	-	+	+	-

Table 5.1: Comparison of different oxy-fuel power cycles

5.4. Oxy-fuel power plant process conditions for PtMtP system

As described in subsection 5.2.3 the CES cycle is based on an internal combustion Rankine cycle. The gas generator, i.e. the main combustor, burns natural gas with oxygen and liquid water is injected to moderate the temperature. The working fluid is then expanded in a steam turbine like HP turbine (HPT). After the expansion to an intermediate pressure the working fluid is reheated by an additional combustion of fuel with oxygen. Through the IP turbine (IPT) and the LP turbine (LPT) the steam mixture is expanded to vacuum condenser pressure. The condenser separates CO₂ and water at vacuum conditions. The liquid water is then recycled to the gas generator. The water is preheated by the LP turbine exhaust gas. The HP steam is approximately 80–105 bar and 600 °C – 900 °C. The IP inlet temperature is in the range of 1200 °C – 1500 °C and the condenser pressure between 0.05 and 0.15 bar [49]. A higher condenser pressure leads to a higher CO₂ purity after the condenser and lower

CO₂ compression power but still an overall reduced efficiency [18]. Oxygen pressure at gas generator inlet could be up to 100 bar [49]. The oxygen and CH₄ inlet flows are modelled to be at 15 bar. Much CO₂ compression energy is needed because the CO₂ is extracted from the vacuum condenser. Due to the low condenser pressure, the water content of approx. 40% in the CO₂ has to be reduced by intercooled compression with condensation [16]. The CES cycle is modeled as an oxy-fuel combined heat and power cycle (OF-CHP). Waste heat is extracted from the plant as much as possible to use for heating purposes as district heating or greenhouse heating. The minimum load of the OF-CHP is assumed to be the same as that of a NGCC, i.e. 20% [26]. However, this minimum load is not used in the model in this thesis as shutting down and starting up a power plant is less costly and time consuming than chemical plants. It is assumed that the OF-CHP is shut down during green electricity deficit hours. In reality, whether the power plant is shut down or not is an economic consideration. Keeping the power plant in operating during surplus hours can be costly due to low or even negative electricity prices. On the other hand, shutting the plant down means that the plant has to be start up again as some point, which brings extra costs. When the operational costs during surplus hours exceed the start-up costs, the plant is shut down. This economic consideration is neglected in this research and it is assumed that the plant is always shut down during surplus hours. The process conditions are taken from [6] and are listed in table 5.2

Inlet pressure HPT	85 bar
Inlet pressure IPT	8.47 bar
Inlet pressure LPT 2	3 bar
Condenser pressure	0.26 bar

Table 5.2: Equipment specifications of oxy-fuel combined heat and power cycle in PtMtP system

6

Gas Storage and Transport

Gas can be stored underground at high pressure or above ground (i.e. in tanks) either under high pressure or liquified. Liquified gas has the advantage of being much more compact than compressed gas resulting in smaller storage tanks and less space requirements. However liquifying gas consumes more energy than compressing gas. Because of their large capacities and low cost, underground compressed gas systems are generally most suitable for large quantities and/or long storage times. Four types of underground solutions can be distinguished: depleted oil or gas fields, aquifers, excavated rock caverns and salt caverns [33]. Underground storage is reported to be the cheapest solution for storage of large quantities of gas, up to two orders of magnitude less expensive than other methods]. An abandoned natural gas well was reported to be the least expensive [33]. The operating costs for underground storage are limited to the energy and maintenance costs related to compressing the gas into underground storage and possibly boosting the pressure coming back out [2]. The drop in pressure due to the reduction of the hydraulic head along the pipeline is compensated by adding recompression stations. Larger diameter pipelines allow lower flow rates with smaller pressure drop and therefore a reduced number of recompression stations. However larger pipelines are more expensive. Both temporary gas storage buffers and pipeline networks and hubs can be useful ways to control the flow in a pipeline or set of pipelines to minimize compositional and/or mass flow rate variations. The supply of gas with a power-to-methane-to-power system fluctuates both on a short-term (minute-to-minute) and a longer-term (seasonal) basis. The impact of a varying mass flow rate on pipeline and storage operation is not fully understood in terms of either operability or infrastructure robustness [34].

6.1. Carbon dioxide storage and transport

During green electricity deficit hours, CO₂ is produced at the oxy-power plant. The gas is stored until peak hours occur, in which it is used as a reactant for methane production. Since methanation shut down and start up is a very costly, slow and energy intensive process the methanation plant runs at 40% during deficit hours. In these hours the CO₂ produced by the oxy-power plant could be directly transported to the methanation plant so that energy for storage (i.e. compression and transport) can be saved. The oxy-power plants is more flexible and during peak green electricity hours it is shut down or operates at a minimum load of 20%, depending on the duration and high of the peak.

The Dutch research institute TNO investigated the potential of underground gas storage in the Netherlands and concluded CO₂ could be stored in depleted gas fields [24]. This only concerns permanent CO₂ storage. As salt caverns are suited for temporary storage and buffering of natural gas and other industrial gases [43] it is assumed that these caverns are also suited for temporary CO₂ storage. Depleted gas fields have a pressure range of 100 – 200 bar where the temperature varies between 80 – 140 °C. In salt caverns the pressure varies between 80 – 180 bar. The dept of the caverns is between 500 – 1500 m [24] and with a temperature increase of 1.6 °C per 100 meters the temperature in the caverns will be between 8 – 24 °C above surface temperature. For Dutch salt caverns a surface temperature of 15 °C is taken, resulting in a cavern temperature between 23 – 39 °C.

Storage technology	Gas fields	Oil fields	Aquifers	Salt caverns	Mine aisles
Natural gas storage	Yes	No	Maybe	Yes	No
Hydrogen storage	Yes	No	Maybe	Yes	No
CO ₂ storage	Yes	No	Maybe	No	No
Compressed air storage	Maybe	No	Maybe	Yes	No
HTO	No	No	Yes	No	Maybe

Table 6.1: Underground gas storage potential in the Netherlands for different gases taken from [24]

TNO and the Dutch company Gasunie found potential underground storage space on land and at sea. The effective underground CO₂ storage capacity is 1678 Mt in 104 fields. At land an effective capacity of 1060 Mt in 54 fields was found. [24]

Pipelines are considered to be the most viable method for onshore transport of high volume of CO₂. Pipelines are also the most efficient way for CO₂ transport when the source of CO₂ is a power plant which lifetime is longer than 23 years. For shorter period road and rail tankers are more competitive. Super-critical is the preferred state for CO₂ transported by pipelines, which implies that the pipelines operative temperature and pressure should be maintained within the CO₂ supercritical envelop. The typical range of pressure and temperature for a CO₂ pipeline is between 85 and 150 bar, and between 13 °C and 44 °C to ensure a stable single-phase flow through the pipeline. Impurities in the CO₂ stream represent a serious issue because their presence can change the boundaries of the pressure and temperature envelope within which a single-phase flow is stable. Moreover, the presence of water concentration above 50 ppm may lead to the formation of carbonic acid inside the pipeline and cause corrosion problems [37].

6.2. Methane storage and transport

During green electricity surplus hours, methane is produced in the Methanation plant. The gas is stored until deficit hours occur during which it is burned in the oxy-power plant. Since methanation shut down and start up is a very costly, slow and energy intensive process the methanation plant runs at 40 % during deficit hours. In these hours the produced methane could be directly transported to the oxy-power plant so that energy for storage (i.e. compression and transport) can be saved. According to TNO both gas fields and salt caverns are suited for natural gas storage in the Netherlands. However Dutch natural gas has a different composition < 0.02 % H₂ than the gas produced in this research, it is assumed that the latter can be stored the same way as Dutch natural gas. The potential storage capacity for underground natural gas storage in empty gas fields is 109 billion Nm³ onshore and 79 billion Nm³ offshore. Pressure and temperature range are the same as for CO₂ storage in depleted gas fields. The potential storage capacity for natural gas in salt caverns is 17 billion m³, all onshore. The storage pressure varies between 50 – 180 bar. Transportation of methane is possible in the form of compressed or liquified gas through pipes or liquified gas transported with trucks. It is assumed that, as with CO₂, pipelines are the most viable method for large amounts of onshore transport, with a system lifetime of over 23 years. In the Netherlands natural gas is currently transported via the natural gas grid at a temperature of 5 – 30 °C and a pressure of 45 – 70 bar bar [52].

6.3. Oxygen storage and transport

Oxygen is produced at the electrolysis stacks during green electricity surplus hours and stored until deficit hours. During deficit hours it is burned with methane for power generation. The electrolysis stacks are shut down during green electricity deficit hours, where the oxy-power plant is less flexible. Depending on the duration and the high of a green electricity surplus peak the power plant is either shut down or runs at minimum load. During minimum load oxygen could directly be transported from the electrolysis stacks to the power plant to save energy needed for storage. No literature was found on the underground storage of oxygen. The state of the art of oxygen storage is in liquid form in tanks. Production of pure oxygen usually happens in an ASU which provides oxygen in liquid form. Underground storage of compressed air however is investigated and for this research it is assumed that the opportunities and limitations of compressed air storage also hold for compressed oxygen storage. Nevertheless, this is not proven and more research to underground oxygen storage needs to be done.

According to TNO salt caverns are suited for storing compressed air. Compressed air has a lower storage efficiency than compressing and storing a fuel gas like natural gas or hydrogen. TNO reports compressed air should be stored under lowest possible pressure to achieve a reasonable storage efficiency. Low pressure storage cannot take place at high depths and therefore not all salt caverns suited for compressed air storage. For the power-to-methane-to-power system is this research a lot of gas needs to be stored, decreasing the round trip efficiency. A low pressure storage facility could be an interesting solution for a reasonable storage efficiency. The potential storage capacity of low depth salt caverns in the Netherlands is $16 \times 10^9 \text{ Nm}^3$, all onshore. This almost equals the total amount of salt caverns storage capacity of $17 \times 10^9 \text{ Nm}^3$, meaning only a couple of caverns are located at high depth. The pressure of the low depth caverns varies between 70 – 100 bar with a minimum pressure of 50 – 80 bar.

6.4. Hydrogen storage and transport

Hydrogen is produced during green electricity surplus hours and ideally all hydrogen is directly converted to methane. Due to flexibility limitations of the methanation plant, extra hydrogen needs to be produced during peak hours to supply to the methanation plant with hydrogen during deficit hour (i.e. when the methanation plant runs at minimum load). Therefore a hydrogen storage facility is required. Large amounts of hydrogen are most suited to be stored undergrounds, where small hydrogen buffers could also be stored and transported in tanks as high pressure gas or in liquid form. TNO reports that hydrogen could be stored in salt caverns and depleted gas fields 6.1. In their research they found that the caverns and fields suited for natural gas could also be used for hydrogen. However the operational volume for hydrogen is only 85 % of the volume for natural gas due to fact that on Nm^3 of hydrogen occupies a larger volume than natural gas at 100 - 200 bar and 80 - 140 °C. This results in a potential storage capacity of 93 Nm^3 onshore and 60 Nm^3 offshore in depleted gas fields and $14 \times 10^9 \text{ Nm}^3$ in salt caverns [24] Hydrogen storage in tanks carried out between 350 – 700 or in liquid form. Hydrogen storage requires more compression energy and therefore operational costs will rise. When storing gases in empty gas fields or salt caverns special infrastructure needs to be build which causes an increase in capital costs. Underground hydrogen storage will only be feasible when large amounts has to be stored. The required hydrogen storage capacity is calculated in section 8.3. Transportation of hydrogen is possible in the form of compressed gas through pipes or liquified gas transported with trucks. It is assumed that, as with CO_2 , pipelines are the most viable method for large amounts of onshore transport, with a system lifetime of over 23 years.

6.5. Conclusion on storage and transport

All gases are stored in underground caverns. According to TNO caverns are not suited for CO_2 , however TNO only considered the long term storage of CO_2 . It is assumed that temporary storage of CO_2 can take place in salt caverns. Large scale oxygen gas storage is a field with only little expertise. Since compressed air can be stored in underground caverns, it is assumed that caverns are also suited for CO_2 storage. The most suitable storage conditions in terms of energy efficiency is at low pressure, therefore gases are storage in low pressure caverns at 80 bar. The average temperature in these caverns is 31 °C. It is assumed that both the power-to-gas installation and the methane-to-power installation are located near the storage facility and that gas transport losses can be neglected.

7

Modeling

7.1. Oxy-fuel power plant

The CES cycle is modelled in Cycle Tempo as a 44 MW oxy-fuel combined cycle (OFCC) to check electrical efficiencies found in literature and to find the amount of energy available for district heating (heat efficiency). Heat for district heating is extracted in the form of hot water. With a power output of 44 MW, the modelled plant is a factor 10 smaller than an existing gas power plant in the Netherlands, owned by Vattenfall. Gas with a composition from table 7.2, a temperature of 20.0 °C and a pressure of 15.0 bar leaves fuel source 100 with a mass flow of 1.63 kg s⁻¹. The fuel composition matches the Aspen model gas product described in the next sub section.

Component	Vol%
CH ₄	95.30 %
H ₂	4.20 %
H ₂ O	0.30 %
CO ₂	0.20 %

Table 7.1: Fuel composition of OFCC model

The fuel is transported through pipe 101 to compressor 101 where part of the fuel gas is compressed to 85.0 bar and a part is expanded to 8.47 bar. The model subtracts the energy released during fuel expansion from energy required for compression. The compressed fuel is fed to combustion chamber 103 and the expanded fuel is fed to combustion chamber 121. Oxygen at 15.0 bar and 20.0 °C leaves oxygen source 131 with a mass flow of 6.56 kg s⁻¹. In compressor 133 part of the oxygen is compressed to 84.5 bar and fed to combustion chamber 103. The left over oxygen stream is expanded to 8.47 bar and fed to combustion chamber 121. In node 134 pressurized oxygen is mixed with liquid water with a pressure of 84.5 bar and a temperature of 299 °C. In node 135 expanded oxygen is mixed with liquid water with a pressure of 8.47 bar and a temperature of 173 °C. Liquid water is evaporated in the combustion chambers. This is modelled as a combustion chamber and a heat exchanger (103 + 115 and 121 + 106) where CH₄ is combusted with oxygen in the combustion chambers and water is converted into steam in the heat exchangers.

After combustion the high pressure water vapour and CO₂ mixture in pipe 106 is expanded in high pressure turbine (HPT) 105 to a pressure of 8.47 bar. The fluid is reheated in heat exchanger 106 and expanded in intermediate pressure turbine (IPT) 108 to 3 bar. The working fluid consist now of 91 % H₂O and 9 % CO₂ which strikes with literature [49]. After the IPT the fluid is expanded again to 0.26 bar in low pressure turbine (LPT) 109. The turbine inlet temperatures are listed in table 7.2. They are all in the temperature range described in section 5.4.

Heat exchanger 113 cools the stream down after which it is further cooled in moisture separator 203. The cooling water used for this step comes from source 201 at a temperature of 35 °C and a pressure of 2 bar. This is a typical temperature for a cold district heating stream. Pump 202 pumps the water from the source to the moisture separator to extract 43.6 MW, creating a hot water stream of 65 °C. Sink 141

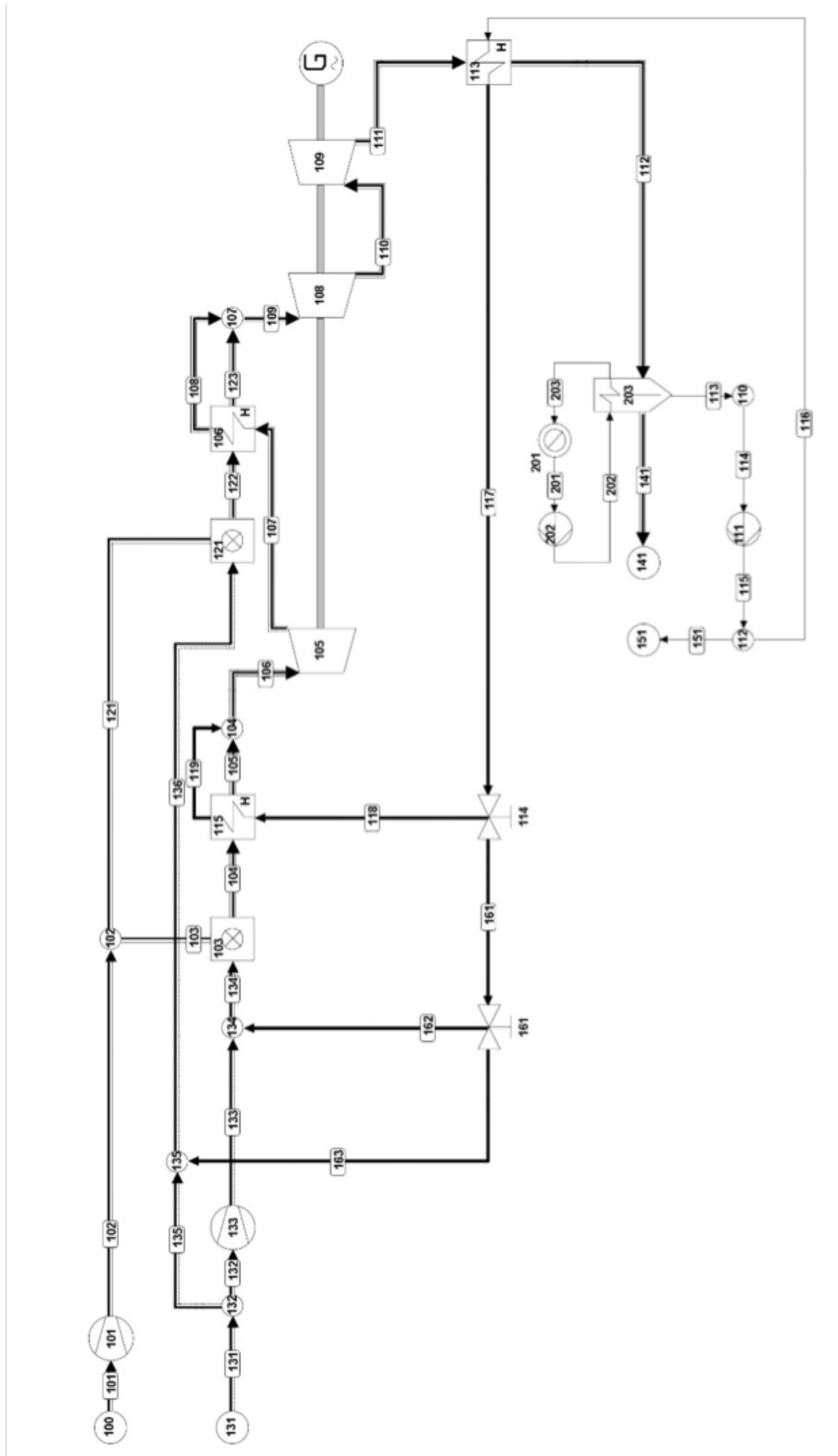


Figure 7.1: Oxy-fuel powerplant model from Cycle Tempo

HPT inlet temperature	1000 °C
IPT inlet temperature	1330 °C
LPT inlet temperature	1104 °C

Table 7.2: Turbine inlet temperatures for OF-CHP model

collects the CO₂ and stream 113 represents the cold water stream. Part of the stream is compressed to 85 bar in compressor 111 and the other part is compressed to 8.5 bar. After compression the stream is separated in node 112 after which 12.5 % of the water is purged. The remaining streams (116) at 85 bar and 8.5 bar are heated in heat exchanger 113. The 8.5 bar stream is mixed with oxygen in node 135. The remaining 85 bar stream is partly mixed with oxygen in node 134 and the rest is evaporated in heat exchanger 115. The equipment specifications are listed in table 7.1.

Compressor 101 isentropic efficiency	80 %
Compressor 133 isentropic efficiency	80 %
Pump 111 efficiency	70 %
HP Turbine 105 isentropic efficiency	85 %
IP Turbine 108 isentropic efficiency	87 %
LP Turbine 109 isentropic efficiency	87 %
Heat exchanger 106 hot stream pressure drop	0 bar
Heat exchanger 106 cold stream pressure drop	0.2 bar
Heat exchanger 113 hot stream pressure drop	0.02 bar
Heat exchanger 113 cold stream pressure drop	0.5 bar
Heat exchanger 115 hot stream pressure drop	0 bar
Heat exchanger 115 cold stream pressure drop	1.8 bar
Combustion chamber 103 pressure drop	1.8 bar
Combustion chamber 106 pressure drop	0.2 bar
Moisture separator 203 liquid stream pressure drop	0.5 bar
Moisture separator 203 gas stream pressure drop	0.02 bar
Generator mechanical efficiency	98 %

Table 7.3: Equipment specifications of OFCC

The output of the power plant is a trade-off between high value electricity and usable heat. An increase in electrical efficiency of the plant comes with a decrease in hot water output temperature. For tap water (including kitchen tap and shower) warm water circulates inside the house at a minimum of 60 °C to prevent growing of Legionella bacteria. Heat is transferred from the hot water grid towards the households via heat exchangers resulting in a hot water stream within the house that is approximately 5 °C lower than the incoming stream from the grid. To make OFC plant heat output suited to heat tap water the temperature of the hot water output stream should be at least 65 °C. A higher temperature is beneficial since high temperature streams require smaller mass flows and thus pipes to exchange the same amount of heat. It is assumed that in 2030 enough houses are facilitated with district heating so that the total hot water stream can be used for tap water heating. The results of the Cycle Tempo model are presented in chapter 8 and discussed in chapter 10. Carbon dioxide is captured from stream 141 in a flash tank, which is not shown in the model in figure 7.1. Stream 141 is compressed for storage. Somewhere in between two compressor stages the stream is transferred to a flash vessel to flash out the water. All CO₂ is captured. Energy consumption of this compression is modelled in section 7.5.7.

7.2. Methanation plant

The fuel consumption of the OFCC is 1.63 kg s⁻¹. As reported in section 2.4 the number of operating hours the OFCC plant is 6137. Of these hours, 22 hours are part load operation, meaning the electricity deficit is between 0 – 44 MW during these hours. In the calculation of the annual fuel consumption, the fuel hourly fuel consumption is scaled to the load during part load hours. In example, if the electricity deficit is 11 MW the fuel consumption is 0.25 × 1.63 kg s⁻¹. Deviation of fuel consumption during start-up and shut down are neglected. Based on the above assumptions the annual fuel consumption of

the OFCC is calculated by coupling the oxy-fuel power plant to the 2030 grid analysis, resulting in an annual consumption of $2.35 \times 10^6 \text{ kmol y}^{-1}$ per year or 36 kt y^{-1} per year. Ideally the methanation plant would only produce methane during green electricity surplus hours, however the flexibility of the plant does not allow this. During peak green electricity hours the methanation plant operates at full load and when the green electricity supply is lower than the electricity demand the methanation plant runs at 40 % load. This means the capacity of the methanation plant is lower than that of a plant that would only produce methane during green electricity surplus hours.

The capacity of the methanation plant is calculated via an iterative process. Ideally the methanation plant load follows the hydrogen production, meaning when there is enough surplus electricity for the SOEC's to run at 50 % load, the methanation plant too runs at 50 % load. However, to calculate the methane production as a function of the hydrogen production, the amount of installed capacity SOEC's is needed. The installed capacity SOEC's can only be calculated after a first assumption of the methanation plant capacity. Therefore flexibility of a SOEC-load following process is neglected in the first assumption of the methanation plant capacity and it is assumed that the plant runs at 100 % load during surplus hours and 40 % load during deficit hours. The actual capacity of the plant will become a bit higher, accounting for the fact that the plant does not always run at 100 % during surplus hours. According to the 2030 grid analysis from section 2 the amount of intermediate load hours only 108 hours in one year so the deviation in plant capacity will be very small.

Based on the annual fuel production, the number of full load and minimum load operating hours and a total of 8000 operating hours per year, the methanation plant capacity is calculated. The plant is shut down for maintenance during the month of December, resulting in 8000 operating hours per year. The month of December is chosen since it is the month with most deficit hours in the 2030 grid analysis. The amount of surplus hours in the rest of the year is 2420 and the amount of deficit hours is 5596. This means the Sabatier plant runs at 100 % load during 30 % of the time and it runs at 40 % during 70 % of the time. In MATLAB the plant capacity is calculated to be $505.3 \text{ kmol h}^{-1}$, with a minimum (i.e. 40 % load of $202.1 \text{ kmol h}^{-1}$). The reactant rates required to operate at full capacity are listed in table 7.4.

Reactant	Flow rate [kg h^{-1}]	Flow rate [kmol h^{-1}]
CO ₂	2.18×10^4	487
H ₂	3.98×10^3	1.95×10^3

Table 7.4: Reactant flow rates methanation plant

Operating at 100 % load during peak hours and at 40 % during low hours, the methanation plant is almost 2 times smaller than a plant that would operate only at 100 % during peak hours. The latter case requires a plant capacity of $972.7 \text{ kmol h}^{-1}$ to meet the annual fuel production requirements. A smaller plant reduces CAPEX of the methanation plant on the one hand but the limit in flexibility forces the plant to run on expensive electricity during deficit hours, increasing the OPEX on the other hand. Also, since the electrolysis plant only produces hydrogen during peak hours, a smaller but less flexible plant needs a hydrogen buffer to run at minimum load when there is no hydrogen production. A hydrogen requires hydrogen compression and transport which can be a costly operation.

The composition of the methanation plant product gas has to match the OFCC fuel inlet gas. This is achieved with one iteration step. After modeling the OFCC plant with a fuel composition estimate, the methanation Aspen model is scaled to the OFCC fuel consumption. The exact gas quality from the methanation plant is known after the Aspen model is finished. The final fuel composition is plugged into the OFCC model to find the final fuel requirement. The Aspen model is slightly adjusted to the new target output, a process in which the final product gas composition remains the same. The final composition of the product gas is shown in table 7.3.

The methanation plant is modeled in Aspen. It is a simple system that comprises of two reactors in series. The first reactor operates at a temperature of $700 \text{ }^\circ\text{C}$ and the second reactor at $350 \text{ }^\circ\text{C}$. The operating pressure of the system is 30 bar. There is intermittent water removal between the two reactors product gases are purified in flash vessels. The product gas has a purity of 95.3 % CH₄, the rest of the gas is mostly H₂ (4.2 %) and some H₂O (0.3 %) CO₂ (0.2 %) and CO (<0.1 %). A higher CH₄ purity can be achieved in a more complex plant with more reactors in series. The feed streams are modeled as pure CO₂ and pure H₂ streams. Since CO₂ is stored at high pressure there is no need for compressing this feed stream. In contrary, CO₂ is partly expanded before entering the methanation system. The energy

released during expansion is not modeled.

CO₂ enters the system at a pressure of 30 bar (stream 1) and is mixed with H₂ in MIX. Hydrogen enters the system at the SOEC output temperature and pressure of 800 °C and 10 bar (stream 11) and is compressed to 30 bar. Several compressors with intermediate cooling are modeled as one compressor (COMP) and one heat exchanger (HEX1). Compressed H₂ flow to the mixer at a temperature of 75 bar (stream 13). The mixture flows into REAC 1 (stream 2) where it reacts at a temperature of 700 °C and a pressure of 30 bar. Afterwards the gases are cooled down to 141 °C in HEX2 and transported to FLASH1 (stream 4). Here most of the water is flashed out. The left-over gas mixture flows to REAC2 (stream 5) and a second methanation step takes place at 300 °C and 30 bar. Afterwards the gases are cooled down to 80 °C in HEX3 and water is flashed out in FLASH2. Left-over gases flow to HEX4 (stream 8) in which they are cooled down to 40 °C. Afterwards the last water removal step takes place in FLASH3.

Gas cooling in the heat exchangers is used to produce steam for the SOEC's and warm water for district heating. Demineralized water is used for steam production and the cooling water system is at 4 bar. Cold water at a temperature of 15 °C and a pressure of 4 bar enters HEX3 (stream 20) and is heated up to 70 °C. This is the highest possible cold stream outlet temperature in HEX3. Part of the warm water (stream 26) can be used for district heating. The rest of the flow (stream 22 and 24) is further heated to steam of 150 °C. HEX4 cools the gases down before the final separation tank (FLASH3). Cold water at 4 bar and 15 °C enters the heat exchanger and is heated up to 35 °C. This water does not have to be demineralized as it is not used for steam production. Other purposes for this warm water stream are discussed in 10. The equipment specifications are listed in table 7.5.

Compressor isentropic efficiency	80 %
Temperature reactor REAC 1	700 °C
Temperature reactor REAC 2	300 °C
Pressure drop in all heat exchangers	0 bar
System pressure	30 bar

Table 7.5: Equipment specifications methanation plant

7.3. Electrolysis plant

For the electrolysis plant Sunfire-Hylink solid oxide electrolysis stacks are chosen due to its low energy consumption of 3.37 kWhNm⁻³ and operating pressure of 11 bara. The stack specifications are listed in table 7.6.

Power (AC)	150 kW
Specific electric energy	3.37 kWhNm ³
H ₂ production	40 Nm ³ h ⁻¹
Pressure	10 barg
H ₂ purity after gas cleaning	100.00 %
Steam input mass flow	40 kg h ⁻¹
Steam input temperature	150 °C
Steam input pressure	3 bar(g)
Steam conversion	81 %
Load variation	0 % - 125 %

Table 7.6: Electrolyzer specifications Sunfire SOEC [25, 30]

The stack consumes a steam input of 40 kg h⁻¹ at an absolute pressure of 4 bar and a temperature of 150 °C. Note that this is not the operating temperature of the stack. During electrolysis in SOEC's the steam temperature rises in the stack. After electrolysis hydrogen is further compressed to 11 bar within the electrolyzer. The number of stacks can be calculated from the required annual hydrogen production and the number of operating hours. The annual hydrogen production is based on the annual OFCC fuel consumption and not the methanation hydrogen consumption. This is due to the fact that the SOEC stacks at full load produce more hydrogen than the methanation plant needs at full load. This way a buffer is created for the methanation plant to run at part load during electricity deficit hours. The first

step is to calculate how much hydrogen is needed for the production of fuel gas. From the Aspen model it is found that 3.93 moles of hydrogen are needed to produce one mole of fuel (with a composition from table 7.1). The annual hydrogen production is now calculated via the following formula:

$$\text{Annual H}_2 \text{ production} = \text{OFCC annual fuel consumption} \times 3.93 \quad (7.1)$$

This gives a production of $9.24 \times 10^6 \text{ kmol y}^{-1}$. Based on the assumption that the SOEC stacks always run at full load during surplus hours and at zero load during deficit hours, the hourly H₂ consumption in kmol/h becomes:

$$\text{Hourly H}_2 \text{ production} = \frac{\text{Annual H}_2 \text{ consumption}}{\text{surplus hours}} \quad (7.2)$$

Resulting in an hourly production of 3523 kmol h^{-1} (or 7 t h^{-1}) during electricity surplus hours. From table 7.6 it can be calculated that the stacks produce $1.79 \text{ kmol h}^{-1} \text{ H}_2$, meaning a total of 1973 stacks is needed for hydrogen production. One stack has a power of 150 kW, resulting in a total installed capacity SOEC stacks of 296 MW. The scenario described above, where the SOEC stack always run at 100 % during surplus hours is a simplified case. When accounting for the fact that hydrogen production is a load following process, the SOEC stacks do not always run at 100 % during surplus hours. When the electricity surplus is lower than the installed capacity of stacks, the stacks will run at a lower load. Therefore the actual amount of installed SOEC capacity is a bit higher than the initial value calculated above, to meet the annual hydrogen requirement. The final value is calculated in the next sub section. The initial production and consumption values are listed in table 7.7. They are plugged in an excel sheet and coupled to the 2030 grid analysis. Now the actual methanation plant capacity can be determined and with that the annual hydrogen production and the required installed capacity of SOEC's.

OF-CHP fuel consumption (full load)	383 kmol h^{-1}
OF-CHP annual fuel consumption	$2.35 \times 10^6 \text{ kmol y}^{-1}$
Methanation plant capacity (full load)	505 kmol h^{-1}
Methanation CO ₂ input (full load)	497 kmol h^{-1}
Methanation H ₂ input (full load)	1987 kmol h^{-1}
Methanation annual H ₂ input (full load)	$9.24 \times 10^6 \text{ kmol y}^{-1}$
SOEC H ₂ production (full load)	$3.52 \times 10^3 \text{ kmol h}^{-1}$
Installed capacity SOEC's	296 MW

Table 7.7: Values for PtMtP system capacity based on first assumption as explained in section 7.2-7.3

7.4. Final system values

7.4.1. Methanation and electrolysis plant final capacity

After coupling the data from table 7.7 to the hourly 2030 grid balance there is an annual fuel deficit and a hydrogen deficit. As explained in section 7.2 this is caused by the neglect that the methanation plant does not always run at full production load during surplus hours and the same holds for the SOEC's. In fact they run between minimum load and full load for 108 hours per year. This results in an annual fuel deficit of 18 074 kmol or ... ton and a hydrogen deficit of 288 333 kmol or... ton. The methanation plant capacity and the installed capacity SOEC's are scaled up slightly to meet the OF-CHP fuel demand, resulting in a methanation capacity of 510 kmol h^{-1} and 306 MW SOEC's. This and the other new system parameters are listed in table 7.8. Note that the hourly and annual fuel consumption remain the same, as well as the annual hydrogen input to the methanation plant.

OFCC fuel consumption (full load)	383 kmolh ⁻¹
OFCC annual fuel consumption	2.35 × 10 ⁶ kmoly ⁻¹
Methanation plant capacity (full load)	510 kmolh ⁻¹
Methanation CO ₂ input (full load)	501 kmolh ⁻¹
Methanation H ₂ input (full load)	2004 kmolh ⁻¹
Methanation annual H ₂ input (full load)	9.24 × 10 ⁶ kmoly ⁻¹
SOEC H ₂ production (full load)	3.64 × 10 ³ kmolh ⁻¹
Installed capacity SOEC's	306 MW

Table 7.8: Final values for PtMtP system capacity based on first assumption as explained in section 7.4.1

The numbers from table 7.8 differ only slightly from the number from table 7.7. This is explained by the small amount of hours (108) in the year that the hydrogen and methane production deviates from the simplified case. However, if the installed capacity of SOEC's increases the number part load hours increases as well and system parameters for the load following case will deviate more from the simplified case. In example, when a ten times larger capacity of 3 GW SOEC's is installed the amount of part load hours is 898, which is more than 10% of the year.

7.4.2. Steam production and consumption

After sizing the system the final steam output of the methanation plant and the steam requirements of the SOEC stacks are determined. Based on a methanation plant capacity from table 7.8, i.e. 510 kmol h⁻¹, streams 23 and 25 together produce 2985 kmol h⁻¹ of steam at SOEC inlet conditions (4 bar and 150 °C). Reactors 1 and 2 operate at constant temperature resulting in a total of 8.62 MW of heat that needs to be disposed of. By cooling the reactors with water another 640 kmol h⁻¹ of steam (at 4 bar and 150 °C) can be generated. The latter steam flow in kmol h⁻¹ is calculated as follows:

$$\dot{m}_{\text{steam}} = \frac{\dot{Q}}{cp_l * \Delta T_l + H_v + cp_g * \Delta T_g} \quad (7.3)$$

Where

\dot{Q}	=	Heat from reactors in MW
cp_l	=	average cp of water at 4 bar and between 15 °C and 144 °C
cp_g	=	average cp of steam at 4 bar between 144 °C and 150 °C
ΔT_l	=	$T_{boil} - T_0$
ΔT_g	=	$T_e - T_{boil}$
T_0	=	15 °C
T_{boil}	=	144 °C
T_e	=	150 °C
H_v	=	Heat of vaporization of water at 4 bar

Heat transfer losses in steam production from reactor cooling are neglected. All together the methanation plant produces 3625 kmol h⁻¹ of steam, when operating at full load. The steam SOEC steam consumption is calculated from the hydrogen production and the steam conversion of the stacks. Operating at full load, the SOEC stacks produce more hydrogen than needed for the methanation plant. This is to build a buffer for the methanation plant to run at 40% load during electricity deficit hours. At full load, the SOEC stacks steam consumption is calculated as follows:

$$\dot{m}_{\text{steam,consumption}} = \dot{m}_{\text{steam per stack}} * n_{\text{stacks}} \quad (7.4)$$

This gives a steam input of 2.2 kmol h⁻¹ per stack and a system steam input of 4585 kmol h⁻¹ when operating at full load. The full load SOEC steam consumption is higher than the full load methanation steam production. However at the end of the year there is a steam surplus of 650 × 10⁴ kmol. This is caused by the fact that during deficit hours, when there is no hydrogen production, there is still 40% steam production. On a yearly base 36% of the steam produced by the methanation plant is

overproduction and could be used for other purposes not related to this power-to-methane-to-power system.

7.5. Transport and storage

7.5.1. Transport

It is assumed that, for the 2030 system, the oxy-fuel power plant, methanation plant and electrolyzers are located at the storage facility and that transport losses can be neglected. In section ?? the 2030 system is scaled up to facilitate an all wind and solar grid in 2050 and the results in terms of storage capacity and carbon emissions are evaluated. In this section transport losses are calculated since it is unsure if all power plants, methanation plants and electrolyzers can be located near salt carvens and depleted gas fields.

7.5.2. Storage losses and capacity calculation

The energy required for storage is simplified to energy needed for gas compression [2]. Compressors are modeled in Aspen to find work needed for compression as well as the heat production during compression. The heat is used for the production of steam and warm water. The storage capacity for different gases is calculated with the use of the hourly 2030 grid balance. The hourly production and consumption for each gas (based on the hourly amount of electricity surplus or deficit) are subtracted from each other. This is more briefly explained with examples in the rest of this section.

7.5.3. Methane storage

Methane is produced at the methanation plant during surplus hours. The CH_4 production rate is 510 kmol h^{-1} when the plant runs at full load. The hourly methane production depends on the hourly grid balance. When the electricity surplus equals, or is more than the installed capacity electrolysis cells, i.e. 306 MW, the methanation plant operates at full load. When the surplus is less than 306 MW it operates at part load and when surplus is less than 40% of the installed capacity SOEC's, it runs at minimum load, i.e. 40%. As an estimate, the CH_4 production is scaled linearly with the load. Methane is consumed by the oxy-power plant during deficit hours. The consumption rate is 383 kmol h^{-1} when the power plant runs at full load, i.e. when the electricity shortage is 44 MW or more. During surplus hours the power plant is shut down resulting in zero methane consumption. It is assumed that, between 0 and 44MW electricity shortage, the methane consumption is scaled linearly with the grid load. The methane production and consumption rates are listed in table 7.9

Grid load	Production rate [kmol h^{-1}]	Consumption rate [kmol h^{-1}]
$\geq 306 \text{ MW}$	510	0
122 MW-306 MW	Linearly scaled	0
0 MW-122 MW	204	0
-44 MW-0 MW	204	Linearly scaled
$\leq -44 \text{ MW}$	204	383

Table 7.9: Methane production and consumption rates for PtGIP system, depending on the grid load

When coupled to the 2030 grid balance this results in a yearly CH_4 production as shown in figure 7.3. The flat end of the line indicated the shut-down of the methanation plant in the month December (described in section 7.2), where no methane is produced.

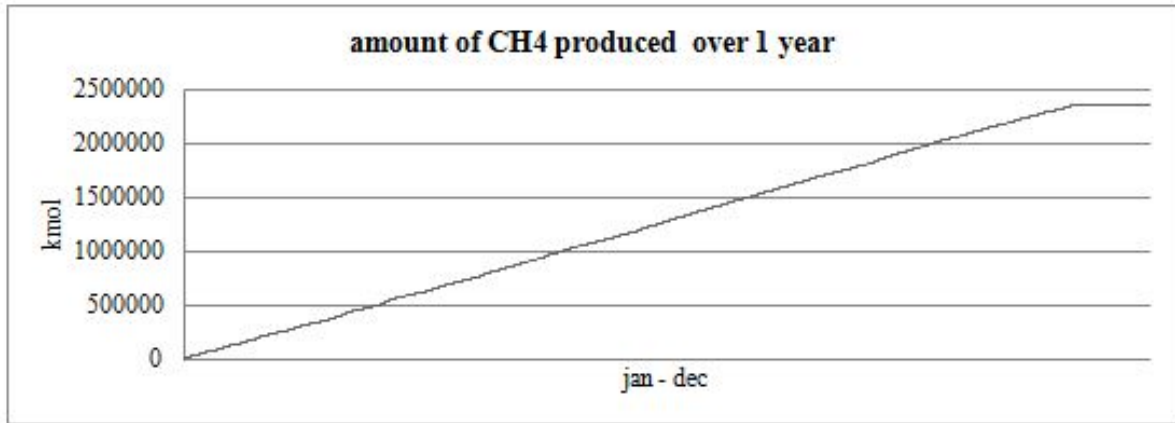


Figure 7.3: Total amount of CH₄ produced by methanation plant per hour over the year 2030

In figure 7.4 the CH₄ consumption of one year is plotted. The graph ends at approximately the same value of kmol methane as figure 7.3 since the annual fuel production is calculated to meet the annual fuel consumption.

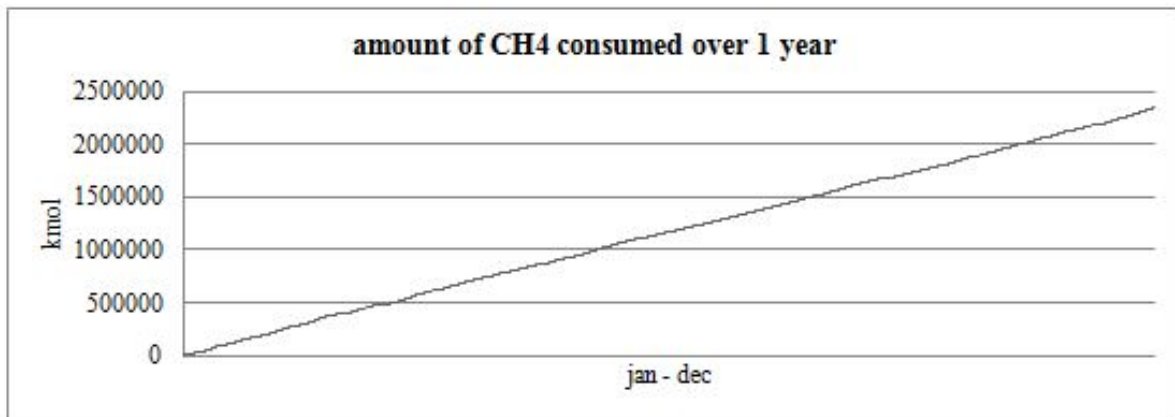


Figure 7.4: Total amount of CH₄ consumed by power plant per hour over the year 2030

Subtracting the graph 7.4 from graph 7.3 gives the methane balance over the year. It represents the amount of methane stored. The result is presented and discussed in section 8.1.

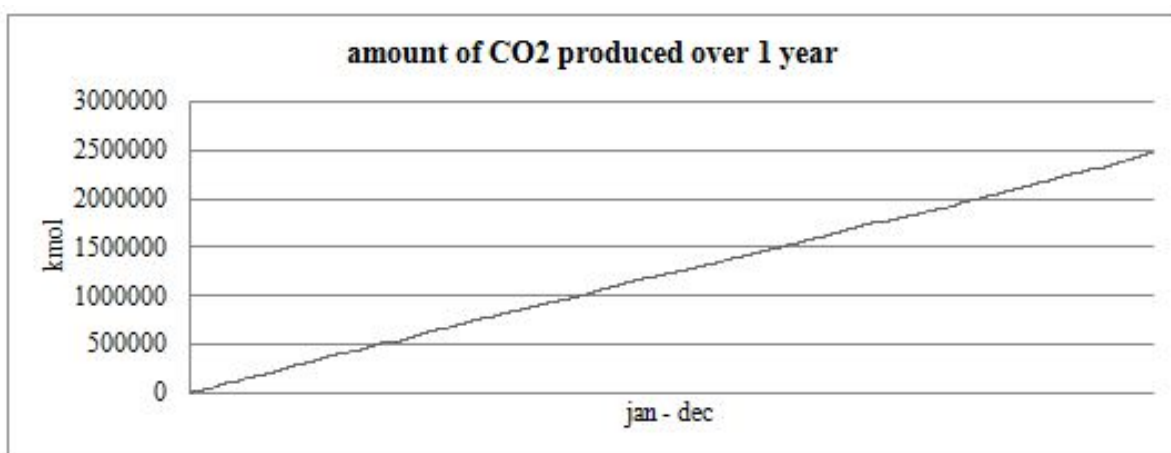
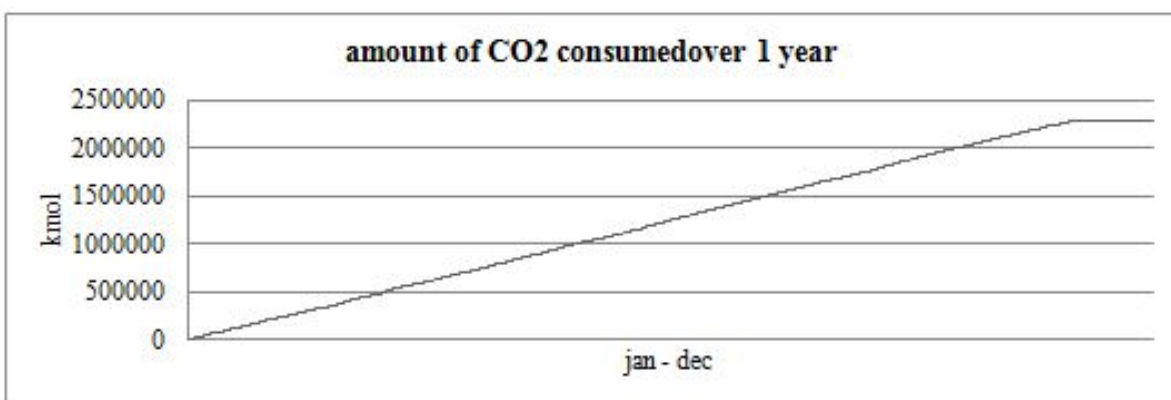
7.5.4. Carbon dioxide storage

Carbon dioxide is produced at the power plant during deficit hours. The CO₂ production rate is 364 kmol h⁻¹ when the plant runs at full load. The hourly methane production depends on the hourly grid balance. When the electricity deficit equals, or is more than the power plant capacity, i.e. 44 MW, the power plant operates at full load. When the deficit is less than 44 MW it operates at part load and when there is a surplus the plant is shut down. As an estimate, the CO₂ production is scaled linearly with the load. Carbon dioxide is consumed by the methanation plant during surplus hours. The consumption rate is 497 kmol h⁻¹ when the power plant runs at full load, i.e. when the electricity surplus is 306 MW or more. During deficit hours the methanation plant runs at minimum load resulting in a CO₂ consumption of 199 kmol h⁻¹. It is assumed that, between 0 MW and 306 MW electricity surplus, the methane consumption is scaled linearly with the grid load. The carbon dioxide production and consumption rates are listed in table 7.10

Grid load	Production rate [kmol h ⁻¹]	Consumption rate [kmol h ⁻¹]
≤-44 MW	364	199
-44 MW-0 MW	Linearly scaled	199
0 MW-122 MW	0	199
122 MW-306 MW	0	Linearly scaled
≥306 MW	0	496

Table 7.10: Carbon dioxide production and consumption rates for PtGtP system, depending on the grid load

When coupled to the 2030 grid balance this results in a yearly CO₂ production as shown in figure 7.5. In figure 7.6 the CO₂ consumption of one year is plotted. The flat end of the line indicated the shut-down of the methanation plant in the month December (described in section 7.2), where no carbon dioxide is consumed. Subtracting the graph 7.6 from graph 7.5 gives the carbon dioxide balance over the year. It represents the amount of carbon dioxide stored. The result is presented and discussed in section 8.1

Figure 7.5: Total amount of CO₂ produced by methanation plant per hour over the year 2030Figure 7.6: Total amount of CO₂ consumed by methanation plant per hour over the year 2030

7.5.5. Oxygen storage

Oxygen is produced at the electrolyzers during surplus hours. The O₂ production rate is 1820 kmol h⁻¹ when the electrolysis stacks operate at full load. The hourly oxygen production depends on the hourly grid load. When the electricity surplus equals, or is more than the installed capacity electrolysis stacks, i.e. 306 MW, the stacks operate at full load. When the surplus is less than 306 MW they operate at part

load and when there is a deficit the production is zero. As an estimate, the O_2 production is scaled linearly with the load. Oxygen is consumed by the oxy-power plant during deficit hours. The consumption rate is 738 kmol h^{-1} when the power plant runs at full load, i.e. when the electricity shortage is 44 MW or more. During surplus hours the power plant is shut down resulting in zero oxygen consumption. It is assumed that, between 0 MW and 44 MW electricity shortage, the oxygen consumption is scaled linearly with the grid load. The oxygen production and consumption rates are listed in table 7.11

Grid load	Production rate [kmol h^{-1}]	Consumption rate [kmol h^{-1}]
$\geq 306 \text{ MW}$	1820	0
0 MW-360 MW	Linearly scaled	0
-44 MW-0 MW	0	Linearly scaled
$\leq -44 \text{ MW}$	0	738

Table 7.11: Oxygen production and consumption rates for PtGtP system, depending on the grid load

When coupled to the 2030 grid balance this results in a yearly O_2 production as shown in figure 7.7. In figure 7.8 the O_2 consumption of one year is plotted. Subtracting the graph 7.8 from graph 7.7 gives the oxygen balance over the year. It represents the amount of oxygen stored. The result is presented and discussed in section 8.1

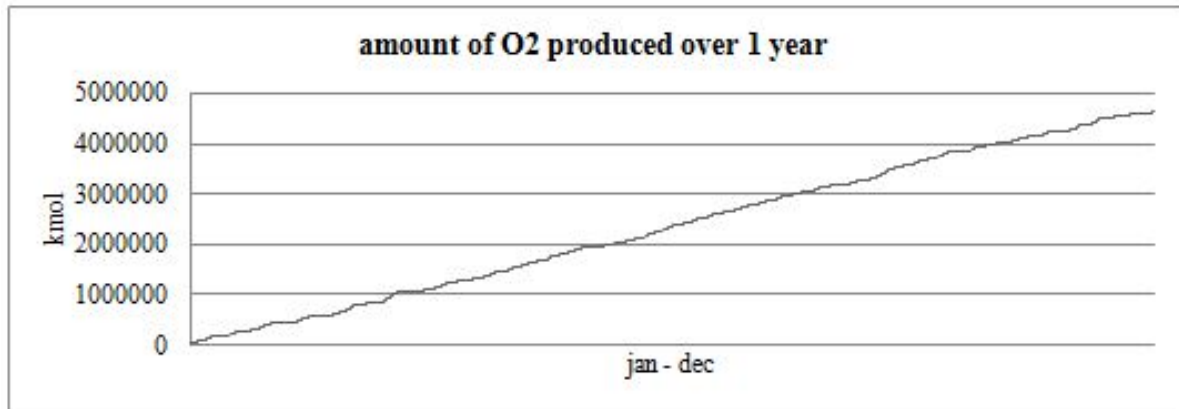


Figure 7.7: Total amount of O_2 produced by methanation plant per hour over the year 2030

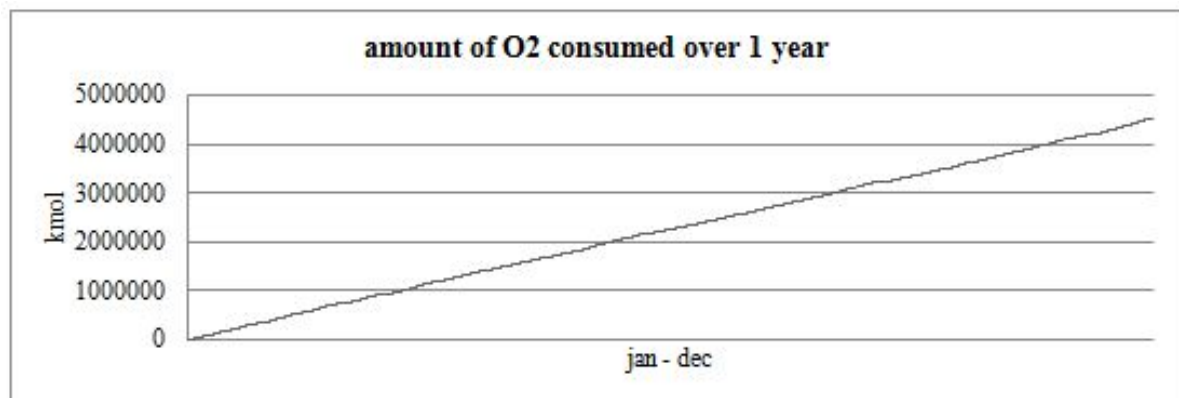


Figure 7.8: Total amount of O_2 consumed by methanation plant per hour over the year 2030

7.5.6. Hydrogen storage

Hydrogen is produced at the electrolyzers during surplus hours. The H_2 production rate is 3640 kmol h^{-1} when the electrolysis stacks operate at full load. The hourly hydrogen production depends on the hourly

grid load. When the electricity surplus equals, or is more than the installed capacity electrolysis stacks, i.e. 306 MW, the stacks operate at full load. When the surplus is less than 306 MW they operate at part load and when there is a deficit the production is zero. As an estimate, the H₂ production is scaled linearly with the load. Hydrogen is consumed by the methanation plant during surplus hours. The consumption rate is 2004 kmol h⁻¹ when the methanation plant runs at full load, i.e. when the electricity surplus is 306 MW or more. When the grid load is less than 40% of the installed capacity of SOEC's, i.e. 122 MW, the methanation plant runs at minimum load resulting in a hydrogen consumption of 802 kmol h⁻¹. It is assumed that, between 122 MW and 306 MW electricity surplus, the hydrogen consumption is scaled linearly with the grid load. The hydrogen production and consumption rates are listed in table 7.12.

Grid load	Production rate [kmol h ⁻¹]	Consumption rate [kmol h ⁻¹]
≥306 MW	3640	2004
122 MW-306 MW	Linearly scaled	Linearly scaled
0 MW-122 MW	Linearly scaled	802
≤0 MW	0	802

Table 7.12: Hydrogen production and consumption rates for PtGtP system, depending on the grid load

When coupled to the 2030 grid balance this results in a yearly O₂ production as shown in figure 7.9. In figure 7.10 the H₂ consumption of one year is plotted. The flat end of the line indicates the shut-down of the methanation plant in the month December, where the hydrogen production is zero.

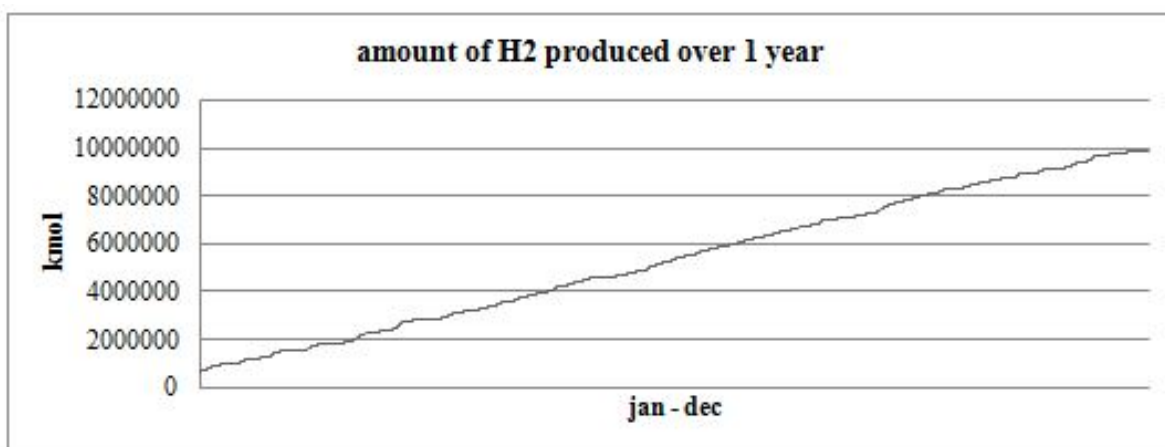


Figure 7.9: Total amount of H₂ produced by SOEC's per hour over the year 2030

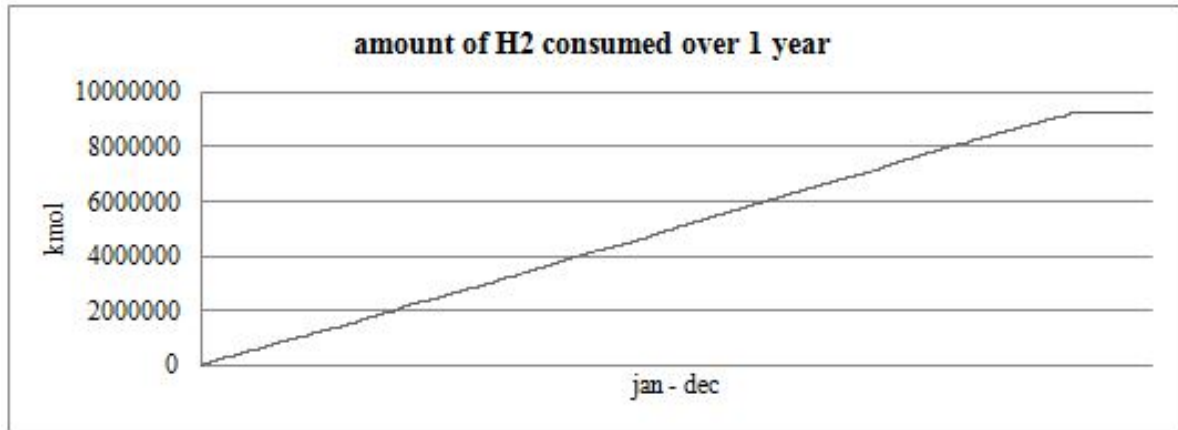


Figure 7.10: Total amount of H₂ consumed by the methanation plant per hour over the year 2030

Subtracting the graph 7.10 from graph 7.9 gives the oxygen balance over the year. It represents the amount of oxygen stored. The result is presented and discussed in section 8.1

7.5.7. Gas compression

Energy consumption for storage decreases with storage pressure, therefore the lowest cavern pressure is the most optimal one in terms of system efficiency. As described in section 6.1 this is 80 bar. A low storage pressure however 10. The initial conditions of the gases before compression are based on the production method and listed in table 7.13. Note that the temperature of the hydrogen stream is lower than right after electrolysis. This is modeled like this because the heat of the hydrogen stream is already included in the calculation of steam production from the methanation plant as modeled in section 7.2.

	Pressure [bar]	Temperature [celsius]
CH ₄	30	40
CO ₂	0.26	50
H ₂	10	800
H ₂ O	10	94

Table 7.13: Initial conditions gases before compression for storage

Oxygen is cooled before compressions as a lower gas temperature decreases the energy consumption of compression. For hydrogen, methane and carbon dioxide this effect is very small since they are not at a high temperature before being compressed. Carbon dioxide is compressed with water vapor (stream 141 from section 7.1) during the first compression step. After that liquid water is flashed out and CO₂ is further compressed to storage conditions. Figure 7.11 shows the Aspen flow sheet used to calculate the compressor work and the usable heat output oxygen compression. For hydrogen, methane and carbon dioxide compression the same flowsheet is used, but without a heat exchanger before compression (i.e. B7 in figure 7.11).

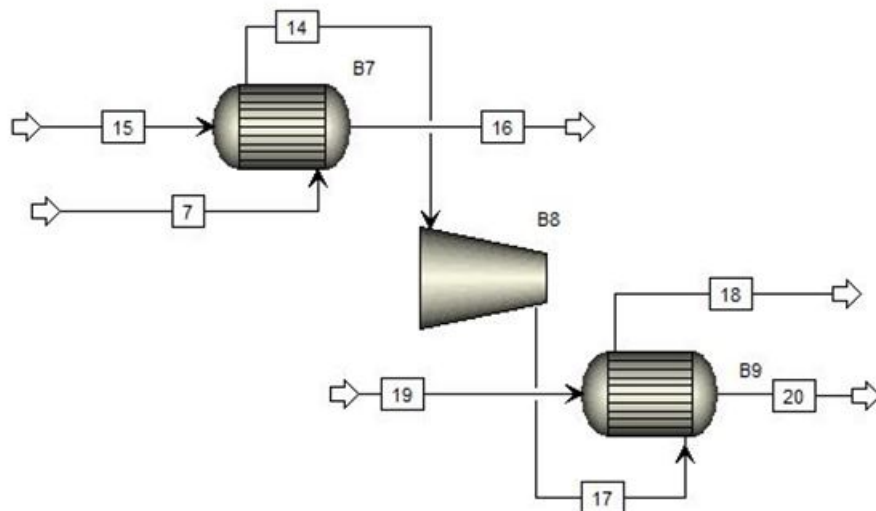
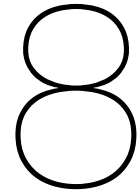


Figure 7.11: Flow sheet from Aspen for gas compression with heat extraction

For oxygen compression hot gas (stream 7) enters a heat exchanger (B7) and is cooled with cold water (stream 15) of 15 °C at 3 bar. The water is converted into steam of 150 °C at 3 bar (stream 16). The steam can be used for external purposes, more on this is chapter 10. The cooled gas (stream 14) is compressed. Multiple compressor stages with intercooling are modeled as one compressor with an isentropic efficiency of 80% (B8) followed by one heat exchanger (B9). Cold water (stream 19) of 15 °C at 3 bar is converted to steam at 150 °C and 3 bar. Note that, to produce high quality heat in the form of steam, compressor temperature may not drop below 150 °C. Last, pressure drop in heat exchangers is neglected. For hydrogen methane and carbon dioxide compression approximately the same procedure is followed as described above. Only here gases do not pass through B7 and enter the compressor at conditions from table 7.4. Due to its high initial pressure and low initial temperature it is not possible to produce steam from methane compression. Therefore hot water is produced at 100 °C and 3 bar. This could be used for external purposes, for instance district heating or greenhouse heating. Energy required for pumping the cooling water around is neglected. It is assumed that no compression energy is recovered through gas expansion after storage. More on this is discussed in chapter 10.



Results

8.1. Gas storage capacity

With the production and consumption rates of the different gases and the hourly electricity balance of 2030, the required gas storage capacity per gas is calculated. Methane is produced by the methanation plant and stored green during electricity surplus hours. It is consumed by the oxy-fuel power plant during electricity deficit hours. Oxygen is produced by the electrolyzer stacks and stored during electricity surplus hours. It is consumed by the oxy-fuel power plant during electricity deficit hours. Carbon dioxide is produced by the oxy-fuel power plant and stored during electricity deficit hours. It is consumed by the methanation plant during the whole year ranging between 40 % during electricity deficit hours and 100 % during electricity surplus hours. Last, hydrogen is produced by the electrolyzer stacks and stored during electricity surplus hours. It is consumed by the methanation plant during the whole year ranging between 40 % during electricity deficit hours and 100 % during electricity surplus hours.

8.1.1. Methane storage capacity

The methane production and consumption rates are listed in table 7.9. The hourly CH₄ production and consumption for the system in 2030, based on the electricity supply and demand in 2030, are calculated in Excel. The amount of CH₄ produced and consumed is shown in graphs 7.3 and 7.4 respectively. Subtracting the hourly consumption graph from the hourly production graph gives graph 8.1. The graph shows the amount of CH₄ stored per hour. The peak at the end of the year is caused by the fact that the methanation plant is shut down in the month of December. In 11 months, the plant produces the amount of fuel that is burned by the power plant in 12 months. To make sure the amount of CH₄ stored is never a negative value and there is always enough CH₄ available for combustion, the starting volume of the storage facility is 0.927×10^4 kmol (in January). The CH₄ plant capacity is scaled to produce the amount of fuel in one year that is consumed by the power plant in one year. Therefore the end value of the CH₄ stored approximately matches the starting value, with a small overproduction of 496 kmol.

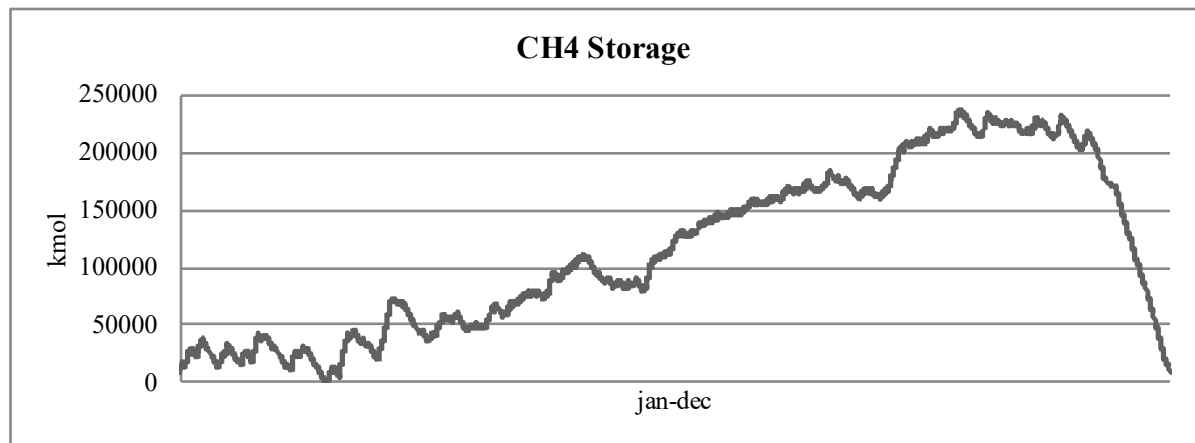


Figure 8.1: Amount of CH₄ stored per hour

The required volume of the methane storage facility is based on the highest peak in graph 8.1, i.e. 23.7×10^4 kmol or 7.49×10^4 m³ under storage conditions described in section 6.5.

8.1.2. Carbon dioxide storage capacity

The carbon dioxide production and consumption rates are listed in table 7.11. The hourly CO₂ production and consumption for the system in 2030 are calculated in Excel, based on the electricity supply and demand in 2030. The amount of CO₂ produced and consumed is shown in graphs 7.5 and 7.6 respectively. Subtracting the hourly consumption graph from the hourly production graph gives graph 8.2. The graph shows the amount of CO₂ stored per hour. To make sure the amount of CO₂ stored is never a negative value, meaning there is not enough CO₂ available for methanation, the starting value of the CO₂ stored is 26.6×10^4 kmol (in January). From the graph it can be seen that the amount of CO₂ consumed by the methanation plant is larger than the CO₂ produced by the power plant. This is explained by the fact that some of the CO₂ ends up in purge gas during methanation and not all CO₂ is captured after combustion. Also there is a small methane surplus at the end of the year. This results in a CO₂ deficit of 56 630 kmol, which has to be supplemented from carbon capture to create an actual zero emission system. More on this is discussed in chapter 10.

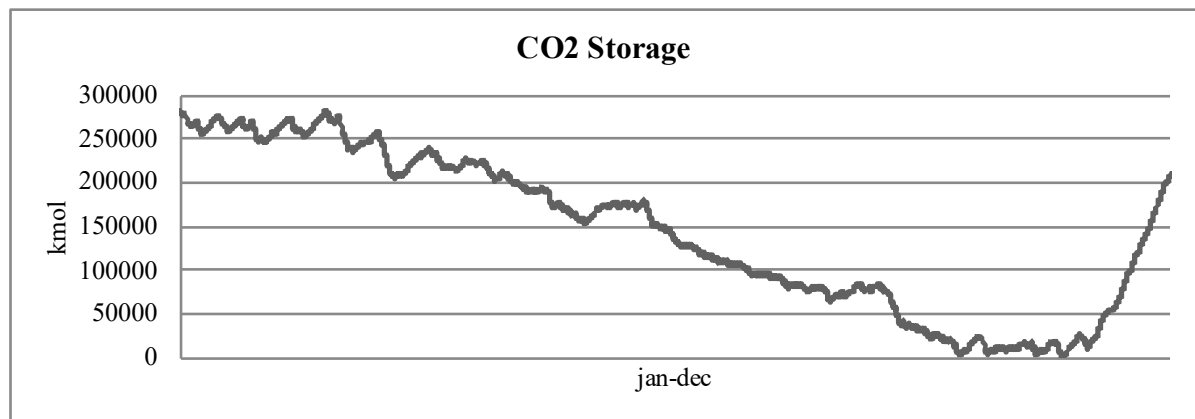


Figure 8.2: Amount of CO₂ stored per hour

The required volume of the carbon dioxide storage facility is based on the highest peak in graph 8.2, i.e. 28.5×10^4 kmol or 9.00×10^4 m³ under storage conditions described in section 6.5

8.1.3. Oxygen storage capacity

The oxygen production and consumption rates are listed in table 7.11. The hourly O₂ production and consumption for the system in 2030 are calculated in Excel, based on the electricity supply and demand in 2030. The amount of O₂ produced and consumed is shown in graphs 7.7 and 7.8 respectively.

Subtracting the hourly consumption graph from the hourly production graph gives graph 8.3. The graph shows the amount of O₂ stored per hour. To make sure the amount of CO₂ stored is never a negative value, meaning there is not enough O₂ available for combustion, the starting value of the O₂ stored is 12.9×10^4 kmol (in January). From the graph it can be seen that the amount of O₂ consumed by the power plant is smaller than the amount of O₂ produced by the Electrolysis stacks. This can be explained. For every two moles of hydrogen produced by the SOEC's, one mole of oxygen is produced. During methanation some of the hydrogen ends up in the purge gas, meaning it is lost by the system. At the oxy-power plant methane and hydrogen react stoichiometrically. At the end of the year there is a O₂ surplus of 9.85×10^4 kmol.

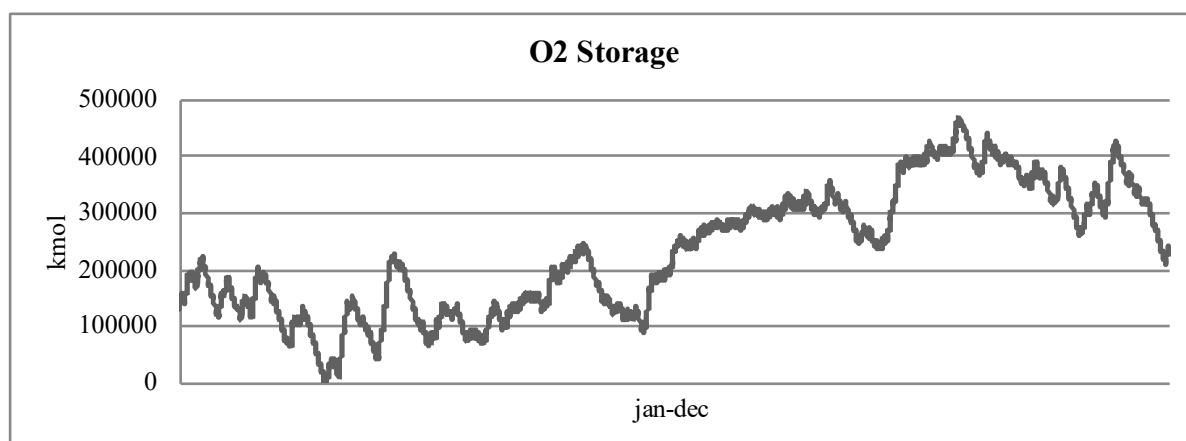


Figure 8.3: Amount of O₂ stored per hour

The required volume of the oxygen storage facility is based on the highest peak in graph 8.3, i.e. 46.7×10^4 kmol or 14.8×10^4 m³ under storage conditions described in section 6.5

8.1.4. Hydrogen storage capacity

The hydrogen production and consumption rates are listed in table 7.12. The hourly H₂ production and consumption for the system in 2030 are calculated in Excel, based on the electricity supply and demand in 2030. The amount of H₂ produced and consumed is shown in graphs 7.9 and 7.10 respectively. Subtracting the hourly consumption graph from the hourly production graph gives graph 8.4. The graph shows the amount of H₂ stored per hour. To make sure the amount of H₂ stored is never a negative value, meaning there is not enough H₂ available for methanation, the starting value of the H₂ stored is 67.5×10^4 kmol (in January). The installed capacity of SOEC's is scaled to the annual H₂ consumption of the methanation plant in one year. Therefore the amount of H₂ stored at the end of the year is approximately the same as the starting value, with a hydrogen surplus of 514 kmol at the end of the year.

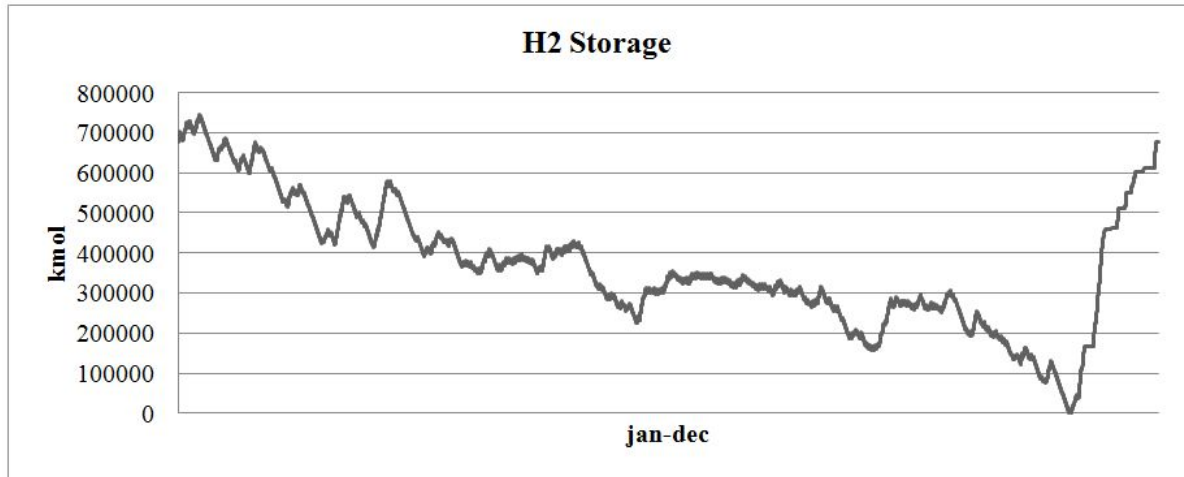


Figure 8.4: Amount of H₂ stored per hour

The required volume of the methane storage facility is based on the highest peak in graph 8.4, i.e. 74.4×10^4 kmol or 23.5×10^4 m³.

8.1.5. Total gas storage capacity

The sum of required storage capacity for the different gases makes the total gas storage capacity. It is assumed that all gases are stored in caverns under the same as described in section 6.5. It is assumed that the molar volume for all gases is the same at these conditions, i.e. 0.315 m³ kmol. The total amount of gas storage capacity is shown in table 8.3.

	kmol $\times 10^{-4}$	m ³ $\times 10^{-4}$
CH ₄	23.7	7.49
CO ₂	28.5	9.00
O ₂	46.7	14.8
H ₂	74.4	23.5
Total	173	54.7

Table 8.1: Required storage capacity with actual system flows based on calculation described in chapter 7

As explained in sub sections 8.1.2 and 8.1.3 there is an annual O₂ surplus of 9.85×10^4 kmol, which is 21 % of the total storage capacity, and a CO₂ shortage of 7.58×10^4 kmol, which is 27 % of the total storage capacity. The oxygen surplus can be balanced by reducing the amount of oxygen flowing to the storage capacity by 2.1 %, i.e. 97.9 % of the oxygen produced goes to storage. The left-over oxygen could either be used for external purposes or emitted into the air, this is discussed in chapter 10. The CO₂ shortage can be balanced by increasing the CO₂ flow towards the storage capacity with 3.4 %. To create an actual zero emission system the extra CO₂ should come from direct air capture. This is further discussed in chapter 10.

	kmol $\times 10^{-4}$	m ³ $\times 10^{-4}$
CH ₄	23.7	7.49
CO ₂	23.2	7.33
O ₂	39.8	12.6
H ₂	74.4	23.5
Total	161	50.9

Table 8.2: Required storage capacity with balanced system flows

8.1.6. Storage capacity sensitivity to methanation flexibility

The flexibility of the methanation plant has an influence on the gas storage of the system. A larger amount of gas to be stored means higher storage losses. A larger required storage capacity results in a larger cavern and higher costs. Therefore it is interesting to see what parameters, concerning the methanation flexibility, have an effect on the gas storage capacity and how the amount of gas to be stored can be reduced. In this research it is assumed that all CH₄, CO₂ and O₂ produced is compressed and stored. Since the annual fuel consumption is fixed and with that the annual fuel production, the amount of CH₄, CO₂ and O₂ to be stored remain unchanged. The amount of hydrogen to be stored can differ, depending on the flexibility of the system.

Scenario 2

The largest volume of gas that needs to be stored is the hydrogen buffer. Also hydrogen storage has the highest impact on storage efficiency due to the high energy consumption of hydrogen compressors. Graph 8.4 shows that the highest hydrogen peaks are in January and December. This is explained by the shut-down of the methanation plant during the month December, where the SOEC's still produce hydrogen. Since the SOEC's are scaled to produce enough hydrogen per year to match the methanation plant hydrogen consumption, the hydrogen buffers slowly empties from January – November and is filled in the month December. It is expected that the amount of hydrogen to be stored will decrease when the SOEC's are also shut down during the month December. In this scenario the required installed capacity will increase since the stacks have to produce the same amount of hydrogen in a shorter period of time. Also the oxygen storage volume will increase as the oxy-power plant consumed oxygen in December but no oxygen is produced. The excel model is updated with the new SOEC stack operating hours and the new maximum storage volumes are calculated as is the new installed capacity SOEC stacks. The latter slightly effects the methanation plant capacity in this model since the methane production is scaled to the installed capacity of SOEC stacks, as explained in section 7.4. The effect however is so small that is it not visible in table 8.3, where the new system values are listed under 'scenario 2'. The O₂ and CO₂ storage capacity is again balanced as described above.

Scenario 3 – 8592 operating hours

The number of operating hours of the methanation plant also has an influence on the required gas storage volume. Graph 8.2 shows that the annual CH₄ storage builds up towards the month December and decreases quickly during this last month. This is explained by the shutdown of the methanation plant in December where no fuel is produced, yet fuel is consumed by the power plant. For the fuel production to match the fuel consumption, in the months January – November as fuel buffer is built for the month December. Graph 8.2 shows that the amount of CO₂ stored decreases over the year to be built up during December. This too is caused by the methanation plant shut down in this month, where no CO₂ is consumed, yet is it produced by the power plant. It is assumed that the methanation plant operates 8016 hours per year in the original scenario. If this number would be increased to 8592 operating hours per year, corresponding to an annual shut down of one week, the storage volume for CO₂ and CH₄ in expected to decrease. In this scenario the amount of operating hours of the SOEC stacks is also 8592 hours. Besides a reduce in gas storage volume, the methanation plant capacity will decrease as well since the same amount of fuel in made within a longer operating time. The results are listed in table 8.3 under 'scenario 3'. The installed capacity SOEC's is the same as in the original scenario. This is explained by the low amount of green electricity surplus during the shutdown week, which means the same amount of hydrogen is produced in approximately the same amount of operating hours as compared to the original scenario. Therefore the oxygen storage capacity is also the same as for the original scenario. The hydrogen storage capacity decreases due to a more spread out fuel production period over the year. The methanation plant capacity decreases since the same amount of methane is produced with more operation hours.

Scenario 3.1 – 8592 operating hours and 30 % methanation plant minimum load

Another way to decrease the gas storage capacity is to increase the methanation plant flexibility. A lower methanation plant minimum load reduces the amount of hydrogen to be stored to keep the plant running during deficit hours. It will also reduce the maximum hydrogen storage capacity. The capacity of the methanation plant will increase compared to scenario 3, since the production during deficit hours decreases. This has to be compensated during surplus hours. The methane storage will increase

because more methane is produced during surplus hours, which has to be stored until deficit hours. The results are shown in table 8.3 under scenario 3.1. The installed capacity SOEC's is the same as in the original scenario. This is explained by the fact that the annual hydrogen production does not change, as well as the number of SOEC operating hours. Therefore the oxygen storage volume does not change either. The CO₂ storage volume increases which is caused by a larger methanation plant resulting in a larger CO₂ consumption per hour during methanation full load hours. Note that the annual CO₂ consumption is unchanged since the annual fuel production remains the same for all scenarios.

Scenario 3.3 – 8592 operating hours and 12.5 % methanation plant minimum load

As described in section 4.7 the demand for more flexible process plants is likely to grow. Biegger et al. [5] reports about a new honeycomb catalyst used in a multi bed methanation reactor which increases the process flexibility to 12.5 % minimum load. This will decrease the amount of hydrogen to be stored to 22.3 % of the annual production. It will also reduce the hydrogen storage capacity. The methanation plant capacity and the methane and carbon dioxide storage capacity will increase as explained under 'scenario 3.1'. The installed capacity SOEC's and the required oxygen storage volume will remain, as explained under 'scenario 3.1'.

	Original	2	3	3.1	3.3
CH ₄ [kmol] x 10 ⁻⁵	2.37	2.37	1.30	1.43	1.78
CO ₂ [kmol] x 10 ⁻⁵	2.32	2.32	1.27	1.40	1.74
O ₂ [kmol] x 10 ⁻⁵	3.98	7.07	3.98	3.98	3.98
H ₂ [kmol] x 10 ⁻⁵	7.44	3.65	3.02	2.50	1.29
Total [kmol] x 10 ⁻⁵	16.1	15.9	9.57	9.31	8.80
Meth. cap. [kmol/h]	510	510	477	544	719
SOEC cap. [MW]	306	329	306	306	306
Op. hours meth. [h]	8016	8016	8592	8592	8592
Op. hours SOEC [h]	8760	8016	8592	8592	8592

Table 8.3: Required storage capacity for different scenarios

The total amount of CH₄, CO₂ and O₂ that needs be stored in one year corresponds to the end point of graphs 7.3, 7.5. and 7.7, i.e. the total amount of these gases that is produced in one year. The total amount of hydrogen to be stored is only the overproduction during surplus hours. All gas that needs to be stored is shown in table 8.4 for each scenario. As described in this subsection, the amount of CH₄, CO₂ and O₂ to be stored does not change for different scenarios. The amount of hydrogen to be stored however, does change. This results in a different round trip efficiency for each scenario's as a higher amount of gas to be stored gives higher losses.

	Original	2	3	3.1	3.3
CH ₄ [kmol] x 10 ⁻⁶	2.35	2.35	2.35	2.35	2.35
CO ₂ [kmol] x 10 ⁻⁶	2.31	2.31	2.31	2.31	2.31
O ₂ [kmol] x 10 ⁻⁶	4.52	4.52	4.52	4.52	4.52
H ₂ [kmol] x 10 ⁻⁶	4.50	5.18	4.47	3.77	2.06
Total [kmol] x 10 ⁻⁶	13.7	14.4	13.6	13.0	11.2
Meth. cap. [kmol/h]	510	510	477	544	719
SOEC cap. [MW]	306	329	306	306	306
Op. hours meth. [h]	8016	8016	8592	8592	8592
Op. hours SOEC [h]	8760	8016	8592	8592	8592

Table 8.4: Amount of gas to be stored for different scenarios

8.2. Efficiencies

8.2.1. Oxy-fuel power plant efficiency

The oxy-fuel power plant efficiency can be divided into two different forms: electrical efficiency and heat efficiency. The electrical efficiency describes the efficiency of the power plant, only taken into account the electrical output. The heat efficiency only accounts for the heat output, in this model in the form of hot water. The sum of both efficiencies represents the energetic efficiency. The net electrical efficiency of the power plant is:

$$\eta_{\text{elec,OFCC}} = \frac{E_{\text{out,elec,OFCC}}}{E_{\text{in,OFCC}}} = \frac{W_{\text{net,OFCC}}}{\dot{m}_{\text{fuel}} \times \text{HHV}} \quad (8.1)$$

Where

$W_{\text{net,OFCC}}$	=	net electrical output
\dot{m}_{fuel}	=	molar flow rate of fuel at inlet
HHV	=	higher heating value of the fuel

And

$$W_{\text{net,OFCC}} = W_{\text{out}} - W_{\text{aux}} \quad (8.2)$$

Where

W_{out}	=	the work delivered by the shaft
W_{aux}	=	auxiliary power consumption (i.e. pump and compressor work)

The higher heating value of the fuel is used in the calculation for the electrical efficiency as the fuel energy is not only used for heating up the working fluid but also for evaporation of the H₂O in the working fluid. With a fuel inlet of 0.107 kmol s⁻¹, a HHV of 860 kJ kmol⁻¹ and a net electrical output of 42.4 MW, the electrical efficiency of the power plant is 46.3%. According to Bolland et al. [6] the net electrical efficiency of a CES cycle power plant on the short term would be 52%_{LHV} with a potential of 60%_{LHV} on the long term if all process parameters are increased significantly above the technology level of conventional equipment. A net electrical efficiency of 52%_{LHV} corresponds to a an efficiency of 47%_{HHV} which is close to the value found in this research.

The heat efficiency of the power plant is defined as:

$$\eta_{\text{elec,OFCC}} = \frac{E_{\text{out,heat,OFCC}}}{E_{\text{in,OFCC}}} = \frac{Q_{\text{out}}}{\dot{m}_{\text{fuel}} \times \text{HHV}} \quad (8.3)$$

Where

Q_{out}	=	heat output
\dot{m}_{fuel}	=	molar flow rate of fuel at inlet
HHV	=	higher heating value of the fuel

The heat output of the plant is the defined by the amount of heat energy captured by heating up water for external purposes. The heat output is defined as:

$$Q_{\text{out}} = \dot{m}_{\text{water}} \times (h_1 - h_2) \quad (8.4)$$

Where

$$\begin{aligned}\dot{m}_{\text{water}} &= \text{molar flow of cold water circuit} \\ h_1 &= \text{enthalpy of water in pipe 202} \\ h_2 &= \text{enthalpy of water in pipe 203}\end{aligned}$$

This gives a thermal output of 43.7 MW, resulting in a thermal efficiency of 47.7%_{HHV}. The plant heats up 193.2 kmol s⁻¹ (3.549 m³s⁻¹) of water from 35 °C – 65 °C.

The total efficiency of the plant is:

$$\eta_{\text{OFCC}} = \eta_{\text{elec,OFCC}} + \eta_{\text{heat,OFCC}} \quad (8.5)$$

which gives a total efficiency of 94.0%_{HHV}. Note that this efficiency can only be achieved when all heat output of the power plant can be used for other purposes. This is further discussed in chapter 110.

8.2.2. Methanation plant efficiency

The methanation plant efficiency consists of the chemical efficiency (accounting for only fuel as a product) and the heat efficiency (accounting for only heat as a product). The sum of these two efficiencies describes the plant efficiency. The methanation plant chemical efficiency is:

$$\eta_{\text{chem,meth}} = \frac{E_{\text{out,chem,meth}}}{E_{\text{in,meth}}} = \frac{\dot{m}_{\text{fuel}} \times \text{HHV}_{\text{fuel}}}{W_{\text{in}} + \dot{m}_{\text{reac}} \times \text{HHV}_{\text{reac}}} \quad (8.6)$$

Where

$$\begin{aligned}\dot{m}_{\text{fuel}} &= \text{molar flow of fuel output} \\ \dot{m}_{\text{reac}} &= \text{molar flow of hydrogen output} \\ \text{HHV}_{\text{fuel}} &= \text{higher heating value of fuel} \\ \text{HHV}_{\text{reac}} &= \text{higher heating value of hydrogen} \\ W_{\text{in}} &= \text{compressor work}\end{aligned}$$

\dot{m}_{fuel}	509.5 kmol h ⁻¹
\dot{m}_{reac}	2004 kmol h ⁻¹
HHV_{fuel}	860.0 MJ kmol ⁻¹
HHV_{reac}	285.7 MJ kmol ⁻¹
W_{in}	7.959 MW

Table 8.5: Input and chemical output values of methanation plant

The values of the parameters in formula 8.6 are listed in table 8.5. Plugging the values into formula 8.6 gives a chemical efficiency of 72.9%. In this calculation the HHV is used to follow the approach as for the power plant efficiency calculation. Being consequent in choosing either HHV or LHV in different efficiency calculation makes it easier to calculate the round trip efficiency eventually. Besides compressor losses the methanation plant has small losses due to hydrogen that ends up in purge streams. These losses are very small since total of 0.151 kmol/h of H₂ end ups in the purge streams, corresponding to 0.000 075 3 % of the hydrogen input.

Besides a fuel product, the methanation plant provides energy in the form of heat. Part of this heat is used for steam production for the SOEC's while the rest, part in the form of steam and part in the form of hot water, can be used for external purposes. The thermal efficiency of the methanation plant is calculated as follows

$$\eta_{\text{therm,meth}} = \frac{E_{\text{out,therm,meth}}}{E_{\text{in,meth}}} \quad (8.7)$$

$$\eta_{\text{therm,meth}} = \frac{\dot{m}_{\text{steam}}(h_{2,\text{steam}} - h_{1,\text{water}}) + \dot{m}_{\text{hot water}}(h_{2,\text{hot water}} - h_{1,\text{water}}) + \dot{m}_{\text{warm water}}(h_{2,\text{warm water}} - h_{1,\text{water}})}{W_{\text{in}} + \dot{m}_{\text{reac}} \text{HHV}_{\text{reac}}} \quad (8.8)$$

Where

\dot{m}_{steam}	=	molar flow of steam
$\dot{m}_{\text{hot water}}$	=	molar flow of hot water
$\dot{m}_{\text{warm water}}$	=	molar flow of warm water
\dot{m}_{reac}	=	molar flow of hydrogen
HHV_{reac}	=	higher heating value of hydrogen
$h_{1,\text{water}}$	=	enthalpy of cold water inlet (4 bar, 15 °C)
$h_{2,\text{water}}$	=	enthalpy of hot water outlet (4 bar, 70 °C)
$h_{2,\text{steam}}$	=	enthalpy of steam outlet (4 bar, 150 °C)
W_{in}	=	compressor work

The values are listed in table 8.2

\dot{m}_{steam}	2985 kmol h ⁻¹
$\dot{m}_{\text{hot water}}$	3150 kmol h ⁻¹
$\dot{m}_{\text{warm water}}$	768.7 kmol h ⁻¹
\dot{m}_{reac}	2004 kmol h ⁻¹
HHV_{reac}	285.7 MJ kmol ⁻¹
$h_{1,\text{water}}$	1142 kJ kmol ⁻¹
$h_{2,\text{warm water}}$	2649 kJ kmol ⁻¹
$h_{2,\text{hot water}}$	5285 kJ kmol ⁻¹
$h_{2,\text{steam}}$	49 609 kJ kmol ⁻¹
W_{in}	7.959 MW

Table 8.6: Input and thermal output values of methanation plant

Based on the values in table 8.6 the thermal efficiency of the methanation plant is 26.4 %. It is important to mention that this number represents the efficiency of a methanation plant in this specific power-to-methane system. Part of the plant heat output comes from cooling the hot hydrogen input of 800 °C. This energy is partly provided by the SOEC stack. This results in a total methanation plant efficiency of 99.3 %. Also, part of the steam produced by the plant is used elsewhere in the system, i.e. as SOEC stack input. The power-to-gas efficiency is calculated further in this section.

8.2.3. Electrolyzer efficiency

The electrolyzer efficiency is defined by its electricity consumption, which is 3.37 kWh Nm⁻³ (table 7.6) or 75.5 kWh kmol⁻¹. This corresponds to an energy efficiency of 89.8 %_{LHV} and 105 %_{HHV}. An important note is that the heat for steam production comes from the methanation plant. Therefore the above described SOEC stack efficiencies represent an efficiency of a stack specifically in this system. Without a waste heat source, extra energy would be needed for steam production, lowering the efficiency of the stacks.

8.2.4. Storage energy

As described in section 7.5.1 gas transport losses are neglected in the 2030 scenario and storage losses are simplified to the energy required for compression. It is assumed that all produced methane, carbon dioxide and oxygen is stored before it is used and only part of the hydrogen is stored. From the excel in which the gas production and consumption rates are coupled to the grid load, it can be calculated that 48.6 % of the produced hydrogen in one year needs to be stored before it is used. The amount of hydrogen to be stored decreases when methanation flexibility increases as presented in section 8.1.6. This affects the system efficiency which is discussed in section 8.2.8. For now the original system is assumed with a methanation minimum load of 40 % and a yearly shut-down of one month. The energy required for compression is calculated in Aspen. The SOEC and methanation plant capacities are scaled to produce the amount of fuel that is consumed by the power plant in one year. Therefore in this calculation the system is scaled so that:

- The OFCC fuel consumption per hour meets the methanation fuel production per hour.

- The methanation hydrogen consumption per hour meets the SOEC's hydrogen production per hour.
- The OFCC oxygen consumption per hour matches the SOEC's oxygen production per hour. I.e. the surplus oxygen produced by the SOEC's is not compressed for storage.
- The carbon dioxide consumption of the methanation plant matches the carbon dioxide produced by the OFCC, plus some extra. I.e. extra carbon dioxide comes from a different carbon capture process and is compressed for storage.

As shown in table 8.4 the scale of the individual parts of the system does not have an effect on the total amount of CH₄, CO₂ and O₂ that needs to be stored and therefore the scale of the individual parts of the system do not affect the storage efficiency of these gases.

The compressor work for different gas streams calculated by the Aspen model are listed in table 8.7. The heat output Q_{out} is calculated as follows:

$$Q_{out} = \dot{m}_{H_2O}(h_2 - h_1) \quad (8.9)$$

Where

$$\begin{aligned} \dot{m}_{H_2O} &= \text{molar flow of cooling water} \\ h_2 &= \text{enthalpy of steam (150 °C and 3 bar)} \\ h_1 &= \text{enthalpy of cold water (15 °C and 3 bar)} \end{aligned}$$

and the corresponding values for the different gas cooling processes are listed in table 8.8. The heat output results are shown in table 8.8

	Compressor work [MW]	Heat output [MW]
CH ₄	0.366	0.511
CO ₂	3.65	4.09
O ₂	1.81	5.83
H ₂	1.77	1.26
Total	7.23	11.69

Table 8.7: Electrical input and heat output of gas compression for storage

\dot{m}_{H_2O,CH_4}	287 kmol h ⁻¹
\dot{m}_{H_2O,CO_2}	303 kmol h ⁻¹
\dot{m}_{H_2O,O_2}	432 kmol h ⁻¹
\dot{m}_{H_2O,H_2}	93 kmol h ⁻¹
h_1	1140 kJ kmol ⁻¹
$h_{2,hot\ water}$	7555 kJ kmol ⁻¹
$h_{2,steam}$	49 757 kJ kmol ⁻¹

Table 8.8: Heat input and output values for compressor cooling

Most of the heat output values listed in table 8.7 are higher than the electrical work input values, this is caused by the fact that the gas streams are cooled to a lower temperature than their initial temperature before compression. The heat of these gases is compensated for in the other process steps of the PtGtP system. Hydrogen is produced from cold water which is heated up to steam by methanation heat output. The hydrogen is further heated up during electrolysis in the SOEC's. The heat of the hydrogen stream is therefore included in the methanation and electrolysis efficiency. CO₂ is produced and heated in the power plant during combustion so the heat of the CO₂ stream is included in the power plant efficiency. CH₄ is produced and heated during the exothermal methanation process and

its heat is included in the methanation plant efficiency. Last, oxygen is produced from cold water which is converted to steam from methanation heat and the oxygen is further heated up during electrolysis. The oxygen heat is included in the methanation plant efficiency and SOEC efficiency. The CH₄ stream is cooled down to its OFCC input temperature. The other gases are cooled down to a temperature above the input temperature of their next process step. This means that some of their heat is lost in this model.

8.2.5. Power-to-methane efficiency

The power-to-methane efficiency can be divided into a chemical efficiency (only accounting for the chemical output of the system) and a thermal efficiency (only accounting for the heat output of the system). In the power-to-methane efficiency, the energy for intermediate hydrogen storage is not taken into account. The chemical efficiency without storage losses is defined as:

$$\eta_{\text{chem,PtG}} = \frac{E_{\text{out,chem,PtG}}}{E_{\text{in,PtG}}} = \frac{E_{\text{out,chem,metH}}}{E_{\text{SOEC}}\dot{m}_{\text{reac}} + W_{\text{comp}}} \quad (8.10)$$

Where

$E_{\text{H}_2\text{O}}$	=	energy requirement of electrolyzer stack in kWh kmol ⁻¹
\dot{m}_{reac}	=	molar flow of H ₂ inlet to methanation plant in kmol s ⁻¹
W_{comp}	=	compressor work of methanation plant MW

With the values described earlier in this section this results in a chemical efficiency of 76.4 %, which is the same as the power-to-methane value found in project HELMETH [30]. The thermal efficiency without storage losses is defined as:

$$\eta_{\text{therm,PtG}} = \frac{E_{\text{out,therm,PtG}}}{E_{\text{in,PtG}}} \quad (8.11)$$

$$\eta_{\text{therm,PtG}} = \frac{0.36\dot{m}_{\text{steam}}(h_{2,\text{steam}} - h_{1,\text{water}}) + \dot{m}_{\text{hot water}}(h_{2,\text{hot water}} - h_{1,\text{water}}) + \dot{m}_{\text{warm water}}(h_{2,\text{warm water}} - h_{1,\text{water}})}{E_{\text{SOEC}} \times \dot{m}_{\text{reac}} + W_{\text{comp}}} \quad (8.12)$$

On a yearly base, the SOEC stacks need 64 % of the steam generated by the methanation plant, leaving 36 % as waste steam output (section 7.4.2). This gives a thermal efficiency of the power-to-methane system of 11.6 %. Together with the chemical efficiency the total power-to-methane efficiency is 88.0 %. This efficiency is only achieved when all thermal output is useful heat. This is further discussed in section 10.

8.2.6. Methane-to-power efficiency

The methane-to-power efficiency includes oxy-fuel power generation and carbon dioxide compression. During green electricity deficit hours methane is converted into electricity and the exhaust CO₂ is captured and compressed for storage. The compressor work for CO₂ compression is therefore subtracted from the OFCC net output to find the methane-to-power net electrical output. Heat recovered from CO₂ compression is added up to the heat output of the power plant to find methane-to-power heat output. The methane to power electrical efficiency (only accounting for electrical output) is defined as:

$$\eta_{\text{elec,GtP}} = \frac{E_{\text{out,elec}}}{E_{\text{in}}} = \frac{W_{\text{net,OFCC}} - W_{\text{comp,CO}_2}}{\dot{m}_{\text{fuel}}\text{HHV}} \quad (8.13)$$

With $W_{\text{comp,CO}_2}$ is the work of the CO₂ compressor from table 8.7. This gives an electrical efficiency of 42.4 %. Note that this is 4 percent points lower than the OFCC electrical efficiency.

8.2.7. Round trip efficiency

The round trip energy efficiency can be divided into an electrical efficiency (only taken into account electrical output) and a thermal efficiency (only accounting for the heat output). For the electrical efficiency of the PtGtP system the same scaling is used as described in section 8.2.4, again assuming that 48.6 % of the hydrogen produced per year needs to be compressed for storage.

The round trip electrical efficiency is calculated as:

$$\eta_{\text{elec,round trip}} = \frac{E_{\text{out,elec}}}{E_{\text{in}}} = \frac{E_{\text{out,elec,OFCC}} - E_{\text{comp,CO}_2}}{E_{\text{in,PtG}} + E_{\text{comp,H}_2 + \text{CH}_4 + \text{O}_2}} \quad (8.14)$$

$E_{\text{in,PtG}}$ is described in section 8.2.5. Note that the methanation plant hydrogen consumption, i.e. \dot{m}_{reac} , is scaled as described above. $E_{\text{comp,H}_2 + \text{CH}_4 + \text{O}_2}$ is the total amount of energy required for gas compression for storage of H₂, CH₄ and O₂. Last, $E_{\text{out,elec,OFCC}}$ is W_{net} as described in section 8.2.1 and $E_{\text{comp,CO}_2}$ is energy required for CO₂ compression. This results in a round trip efficiency of 30.9%. The input and electrical output energy flows are visualized in figure 8.5.

The round trip thermal efficiency is calculated as:

$$\eta_{\text{therm,round trip}} = E_{\text{out,therm}}/E_{\text{in}} = \frac{E_{\text{out,therm,OFCC}} + E_{\text{out,therm,PtG}} + E_{\text{out,therm,comp}}}{E_{\text{in,PtG}} + E_{\text{comp}}} \quad (8.15)$$

$E_{\text{in,PtG}}$ and E_{comp} are the input energy streams as described in the explanation of the round trip electrical efficiency. $E_{\text{out,therm,OFCC}}$ is the heat output of the power plant as described in section 8.2.1 and $E_{\text{out,therm,PtG}}$ is the heat output of the methanation plant as described in section 8.2.2. Note that the latter is left-over heat from methanation, meaning the heat for steam production for the SOEC's is not included in this number. Last $E_{\text{out,therm,comp}}$ is the heat recovered from gas compression for storage as described in section 8.2.4. This results in a round trip thermal efficiency of 57.1%. The input and heat output energy flows are visualized in figure 8.6.

The round trip energy efficiency of the system is:

$$\eta_{\text{elec,round trip}} + \eta_{\text{therm,round trip}} \quad (8.16)$$

With the round trip electrical efficiency and round trip heat efficiency as described above, this results in a round trip energy efficiency of 88.0%. An important note is that this efficiency can only be realized when all heat output of the system can be used for external purposes. Losses can be explained by different phenomena. As mentioned in section 8.2.4 some of the heat is lost due to the fact that after compression, gases are cooled down to a higher temperature than their input temperature to the process after storage. Electrical input is lost in compression due a compressor efficiency lower than 100%, meaning some of the compressor work is lost in the form of heat flowing to the environment. A negligible amount of chemical energy is lost in the purge streams of the methanation plant that contain a small amount of hydrogen (section 8.2.2).

8.2.8. Relation between energy efficiency and methanation flexibility

Table 8.9 shows the input energy streams of the PtMtP system scaled as explained in section 8.2.4. It is again assumed that the amount of hydrogen that needs to be compressed for storage is 48.6% on a yearly base.

		Input [MW]	Percentage [%]
Electrical	SOEC electrical input	114	88.4
	Methanation compressor	7.96	6,17
	H ₂ storage compressor	1.77	1.37
	CH ₄ storage compressor	0.336	0.26
	CO ₂ storage compressor	3.56	2.76
	O ₂ storage compressor	1.18	0.91
Heat	-	-	-
Total		129	100

Table 8.9: Energy input of PtMtP system

The OFCC compressor and pump are not listed in table 8.9 as their contribution is processed in the net work delivered by the power cycle. From table 8.9 it can be seen from table that the compressor work for gas storage has a significant influence on the electrical efficiency of the system, i.e. 5.43% of the total energy input. Table 8.10 shows the output energy streams of the system.

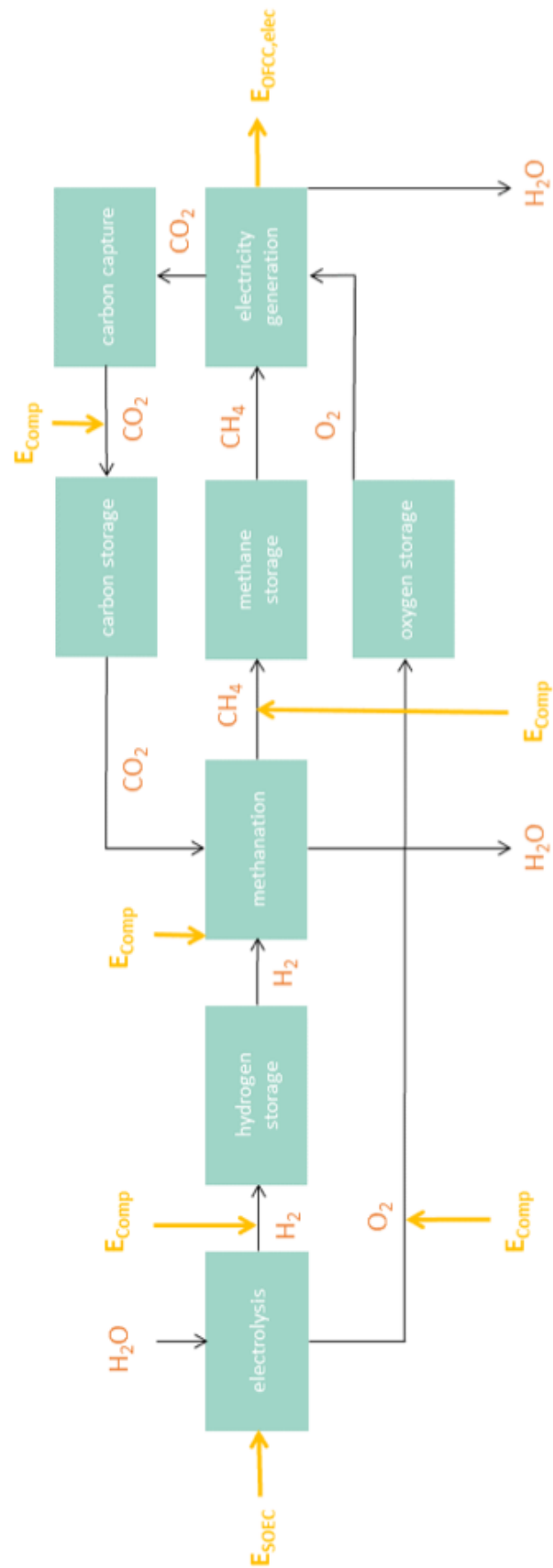


Figure 8.5: System input flows and electrical output flows

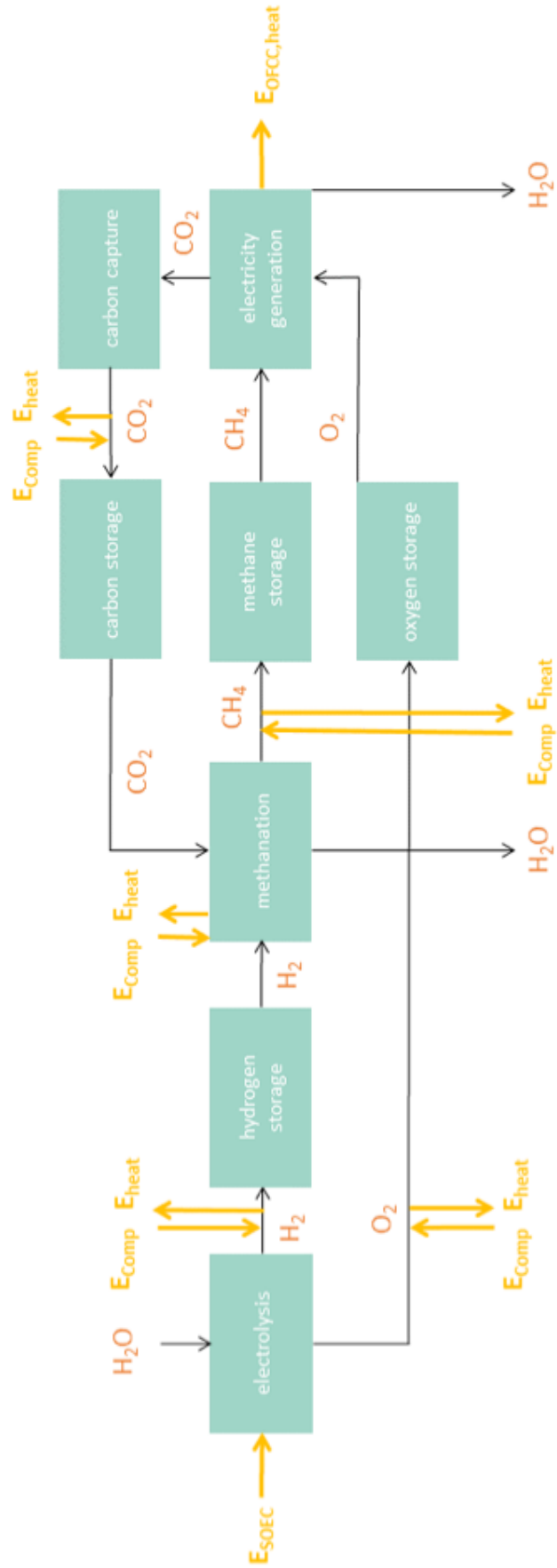


Figure 8.6: System input flows and heat output flows

		Output [MW]	Percentage [%]
Electrical	OFCC net electrical work	42.38	36.48
Heat	OFCC heat output	43.68	37.60
	Methanation heat	18.42	15.86
	H ₂ compression heat	1.256	1.08
	CH ₄ compression heat	0.511	0.44
	CO ₂ compression heat	4.092	3.52
	O ₂ compression heat	5.834	5.02
Total		116.2	100

Table 8.10: Energy output of PtMtP system

Table 8.10 shows that 36.5 % of the total energy output comes out in the form of electricity. The rest of the output energy is produced in the form of heat.

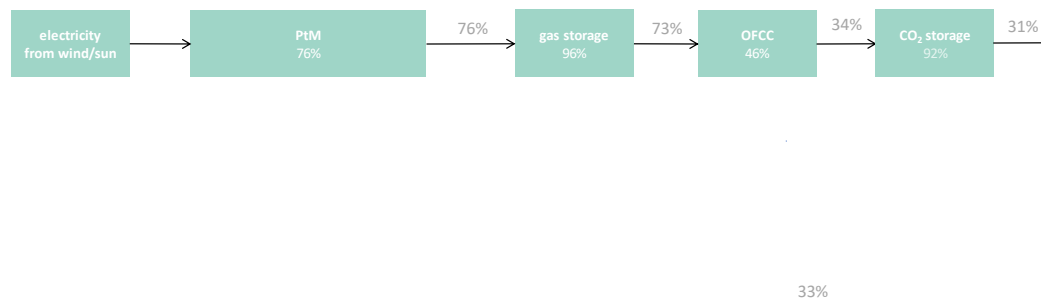


Figure 8.7: Build up of round trip electrical efficiency of PtMtP system

Figure 8.7 shows how the round trip electrical efficiency of the system is built up. A round trip electrical efficiency of 30.9 % means that 69.1 % of the electrical energy is either lost or converted into heat. It can be seen that 3 % of the electrical energy losses is caused by gas compression of CH₄, CO₂ and H₂ for storage. Section 8.2.8 shows that the flexibility of the methanation plant has an influence on the amount of gas that needs to be stored. Most compression energy is consumed for CO₂ compression, however the amount of CO₂, CH₄ and O₂ to be stored does not depend on the methanation flexibility. The amount of hydrogen to be stored decreases when methanation flexibility increases as presented in section 8.2.8. This effects system efficiency as a decrease in the amount of gas to be stored gives a decrease in storage energy consumption. In scenario 3.3 from section 8.2.8 22.3 % of the annual hydrogen production needs to be stored. This results in a higher electrical round trip efficiency of 31.1 %. It reduced the thermal round trip efficiency to 57.9 % as the heat output from hydrogen compression decreases. The total energy efficiency becomes 90.0 %. Although this is slightly lower than the efficiency calculated in section 8.2.7, a more flexible methanation plant is preferred as electricity is a more valuable form of energy than heat.

8.3. Carbon emissions

During its operation the power-to-methane-to-power system emits some carbon dioxide. During methanation part of the reactants are purged to reach a high methane purity. Also equipment manufacturing causes carbon emissions but these are not taken into account in this research. The carbon emissions caused by methanation is $0.278 \text{ kmol h}^{-1}$ at plant full load. For an estimate of the total carbon emissions of the year 2030, the 2030 grid balance is used. The total carbon emissions of the year 2030 are calculated using the 2030 grid balance. With 8000 operating hours, of which 5596 minimum load and 116 part load, the total carbon emission of the methanation plant over one year is 1280 kmol or 56.3 t. Note that the carbon emissions do not depend on methanation flexibility or operating hours, as described in section 8.1.6. It is assumed that the CO_2 emission scales linearly with the load of the plant. In example, when the plant operated at 80 % load, the carbon emission of the plant is $0.8 \times 0.278 \text{ kmol h}^{-1}$. In reality although, it could be that the carbon emission does not scale linearly during ramp up and ramp down. The pressure and temperature in the flash vessels could slightly differ ramping up and down. This results in a new chemical equilibrium and a different composition of purge gases. These variations are expected to small and have a small effect on the carbon emission of the methanation plant.

8.4. Hydrogen system

8.4.1. System design and modeling

A power-to-hydrogen-to-power (PtHtP) system is coupled to the 2030 grid balance to find results in terms of efficiency, storage capacity and carbon emissions. The results are compared to the power-to-methane-to-power system in section 8.6. The system is based on the plan of Vattenfall to realize a hydrogen fired gas power plant. The electrical efficiency of such a plant is 57 %_{LHV} [Vattenfall], corresponding to a fuel inlet of 1139 kmol h^{-1} for a 44 MW plant. PEM cells could be used due to their high flexibility. Efficient PEM cells have an energy consumption of 5 kWh Nm^{-3} , corresponding to an efficiency of 60 %_{LHV} [8]. Without steam supply from waste heat, SOEC's still have a higher efficiency than PEM cells, i.e. 67 %_{LHV} which corresponds to 4.5 kWh Nm^{-3} . A higher cell efficiency reduces system OPEX. The usage of SOEC's however, requires a steam boiler and a heater to keep the cells at high temperature when not in operation. The latter heater is neglected in the energy efficiency of the cells. A steam boiler and a heater increase system CAPEX. The tradeoff between PEM or SOEC cells is a financial one which lays out of the scope of this research. In this thesis it is assumed that the most efficiency option is used, i.e. SOEC's. This is plugged in to the grid balance sheet and the required installed capacity electrolysis cells is found using the following input data:

- The hydrogen consumption is 1139 kmol/h when the electricity deficit is greater than or equal to 44 MW
- The hydrogen consumption scales linearly with the grid load when the deficit is smaller than 44 MW
- The hydrogen production runs at full load when the electricity surplus is equal to or larger than the installed capacity electrolysis cells
- The hydrogen production scales linearly with the grid load when the surplus is less than the installed capacity electrolysis cells.
- The hydrogen annual hydrogen production equals the annual consumption

The required installed capacity electrolysis cells is found to be 276 MW. This includes energy for steam production. The required hydrogen production rate is smaller for the hydrogen system than for the methane system. This is explained by the higher electrical efficiency of the hydrogen power plant and the fact that there are no hydrogen losses during methanation. The hydrogen production and consumption rates are shown in table 8.11.

Grid load	Production rate [kmol/h]	Consumption rate [kmol/h]
≥276	2743	0
0 – 276 MW	Linearly scaled	0
-44 - 0 MW	0	Scaled linearly
≤-44	0	1139

Table 8.11: Hydrogen production and consumption rates, depending on the grid load, for a PtHP system

8.4.2. Storage capacity

Following the same steps as in sections 7.5 and 8.1 table 8.11 result in a hydrogen production, consumption and storage as shown in figures 8.8 – 8.10. To prevent a negative value for the hydrogen stored, a starting value of 21.7 kmol is taken in figure 8.10.

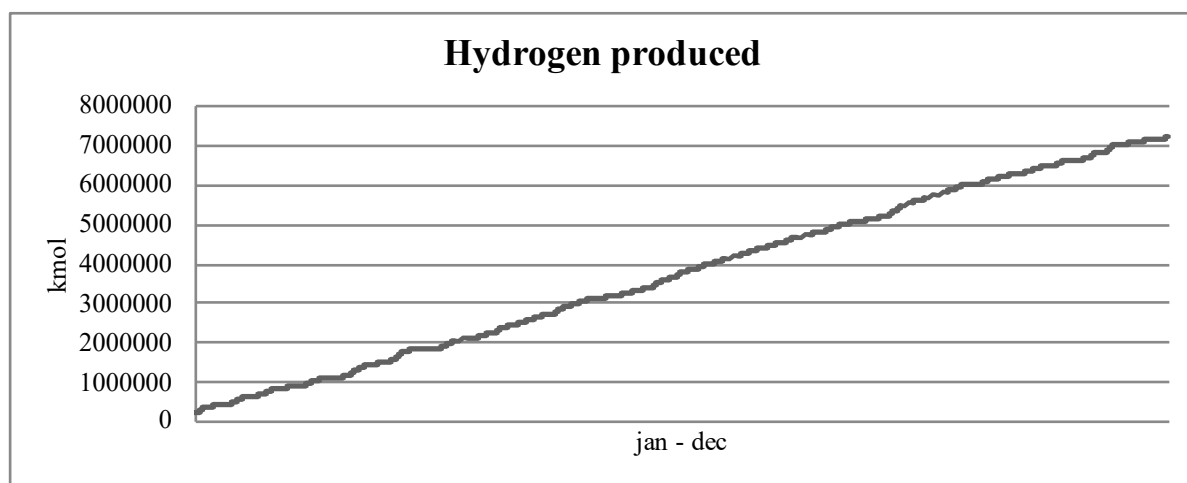


Figure 8.8: Hydrogen produced over one year

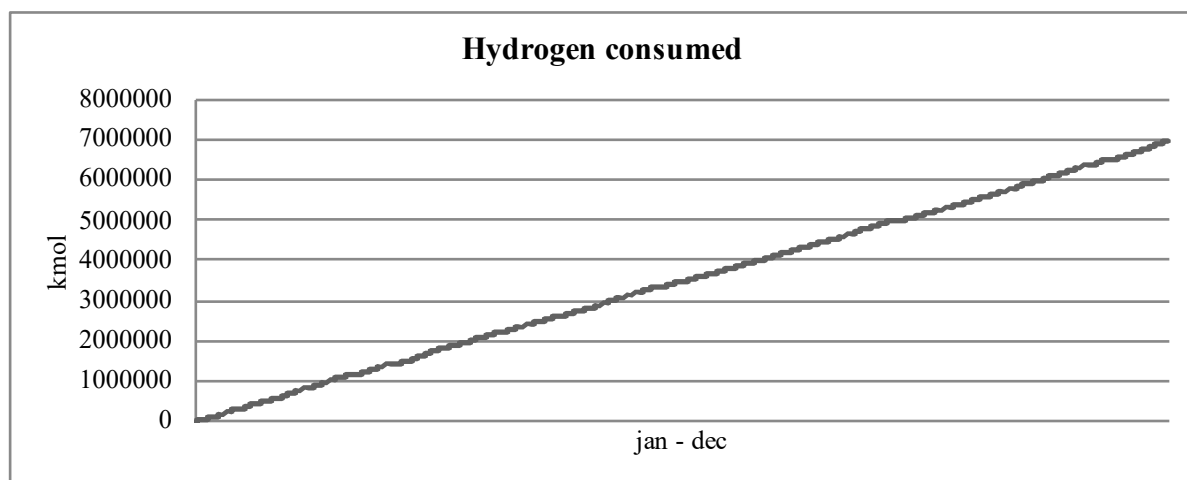


Figure 8.9: Hydrogen consumed over one year

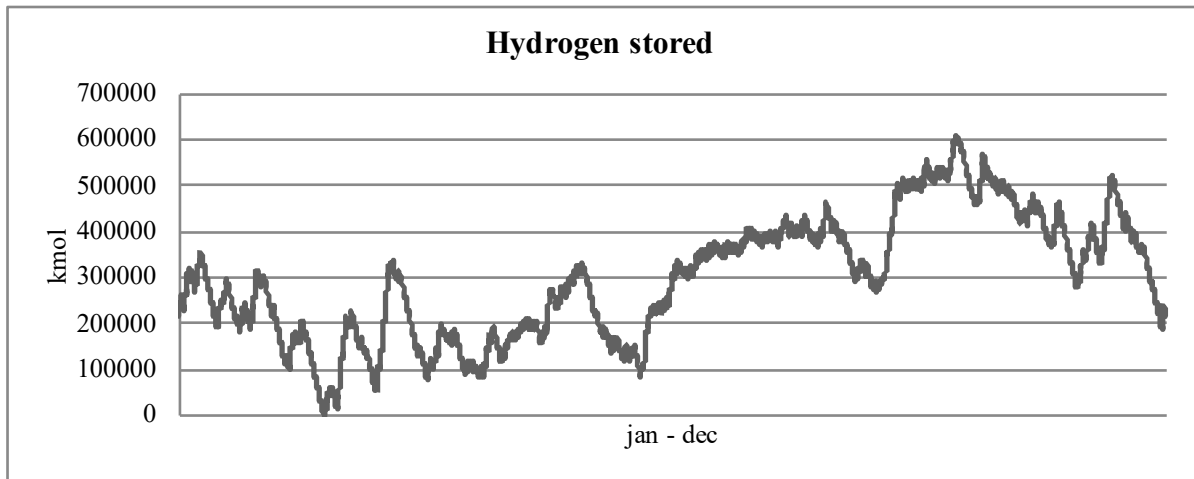


Figure 8.10: Hydrogen stored over one year

The required capacity of the hydrogen cavern is determined by the highest point in graph 8.10, i.e. 6.14×10^5 kmol or 1.94×10^5 m³ (i.e. under storage conditions of 80 bar and 31°C). It is assumed that all hydrogen produced is stored before it is used as a fuel in the hydrogen power plant. The amount of hydrogen to be stored is 6.98×10^6 kmol. This is also the total amount of gas that has to be stored for this system.

8.4.3. Efficiency

Since the PtMtP and PtHtP systems are investigated for electricity grid balance, the electrical efficiency is most important. For the calculation of the round trip electrical efficiency the system is scaled so that

- The power plant hydrogen consumption per hour meets hydrogen production per hour
- The power plant oxygen consumption per hour matches the SOEC's oxygen production per hour. I.e. the surplus oxygen produced by the SOEC's is not compressed for storage and

The round trip electrical efficiency is calculated as:

$$\eta_{\text{elec,round trip,PtHtP}} = \frac{E_{\text{out}}}{E_{\text{in}}} = \frac{E_{\text{out,elec,power plant}}}{E_{\text{SOEC}} \times \dot{m}_{\text{H}_2} + E_{\text{comp}}} \quad (8.17)$$

Where

E_{SOEC}	=	energy consumption of electrolysis cells in kWh kmol ⁻¹
\dot{m}_{H_2}	=	molar flow of hydrogen
E_{comp}	=	compression energy for hydrogen storage
$E_{\text{out,elec,power plant}}$	=	electrical output of hydrogen power plant

It is assumed that all hydrogen is compressed to 80 bar and stored before it is burned. With an electrolyzer energy consumption of 4.5 kWh kmol⁻¹, 2.75 MW compressor work and a power plant electrical output of 44 MW, the results round trip efficiency becomes 37.4 %.

8.5. Comparison between methane system and hydrogen system

8.5.1. Storage capacity

The gas storage capacity for three different systems are shown in table 8.12. The total amount of gas to be stored is listed in table 8.13. The hydrogen system is compared to the original methane system and the long term methane system with a more flexible methanation plant. The total amount of gas that needs to be stored is lowest for the hydrogen system and highest for the short term methane system. However, storing hydrogen requires more compression energy than storing methane, carbon dioxide

or oxygen. The total amount of hydrogen to be stored is lowest for the flexible methane system and highest for the hydrogen system.

	H ₂		3.3		Original	
	kmol × 10 ⁻⁵	m ³ × 10 ⁻⁵	kmol × 10 ⁻⁵	m ³ × 10 ⁻⁵	kmol × 10 ⁻⁵	m ³ × 10 ⁻⁵
CH ₄	0	0	1.78	0.56	2.37	0.75
CO ₂	0	0	1.74	0.55	2.32	0.73
O ₂	0	0	3.98	1.26	3.98	1.26
H ₂	6.14	1.94	1.29	0.41	7.44	2.35
Total	6.14	1.94	8.79	2.78	16.1	5.09
Meth. cap. [kmol/h]	0		719		510	
EC cap. [MW]	276		306		306	
Op. hours meth. [h]	0		8592		8016	
Op. hours EC [h]	8760		8592		8760	

Table 8.12: Storage capacity for different scenarios under storage conditions of 80 bar and 31 °C

	H ₂	3.3	Original
CH ₄ [kmol] × 10 ⁻⁶	0	2.35	2.35
CO ₂ [kmol] × 10 ⁻⁶	0	2.31	2.31
O ₂ [kmol] × 10 ⁻⁶	0	4.52	4.52
H ₂ [kmol] × 10 ⁻⁶	6.98	2.06	4.50
Total [kmol] × 10 ⁻⁶	6.98	11.2	13.7
Meth. cap. [kmolh ⁻¹]	0	719	510
EC cap. [MW]	309	306	306
Op. hours meth. [h]	0	8592	8016
Op. hours SOEC [h]	8760	8592	8760

Table 8.13: Amount of gas to be stored for different scenarios

8.5.2. Efficiency and carbon emissions

The round trip electrical efficiency of the PtMtP system is 30.9% for the original scenario and 31.1% for the flexible scenario. Both numbers are higher than the round trip electrical efficiency of the PtHtP system, i.e. 37.4%. Even in the most flexible case with no hydrogen buffer, the PtHtP plant has a higher round trip efficiency. One explanation is the low gas-to-power efficiency of the methane system, i.e. 42.4% compared to 57.0% for the hydrogen system. This is caused by the low electrical efficiency of the oxy-fuel power plant and the large amount of energy required for CO₂ compression. Another, less significant, reason for the poor behavior of the methane system compared to the hydrogen system is the energy required for oxygen compression. The hydrogen system has no carbon emissions compared to 1280 kmol for the methane system. The CO₂ emitted by the methane system is caused by methanation purge streams. It can be concluded that the hydrogen system scores better in terms of carbon emissions.

9

2050 scenario

9.1. Oxy-fuel power plant capacity

For the 2050 scenario it is assumed that all energy comes from wind and sun. The 2030 system is scaled up to store enough energy to fully back-up the 2050 grid. Three possible 2050 grid scenario's are described in section 2. From the round trip electrical efficiency of 30.9 % it follows that 59.1 % of the electricity is lost during conversion and storage meaning the amount of electricity surplus has to be at least 3.3 times larger than the amount of electricity deficit to balance the grid. The annual surplus and deficit energy for three 2050 scenarios from section 2 are listed in table 9.1.

	Surplus [TWh]	Deficit [GWh]	Deficit as part of surplus [%]
2050 Low	7.44	156	Deficit exceeds surplus
2050 Mid	78.6	73.0	92.8
2050 High	197	36.9	18.7

Table 9.1: Annual surplus and deficit for different scenarios

From table 9.1 it can be seen that only the 2050 high scenario is can be balanced with this power-to-methane-to-power system. In the other scenario's the amount of energy surplus is not high enough to balance the deficit, incorporating a round trip electrical efficiency of 30.9 %. The installed capacity of oxy-fuel power plants is based on the lowest peak of the 2050 high grid balance. In reality the installed capacity of oxy-fuel power plants will be higher for a reliable electricity system. The consequence of this is discussed in section 11. The lowest peak is -35.5 GW, which means that the 44 MW plant has to be scaled up by a factor 802. In reality this would result in several oxy-fuel power plants but in this research this is modeled as one large oxy-fuel power plant with a capacity of 35.5 GW. It is assumed that the fuel and oxygen consumption scales linearly with the plant capacity, resulting in a fuel consumption of 3.08×10^6 kmol h⁻¹. The power plant fuel consumption is coupled to the 2050 hourly grid balance to calculate the annual fuel consumption, following the same procedure as for the 2030 scenario described in section 7.2.

9.2. Methanation plant capacity and electrolysis capacity

Following the same procedure as in section 7.2 – 7.4, the final system values are found and listed in table 9.2.

OFCC fuel consumption (full load)	$3.08 \times 10^6 \text{ kmolh}^{-1}$
OFCC annual fuel consumption	$3.22 \times 10^8 \text{ kmoly}^{-1}$
Methanation plant capacity (full load)	$5.54 \times 10^4 \text{ kmolh}^{-1}$
Methanation CO ₂ input (full load)	$5.00 \times 10^4 \text{ kmolh}^{-1}$
Methanation H ₂ input (full load)	$2.18 \times 10^5 \text{ kmolh}^{-1}$
SOEC H ₂ production (full load)	$2.48 \times 10^5 \text{ kmolh}^{-1}$
Installed capacity SOEC's	20.8 GW

Table 9.2: Final system parameters

The distribution of surplus and deficit hours in the 2050 scenario has changed. The amount of deficit hours is 2657 and the amount of surplus hours is 6095 surplus hours over the year. This results in 69.5 % surplus hours and 30.5 % deficit hours, compared to 30.0 % surplus hours and 70.0 % deficit hours in 2030. This means Although the installed capacity of power plants is approximately 800 times larger, the installed capacity of SOEC's is only 68 times larger due to the decrease in green electricity deficit and increase in green electricity surplus.

9.3. Efficiency

The round trip electricity efficiency of the system is influenced by the amount of hydrogen that needs to be stored 8.2.8. The amount of hydrogen that needs to be stored does not only depend on the flexibility of the methanation plant, but also on the amount of operating hours of the methanation plant. The latter is a result of the amount of electricity surplus hours. The annual amount of hydrogen that needs to be stored in 2050, assuming a methanation minimum load of 40 % and 8000 operating hours per year, is 19.1 %. Following the same calculation as described in chapter 8, this results in a round trip electrical efficiency of 31.1 %, a round trip thermal efficiency of 56.9 % and a round trip energy efficiency of 90.0 %. Assuming a flexible methanation plant as described in scenario 3.3 of section 8.1.5 the amount of hydrogen to be stored is 6.32 %. This gives a round trip electrical efficiency of 31.2 % and a thermal efficiency of 56.9 %. The round trip energy efficiency becomes 90.1 %.

9.4. Storage capacity

Table 9.3 shows the gas storage capacity of the 2050 system for the original methanation plant with a flexibility as described in section 7.2 and for a flexible methanation plant with a flexibility as described in scenario 3.3 of section 8.2.8. The system is scaled as described in section 8.1.5. The gases are compressed to storage conditions of 80 bar and 31C.

	Original		3.3	
	[kmol] $\times 10^{-7}$	[m ³ $\times 10^{-7}$]	[kmol] $\times 10^{-7}$	m ³
CH ₄ [kmol]	3.20	1.01	4.14	1.31
CO ₂ [kmol]	3.68	1.15	4.07	1.29
O ₂ [kmol]	8.71	2.75	8.71	2.75
H ₂ [kmol]	10.9	3.44	1.70	0.54
Total [kmol]	26.4	9.34	18.6	5.88
Meth. cap. [kmolh ⁻¹]	55405		59615	
SOEC cap. [MW]	208		208	
Op. hours meth. [h]	8016		8592	
Op. hours SOEC [h]	8760		8592	

Table 9.3: Gas storage capacity of different gases for a PtMtP system in 2050, designed to store enough gas to provide an electricity grid with input only from wind and solar energy

From table 9.3 it can be seen that the hydrogen storage capacity decreases significantly as methanation flexibility increases. Again CH₄ and CO₂ storage capacity increases with methanation flexibility and the O₂ storage capacity remains the same as explained in section 8.1.6. The methanation plant capacity increases with increasing flexibility and the installed capacity SOEC's remains the same, also

explained in section 8.2.8. The total amount gas storage capacity for the original methanation plant is 9.34×10^7 m³, which is 5.5 % of total potential storage capacity in salt caverns in the Netherlands as described in section 7.5.3.

9.5. Carbon emissions

During its operation the power-to-methane-to-power system emits some carbon dioxide as described in section 8.3. The carbon emissions caused by methanation is 7.55 kmol h^{-1} at full load, resulting in a carbon emissions of 1.79×10^5 kmol or 2.87 kt over the year. It is assumed that the CO₂ emission scales linearly with the load of the plant as described in section 8.1.6. This is 0.0056 % of the current annual carbon emissions caused by the Dutch power generation sector [emissieautoriteit.nl].

10

Discussion and Recommendations

10.1. Grid analysis

The 2030 and 2050 grid balance estimates form the basis of the thesis as the whole system capacity and carbon emissions are based on these data. In the 2030 and 2050 grid balance estimate it is assumed that the weather conditions, as well as the distribution of electricity demand is the same as in 2018 (section 2.1). In reality this is not the case. A change for instance in wind hours and wind force could have a lot of impact on the grid balance, resulting in a different system capacity. It could be useful to check the weather conditions in terms of wind hours, wind force and solar irradiance over the past 30 years to see how this differs over the years. Also the distribution of the electricity demand in 2030 and 2050, compared to 2018 is not unrealistic. For instance, in 2018 midday hours were low demand hours, but with the introduction of smart grids the electricity demand could become more equally spread out. This could effect the amount of installed of power plants.

10.2. Electrolysis

As mentioned in section 3 Co-electrolysis, in which CO₂ and H₂O are reduced in one cell to H₂ and CO, could be an interesting technology for the future. It is not evaluated in this thesis since the technology is not mature enough. Since the heat integration between electrolysis and methanation enhances overall PtM efficiency it is important to investigate this in co-electrolysis. Co-electrolysis could not only decrease required equipment (there is no separate methanation plant) but also have a positive impact on system flexibility. Chemical reactions in electrochemical cells usually have a better system response and shorter shut-down and start-up time than conventional processes in reactor vessels. Last, electrolysis technology is currently widely investigated and develops quickly. Maximum operating pressure and cell efficiency could increase over the coming years for different cells making the choice of SOEC's not the optimal one anymore.

10.3. Methanation

In this research not all options for methanation are explored. For instance, catalytic methanation could also be performed in fluidized bed reactors. These option have to be explored to find the most efficiency PtG route. Anonther option is enhanced adsorption methanation. Also electrochemical methanation is widely investigated and could have a technological break through in the coming years. Electrochemical methanation is of special interesent because in theory electrochemical cells could functions in two modes, a fuel production mode and a fuel consumption mode. This could reduce system space requirements and investment costs.

10.4. Power generation

The oxy-power plant is responsible for the largest electrical energy losses in this research. A more efficient methane-to-power route could drastically inscrease to PtMtP system efficiency. Considering oxy-fuel power plant maturity, no commercial oxy-fuel power plant exist yet, there are only pilot scale

plants. Scaling up plant to commercial scale can influence plant efficiency and operating conditions. HP and LP turbine are considered as a conventional or advanced technology steam turbine and the IP turbine is considered comparable to a gas turbine with advanced materials and cooling technology. These assumptions could work out differently with a large scale oxy-fuel power plant and new operating challenges might come across. A more mature technology is a gas power plant with carbon capture. These plants have a net efficiency of 47-52 %_{LHV} [Leung, Hoffman, Schmidt] which is the same as the plant modelled in this thesis. However, the amount of CO₂ that can be captured with this technology is only 80 % [Leung]. Direct methane fuel cells (DMFC) provide an attractive solution in terms of system dimensions and CAPEX as the fuel cells are smaller than gas power plants and in reverse mode the cells could also be used for methane production, so a separate methanation plant does not need to be built, reducing space requirements and potentially investment costs. However the development of the latter solution is still in a very early stage. Methane conversion to electrical power in solid oxide electrolysis cells (SOFC's) is a promising direction, but it also poses technical difficulties as the methane molecule is difficult to activate and oxidize electrochemically [Gür]. Bloom Energy California is the biggest commercial developer and manufacturer of SOFCs based on methane conversion [Gür] and their largest power generator is the 300 kW Energy Server 5 with an LHV efficiency of 65 %. The Bloom Energy California cells use air for methane oxidation which makes carbon capture challenging and significantly lowers the total net efficiency.

10.5. Gas storage

No research was found on temporary and/or underground storage of CO₂ and O₂. Without large scale storage facilities of these gases the PtMtP system cannot function. Therefore it is important to find out if and how these gases can be stored exactly. Since the total amount of required storage capacity is much smaller than the amount of cavern space available, gases could be stored at the lowest possible pressure to reduce storage losses. In the 2050 scenario transport losses are not taken into account. However, to provide an (almost) zero emission electricity grid with a power-to-methane-to-power system a lot of plants are needed and it is likely that they cannot all be built near a storage facility. Transport losses should therefore be calculated to see what effect this has on the round trip efficiency of the system.

10.6. Modeling

10.6.1. Power plant modeling

The OF-CHP total efficiency is 95 %_{HHV}. Note that this efficiency can only be achieved when all heat output of the power plant is used for other purposes. Assuming all electricity produced by the plant can always be provided to the grid, the plant efficiency depends on the utilization potential of the hot water output. The latter depends highly on the location of the plant. When the plant is located near a district heating network, hot water could be injected in the network and delivered to households. To prevent formation of legionella the minimum hot water temperature is set to be 65°C for tap water. The oxy-power plant meets this requirement. However, located further away from a district heating network transport losses will decrease the water temperature making it unsuitable for heating tap water. A slightly higher electrical efficiency of the OF-CHP can be reached with a colder water outlet stream. However, the risk is created that the water stream temperature becomes too low and the heat cannot be used anymore.

10.6.2. Methanation modeling

In the methanation model hydrogen is first compressed and cooled afterwards. This is a design flaw as it would make more sense to first cool the streams and to compress it afterwards. Compressing a cold stream consumes less work than compressing a hot stream. This would increase system electrical efficiency. Also, compression usually takes place in multiple stages with intercooling to keep the gas temperature, and with that the compressor temperature, as low as possible. However, to produce 150°C steam the temperature of the gas during intercooling must at least be 150°C. It has to be explored if this is technically feasible. In the methanation model it is assumed that all heat from the methanation reactors can be captured to produce steam. Also, there are no heat transfer losses modeled in the heat exchangers. In reality there are some heat transfer losses, reducing thermal efficiency of the system. To find a more accurate result for the amount of heat that can be extracted from the reactors, these

heat transfer losses should be modeled. It is expected that, when accounting for heat transfer losses, still enough steam can be produced for the SOEC's.

10.6.3. Gas storage modeling

Calculation of required capacity

The required gas storage capacity is based on the highest peaks in figure REF-REF. Note that this is a simplification of the required amount of storage capacity. In this estimate the change in distribution of supply and demand over different years is neglected. Two examples: The surplus CH₄ in December might be needed to back up the month of January in a year that there is barely any wind electricity in January. On the other hand, if the difference between the level of CH₄ in January 2030 and December 2030 is zero, there still might be a surplus if January is a very windy month and electricity production from SNG is barely needed. Another example, the stored amount of CO₂ in December 2030 might be higher than the starting level in January 2030. This surplus could be necessary for CH₄ production in January 2031 when this is a very windy month with too little CO₂ production from the oxy-fuel power plant. Instead the surplus CO₂ could not be needed at all and increase even more when the electricity generation from wind in the month of January is very little. Hence, the required amount of gas storage capacity is an indication and meant to calculate the order of magnitude. Also, in the calculation of the required gas storage capacity excess of the oxygen is emitted by the system. This could either be sold or emitted into the air. In the PtMtP system there is an annual CO₂ deficit. Extra CO₂ has to be bought or come from direct air capture, for a truly zero emission system. The latter requires a lot of energy and reduced system efficiency.

Gas compression modeling

As discussed in section 10.6.2 to produce high quality heat in the form of steam, compressor temperature may not drop below 150C. This does not only hold for the compressor in the methanation plant but also for the other compressors in the system. As reported in chapter 8 it is assumed that no compression energy is recovered through expansion after storage. Recovering electricity by gas expansion after storage could be a way to improve system electrical efficiency. This requires extra gas turbines and it should be investigated if there is enough gas expansion potential in the system to cover turbine investment costs over the lifetime of the system. More than half of the compression energy for storage is needed for CO₂ compression. This is explained by the fact that CO₂ is expanded to a low pressure in the OF-CHP and needs to be compressed to a high pressure. A higher CO₂ pressure before compression can be achieved by less expansion in the OF-CHP. However this decreases the electrical efficiency of the power plant. Capturing and storing CO₂ in the PtMtP system is a complicated issue.

10.7. Power-to-gas efficiency

At deficit hours, when the methanation plant runs at minimum load, some of its heat output is used to produce a steam buffer for the SOEC's. This steam is needed so that the cells can directly be put in use when there is an electricity surplus. The heat for steam production is taken into account in the calculation of the heat efficiency of the power-to-gas system. However, the SOEC's can only be put to work very fast when they are already at a high temperature. Therefore some heat from the methanation plant will be needed to keep the SOEC's at high temperature, for instance in the form of hot air blowing against the cells. This heat is not taken into account in the calculation of the power-to-gas efficiency. It will slightly lower the efficiency as more heat from methanation is needed for internal purposes.

10.8. Round trip efficiency

The round trip energy efficiency is calculated only taken into account heat that is considered useful. Hot stream at a temperature lower than 65 °C are not included in the calculation of the energy efficiency. If these streams could be utilized, the round trip energy efficiency would increase. A round trip energy efficiency of 88.0 % can only be reached if the hot water streams can be used for external purposes. Possible purposes for heat output streams are:

- Warm water for heating of buildings (in the district heating network)
- Warm water for green house sector (plant does not have to be located near a city for district heating network)

- Electricity production from excess steam

If heat is to be used for district heating or green house heating, location of the system is very important. When the system is located far away from the heat destination, transport losses are expected to significantly decrease the temperature making the heat less useful a district heating network which is mostly a densely populated area. This is not . To use heat for district means the system should be located near an easy place to build chemical plant and power plants so this comes with a challenge. Also, there has to be an underground cavern nearby the system location to neglect the effect of gas transport losses. Using heat for the greenhouse sector could be easier since green houses are often not build in densely population area's. Other heat purposes should be explored to find the most suited one. Electricity production from excess steam could increase the electrical efficiency of the system. For this purpose steam should be extracted at the highest possible temperature. It should be investigated if enough steam is produced to payback for the steam turbines investment costs during the lifetime of the system. Last, CH₄ and O₂ enter the power plant at 15 bar and are both compressed to before combustion. However, gases come from high pressure storage before entering the power plant and compression is not necessary. This would increase the net work from the power plant which results in a higher system round trip electrical efficiency.

10.9. Hydrogen system

The power-to-hydrogen-to-power system scores better than the methane system in terms of required storage capacity, electrical efficiency and carbon emissions. Also due to higher round trip electrical efficiency, less electrolysis cells have to be installed for the same amount of electrical output of the system. Therefore a higher efficiency does not only reduce OPEX but also CAPEX. Also a methanation plant does have to be built and the total gas storage capacity is smaller, both reducing CAPEX as well. If a power-to-gas-to-power system is used for electricity storage, a hydrogen system seems more suited than a methane system in terms of efficiency, carbon emissions and storage capacity. However, the technical details of of both systems are not explored as well as the investment costs. To find the most convenient and economically feasible system, an economic analysis should be performed.

10.10. 2050 Scenario

Th required gas storage volume for the 2050 system is calculated to be 5.5 % of the total underground storage potential in the Netherlands. To start, this number is based on an estimated 2050 grid balance, not account for a significant change in weather conditions. The number calculated in the 2050 scenario are rough estimates. Second, the gas storage caverns have to be mined first before they can put into use. This is a costly operation. In reality the scale of installed capacity of oxy-power plants in 2050 would be larger than the lowest peak to provide a reliable energy system. This means more power plants have to be build than the 35.5 GW described in this thesis. This emphasizes the need for a combination of different energy storage systems instead of only power-to-gas.

11

Conclusion

This thesis investigated a power-to-methane-to-power system for green electricity storage. In this chapter the research question is answered. First an answer to the sub questions is provided.

Sub question 1: What are the energy efficiency, carbon emissions and required gas storage capacity of a closed loop system that uses methane as an energy carrier?

The energy efficiency of the system modelled in this thesis is 88.0 %. This is the sum of the an electrical efficiency of 30.9 % and a thermal efficiency of 57.1 %. The round trip energy efficiency can only be achieved if all modelled heat outlet streams can be used for external purposes. The round trip electrical efficiency increases slightly with methanation plant flexibility due to a smaller hydrogen buffer. The round trip thermal efficiency and round trip energy efficiency slightly decrease. The round trip electrical efficiency slightly increases with an increase in electrolyzer and methanation plant operating hours, also because of a smaller hydrogen buffer. The required gas storage capacity for a 44MW electrical output system, build in 2030 is estimated to be 16.1×10^5 kmol or 5.09×10^5 m³ under storage conditions of 80 bar and 31 °C. The carbon emissions are estimated to be 56.3 t y^{-1} in 2030.

Sub question 2: How does the allocation between electricity and heat influence the efficiency of the system?

Of the total energy efficiency of the PtMtP system 64.3 % is in the form of heat and 34.8 % is in the form of electricity. Whether an energy efficiency of 88.0 % can be achieved or not depends strongly on the potential of heat utilization, which depends strongly on the location of the system.

Sub question 3: How does the system perform in terms of carbon emissions and storage convenience compared to a power-to-hydrogen system and in an all renewable grid scenario?

The system performs worse in terms of round trip electrical efficiency, storage capacity and carbon emissions compared to a PtHtP system. The round trip electrical efficiency is 6.5 percent points lower than for the hydrogen system. This is mainly caused by the low methane-to-power efficiency. The required gas storage capacity for the methane system is 2.6 times higher than for the hydrogen system and 1.4 times higher than the for the hydrogen system whith a flexible methanation plant. These kind of plants however only function on lab scale. The carbon emissions of the methane system are 56.3 t y^{-1} compared to 0 t y^{-1} for the hydrogen system. When scaling up the system to provide an all renewable electricity grid in 2050 the round trip electrical efficiency slightly increases to 31.1 %. The total carbon emissions become 2.78 kt, which is 0.0056 % of the current annual carbon emissions caused by the Dutch power generation sector. The required gas storage capacity for the system is 9.34×10^7 m³, which is 5.5 % of the total potential salt cavern volume in the Netherlands. When system is used to provide an all renewables electricity grid in 2050, the most optimistic scenario of the PBL has to be realized in term of installed capacity of wind and solar parks and energy consumption. The number of gas power plants has to increase significantly which emphasizes the need for a combination of different energy storage systems instead of only power-to-gas.

Research question: What are the key factors that influence the energy efficiency of a closed

loop system that uses methane as an energy carrier and how does the system perform compared to a system that uses hydrogen as an energy carrier?

The most important factor that influences the electrical efficiency of a power-to-methane-to-power system is the methane-to-power plant as this step causes the greatest electricity losses. The key factors that influence the energy efficiency of a power-to-methane-to-power system are the methane-to-power plant and the potential of usable heat. The latter depends strongly on the location of the system. The PtMtP system performs worse than a PtHtP system in terms of electrical efficiency, storage capacity and carbon emissions. The electrical efficiency of the methane system is lower, the required gas storage capacity is higher and the carbon emissions are higher compared to a PtHtP system.

Bibliography

- [1] R. Allam, B. Forrest, J. Fetvedt, X. Lu, D. Freed and G. Brown, T. Sasaki, M. Itoh, and J. Manning. Demonstration of the allam cycle: An update on the development status of a high efficiency supercritical carbon dioxide power process employing full carbon capture. *Energy Procedia*, 114, 2017.
- [2] W. Amos. Costs of storing and transporting hydrogen. Technical report, National Renewable Energy Laboratory from the US Department of Energy.
- [3] R E Anderson and F Viteri. Adapting gas turbines to zero emission oxy-fuel power plants. In *Proceedings of ASME Turbo Expo 2008: Power for Land, Sea and Air*, 2008.
- [4] Roger E Anderson, Scott Macadam, Fermin Viteri, Daniel O Davies, James P Downs, and Andrew Paliszewski. Proceedings of ASME Turbo Expo 2008: Power for Land, Sea and Air GT. Technical report, 2008.
- [5] Philipp Biegger, Florian Kirchbacher, Ana Roza Medved, Martin Miltner, Markus Lehner, and Michael Harasek. Development of honeycomb methanation catalyst and its application in power to gas systems. *Energies*, 11(7), 2018. ISSN 19961073. doi: 10.3390/en11071679.
- [6] Olav Bolland, Hanne M Kvamsdal, and John C Boden. A THERMODYNAMIC COMPARISON OF THE OXY-FUEL POWER CYCLES WATER-CYCLE, GRAZ-CYCLE AND MATIANT-CYCLE. Technical report.
- [7] B. Buhre, L. Elliott, C. Sheng, R. Gupta, and T. Wall. Oxy-fuel combustion technology for coal-fired power generation. *Progress in Energy and Combustion Science*, 31, 2005.
- [8] Alexander Buttler and Hartmut Spliethoff. Current status of water electrolysis for energy storage, grid balancing and sector coupling via power-to-gas and power-to-liquids: A review, feb 2018. ISSN 18790690.
- [9] Milieu Centraal. Waterkracht. <https://www.milieucentraal.nl/klimaat-en-aarde/energiebronnen/waterkracht/>, 2019. [Online; accessed 19-August-2019].
- [10] Jun Chi and Hongmei Yu. Water electrolysis based on renewable energy for hydrogen production, mar 2018. ISSN 02539837.
- [11] Fernando Climent Barba, Guillermo Martínez-Denegri Sánchez, Blanca Soler Seguí, Hamidreza Gohari Darabkhani, and Edward John Anthony. A technical evaluation, performance analysis and risk assessment of multiple novel oxy-turbine power cycles with complete CO₂ capture. *Journal of Cleaner Production*, 133:971–985, oct 2016. ISSN 09596526. doi: 10.1016/j.jclepro.2016.05.189.
- [12] Energiecourant. Windenergiecourant.nl - Hoofdlijnen Klimaatakkoord 18 tot 24 gigawatt windenergie in 2030. <https://windenergiecourant.nl/offshore/hoofdlijnen-klimaatakkoord-18-tot-24-gigawatt-windenergie-in-2030/>, 2019. [Online; accessed 19-August-2019].
- [13] Energieopwek.nl. Energieopwek.nl. <http://www.energieopwek.nl/>, 2019. [Online; accessed 19-August-2019].
- [14] Entsoe. Entsoe - Power Statistics - Monthly Hourly Load Values. https://www.entsoe.eu/data/power-stats/hourly_load/, 2019. [Online; accessed 19-August-2019].
- [15] F. Heitmeir et al. Graz-cycle; a zero emission power plant of highest efficiency. Technical report, Graz University of Technology, 2005.

- [16] Hustad et al. Optimization of thermodynamically efficient nominal 40 mw zero emission pilot and demonstration power plant in norway. In *ASME Turbo Expo 2010: Power for Land, Sea and Air*, 2005.
- [17] Kvamsdal et al. A quantitative comparison of gas turbine cycles with CO₂ capture. *Energy*, 32, 2006.
- [18] Tak et al. Performance analysis of oxy-fuel power generation systems including CO₂ capture; comparison of two cycles using different recirculation fluids. *Mechanical Science and Technology*, 24, 2010.
- [19] V Evely. Hybridization of solid oxide electrolysis-based power-to-methane with oxyfuel combustion and carbon dioxide utilization for energy storage. *Renewable and Sustainable Energy Reviews*, 108:550–571, 2019.
- [20] Valerie Evely. Hybridization of solid oxide electrolysis-based power-to-methane with oxyfuel combustion and carbon dioxide utilization for energy storage. *Renewable and Sustainable Energy Reviews*, pages 550–571, jul 2019. ISSN 18790690. doi: 10.1016/j.rser.2019.02.027.
- [21] Stefano Falcinelli, Andrea Capriccioli, Fernando Pirani, Franco Vecchiocattivi, Stefano Stranges, Carles Martí, Andrea Nicoziani, Emanuele Topini, and Antonio Laganà. Methane production by CO₂ hydrogenation reaction with and without solid phase catalysis. *Fuel*, 209:802–811, 2017. ISSN 00162361. doi: 10.1016/j.fuel.2017.07.109.
- [22] B Field, J E Campbell, and D B Lobell. Biomass energy: the scale of the potential resource. *Trends Ecol Evol.*, 23(2):65–72, 2008.
- [23] Stefan Fogel, Holger Kryk, and Uwe Hampel. Simulation of the transient behavior of tubular solid oxide electrolyzer cells under fast load variations. *International Journal of Hydrogen Energy*, 44 (18):9188–9202, apr 2019. ISSN 03603199. doi: 10.1016/j.ijhydene.2019.02.063.
- [24] S.van Gessel. Ondergrondse opslag in nederland. Technical report, TNO, 2018.
- [25] Sunfire GmbH. HyLink Factsheet. <https://www.sunfire.de>.
- [26] Miguel Angel Gonzalez-Salazar, Trevor Kirsten, and Lubos Prchlik. Review of the operational flexibility and emissions of gas- and coal-fired power plants in a future with growing renewables, feb 2018. ISSN 18790690.
- [27] Manuel Götz, Amy McDaniel Koch, and Frank Graf. State of the Art and Perspectives of CO₂ Methanation Process Concepts for Power-to-Gas Applications. Technical report, 2014.
- [28] Manuel Götz, Jonathan Lefebvre, Friedemann Mörs, Amy McDaniel Koch, Frank Graf, Siegfried Bajohr, Rainer Reimert, and Thomas Kolb. Renewable Power-to-Gas: A technological and economic review, jan 2016. ISSN 18790682.
- [29] Manuel Gruber, Petra Weinbrecht, Linus Biffar, Stefan Harth, Dimosthenis Trimis, Jörg Brabandt, Oliver Posdziech, and Robert Blumentritt. Power-to-Gas through thermal integration of high-temperature steam electrolysis and carbon dioxide methanation - Experimental results. *Fuel Processing Technology*, 181:61–74, dec 2018. ISSN 03783820. doi: 10.1016/j.fuproc.2018.09.003.
- [30] HELMETH. HELMETH. <http://www.helmeth.eu/index.php>, 2019. [Online; accessed 19-August-2019].
- [31] Sunhwan Hwang, Joongwon Lee, Ung Gi Hong, Jeong Gil Seo, Ji Chul Jung, Dong Jun Koh, Hyojun Lim, Changdae Byun, and In Kyu Song. Methane production from carbon monoxide and hydrogen over nickel-alumina xerogel catalyst: Effect of nickel content. *Journal of Industrial and Engineering Chemistry*, 17(1):154–157, jan 2011. ISSN 1226086X. doi: 10.1016/j.jiec.2010.12.015.
- [32] IEA. CO₂ emissions statistics. <https://www.iea.org/statistics/co2emissions>.

- [33] J. Apt, A. Newcomer, L. Lave, S. Douglas, and L. Dunn. An engineering-economic analysis of syngas storage. Technical report, Carnegie Mellon University and West Virginia University.
- [34] M. Jensen, S. Schlasner, J. Sorensen, and J. Hamling. Operational flexibility of CO₂ transport and storage. *Energy Procedia*, 63, 2014.
- [35] Deqiang Ji, Zhida Li, Wei Li, Dandan Yuan, Yuhang Wang, Yanyan Yu, and Hongjun Wu. The optimization of electrolyte composition for CH₄ and H₂ generation via CO₂/H₂O co-electrolysis in eutectic molten salts. *International Journal of Hydrogen Energy*, pages 5082–5089, feb 2019. ISSN 03603199. doi: 10.1016/j.ijhydene.2018.09.089.
- [36] Jonathan Lefebvre, Manuel Götz, Siegfried Bajohr, Rainer Reimert, and Thomas Kolb. Improvement of three-phase methanation reactor performance for steady-state and transient operation. *Fuel Processing Technology*, 132:83–90, 2015. ISSN 03783820. doi: 10.1016/j.fuproc.2014.10.040.
- [37] Dennis Y.C. Leung, Giorgio Caramanna, and M. Mercedes Maroto-Valer. An overview of current status of carbon dioxide capture and storage technologies, 2014. ISSN 13640321.
- [38] Yu Luo, Yixiang Shi, Wenying Li, and Ningsheng Cai. Dynamic electro-thermal modeling of co-electrolysis of steam and carbon dioxide in a tubular solid oxide electrolysis cell. *Energy*, 89: 637–647, sep 2015. ISSN 03605442. doi: 10.1016/j.energy.2015.05.150.
- [39] Yu Luo, Xiao yu Wu, Yixiang Shi, Ahmed F. Ghoniem, and Ningsheng Cai. Exergy analysis of an integrated solid oxide electrolysis cell-methanation reactor for renewable energy storage. *Applied Energy*, 215:371–383, apr 2018. ISSN 03062619. doi: 10.1016/j.apenergy.2018.02.022.
- [40] V Masson-Delmotte, P Zhai, H O Pörtner, D Roberts and J Skea, P R Shukla, A Pirani, W Moufouma-Okia, C Péan, R Pidcock, S Connors, J B R Matthews, Y Chen, X Zhou, M I Gomis, E Lonnoy, T Maycock, M Tignor, and T Waterfield (eds.). *Ipcc, 2018: Summary for policymakers. In Global Warming of 1.5 degrees Celsius. An IPCC Special Report on the impacts of global warming of 1.5 degrees Celsius above pre-industrial levels and related global greenhouse gas emission pathways, in the context of strengthening the global response to the threat of climate change, sustainable development, and efforts to eradicate poverty*, 2018.
- [41] K. Müller, M. Fleige, F. Rachow, and D. Schmeißer. Sabatier based CO₂-methanation of flue gas emitted by conventional power plants. In *Energy Procedia*, volume 40, pages 240–248. Elsevier Ltd, 2013. doi: 10.1016/j.egypro.2013.08.028.
- [42] Hiroki Muroyama, Yuji Tsuda, Toshiki Asakoshi, Hasan Masitah, Takeou Okanishi, Toshiaki Matsui, and Koichi Eguchi. Carbon dioxide methanation over Ni catalysts supported on various metal oxides. *Journal of Catalysis*, 343:178–184, nov 2016. ISSN 10902694. doi: 10.1016/j.jcat.2016.07.018.
- [43] NLOG. Ondergrondse opslagcapaciteit in nederland. <https://www.nlog.nl/opslag>.
- [44] United Nations Framework Convention on Climate Change. Paris climate agreement. <https://unfccc.int/process-and-meetings/the-paris-agreement/the-paris-agreement>, 2019. [Online; accessed 19-August-2019].
- [45] NET Power. NET Power has reinvented the power plant. <https://www.netpower.com/technology/>.
- [46] Foteini M. Sapountzi, Jose M. Gracia, C. J.(Kees Jan) Weststrate, Hans O.A. Fredriksson, and J. W.(Hans) Niemantsverdriet. Electrocatalysts for the generation of hydrogen, oxygen and synthesis gas, jan 2017. ISSN 03601285.
- [47] O. Schmidt, A. Gambhir, I. Staffell, A. Hawkes, J. Nelson, and S. Few. Future cost and performance of water electrolysis: An expert elicitation study. *International Journal of Hydrogen Energy*, 42(52): 30470–30492, dec 2017. ISSN 03603199. doi: 10.1016/j.ijhydene.2017.10.045.

- [48] Kristian Stangeland, Dori Kalai, Hailong Li, and Zhixin Yu. CO₂ Methanation: The Effect of Catalysts and Reaction Conditions. In *Energy Procedia*, volume 105, pages 2022–2027. Elsevier Ltd, 2017. doi: 10.1016/j.egypro.2017.03.577.
- [49] Rohan Stanger, Terry Wall, Reinhold Spörl, Manoj Paneru, Simon Grathwohl, Max Weidmann, Günter Scheffknecht, Denny McDonald, Kari Myöhänen, Jouni Ritvanen, Sirpa Rahiala, Timo Hyppänen, Jan Mletzko, Alfons Kather, and Stanley Santos. Oxyfuel combustion for CO₂ capture in power plants. *International Journal of Greenhouse Gas Control*, 40:55–125, sep 2015. ISSN 17505836. doi: 10.1016/j.ijggc.2015.06.010.
- [50] Haldor Topsoe. From solid fuels to substitute natural gas using TRESP. <https://www.netl.doe.gov/sites/default/files/netl-file/tresp-2009.pdf>, 2009.
- [51] Brian vad Mathiesen, Iva Ridjan, David Connolly, Mads Pagh Nielsen, Peter Vang Hendriksen, Mogens Bjerg Mogensen, Søren Højgaard Jensen, and Sune Dalgaard Ebbesen. Technology data for high temperature solid oxide electrolyser cells, alkali and pem electrolyzers, 2013.
- [52] Wetten.nl. Regeling gaskwaliteit. <https://wetten.overheid.nl/BWBR0035367/2019-01-01>, 2019. [Online; accessed 19-August-2019].
- [53] Tabbi Wilberforce, Fawwad N. Khatib, Emmanuel Ogungbemi, and Abdul G. Olabi. Water Electrolysis Technology. In *Reference Module in Materials Science and Materials Engineering*. Elsevier, 2018. doi: 10.1016/B978-0-12-803581-8.11273-1. URL <https://linkinghub.elsevier.com/retrieve/pii/B9780128035818112731>.